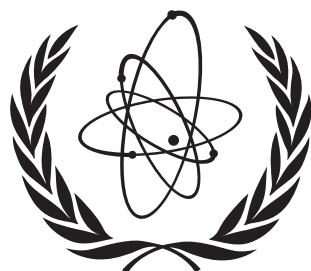


# 21st ATOMIC PROCESSES IN PLASMAS CONFERENCE

15 – 19 MAY 2023  
INTERNATIONAL ATOMIC ENERGY AGENCY  
HEADQUARTERS, VIENNA, AUSTRIA



**IAEA**

*Front cover picture:* Thomas Görlitz

# Contents

Welcome . . . . .	1
Organizing Committee . . . . .	2
Useful Information . . . . .	3
Agenda . . . . .	5
Oral Presentation Abstracts . . . . .	19
Poster Presentation Abstracts . . . . .	91
Tutorial Lecture Abstracts . . . . .	155
Things To Do In Vienna . . . . .	167
Participant List . . . . .	169
Author Index . . . . .	175



---

## Welcome to the 21st International Conference on Atomic Processes in Plasmas

APiP 2023 will be held at the Headquarters of the International Atomic Energy Agency in the Vienna International Centre, Vienna, Austria from 15 – 19 May 2023. This meeting series started in 1977 as an American Physical Society (APS) Topical Conference and was until 2007 held in the US. Since 2007 the meeting has become international to better reflect the true nature of its scope; it is generally held every two years but the COVID-19 pandemic led to the 2021 meeting being postponed until 2023.

The APiP conference focuses on atomic processes that are involved in the study of various plasmas over a wide range of densities and temperatures (eV to a few keVs). The event consists of invited and contributed oral presentations and posters on topics including:

- Astrophysical Plasmas
- Fundamental Data and Modelling
- Atmospheric and Medical Plasmas
- High Energy Density Plasmas
- Low Temperature and Industrial Plasmas
- Magnetically Confined Fusion Plasmas
- Measurements of Atomic Processes
- Powerful Light Sources (XFEL, etc.)
- Small-Scale Plasmas (table-top lasers, EBITs, etc.)
- Warm Dense Matter

---

## International Programme Committee

- **Christian HILL**, IAEA (Chair)
- **Djamel BENREDJEM**, Laboratoire Aimé Cotton, Université Paris-Saclay, France
- **Hyun-Kyung CHUNG**, Korea Institute of Fusion Energy, Republic of Korea
- **Matthew REINKE**, Oak Ridge National Laboratory, USA
- **Hae Ja LEE**, SLAC National Accelerator Laboratory, USA
- **Nobuyuki NAKAMURA**, Institute for Laser Science, University of Electro-Communications, Japan
- **Oleksandr MARCHUK**, Forschungszentrum Jülich (FZJ), Germany
- **Olivier PEYRUSSE**, Aix-Marseille Université, CNRS, Laboratoire LP3, France
- **Taisuke NAGAYAMA**, Sandia National Laboratories, USA

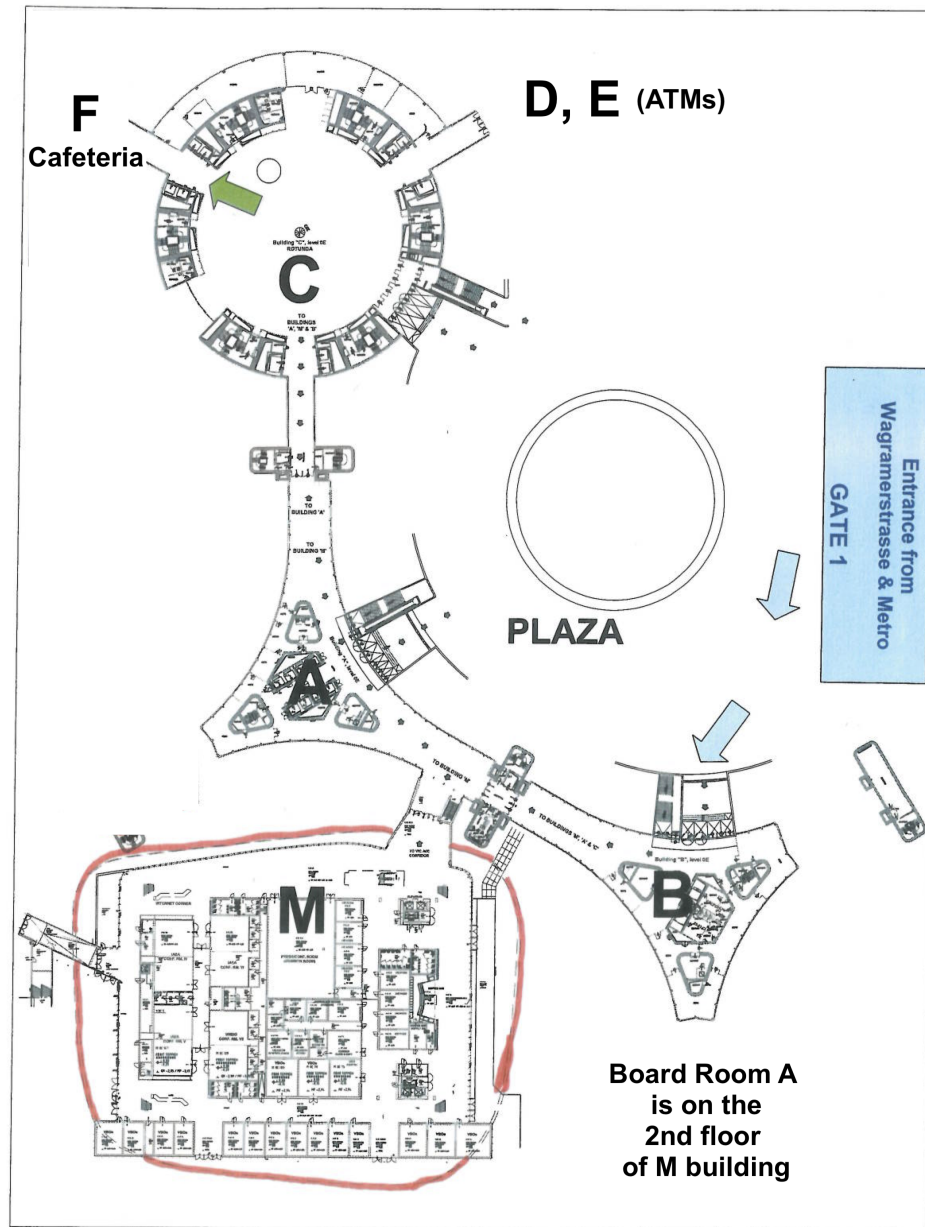
## Local Organizers

- **Christian HILL**, IAEA
- **Dipti**, IAEA
- **Kalle HEINOLA**, IAEA
- **Charisse MONFERO**, IAEA
- **Lidija VRAPCENJAK**, IAEA

---

## Useful Information

The conference meeting room is Board Room A, on the second floor of the M-building of the Vienna International Centre. Coffee breaks and the poster session will be held in the space immediately outside the meeting room itself. There is elevator and escalator access to this floor.



- 
- Visitors are requested to wear their visitor badges visibly at all times whilst at the Vienna International Centre.
  - There are currently no specific requirements for participants concerning COVID-19 for this meeting.
  - Two additional rooms on the ground floor of the M-building, M0E-05 and M0E-07, are available for breakout meetings: please contact the meeting organisers for details.
  - There is a cafeteria on the ground floor of the F-building; *only cash (in Euros) is accepted* but there are ATMs on the ground floor of the E-building and the first floor of the C-building rotunda.
  - There is an IAEA souvenir shop in the F-building, next to the rotunda (open Monday, Wednesday and Friday from 11 am – 2 pm) and a UN Gift Shop at Gate 1 (the main visitors' entrance).
  - Please contact the local organisers, Christian Hill ([ch.hill@iaea.org](mailto:ch.hill@iaea.org)) or Charisse Monfero ([c.monfero@iaea.org](mailto:c.monfero@iaea.org)) with any questions concerning the conference.



## **AGENDA**



---

## Monday, 15 May 2023

10:00 – 10:20 **Melissa DENECKE**  
*Director, Division of Physics and Chemistry Sciences,  
Department of Nuclear Applications, IAEA*  
Welcome and Meeting Opening

### Session 1: Magnetic Confinement Fusion Plasmas I

*Chair: Chihiro SUZUKI*

- 10:20 – 10:40 **Izumi MURAKAMI**  
[#57] *National Institute for Fusion Science, Japan*  
Evaluation of extreme ultraviolet spectral models for mid-charged tungsten ions with LHD experiments
- 10:40 – 11:00 **Dmitriy BORODIN**  
[#118] *Forschungszentrum Jülich (FZJ), Germany*  
Tracking of internal states in collisional-radiative models employed in the transport codes
- 11:00 – 11:30 Coffee Break
- 11:30 – 11:50 **Rémy GUIRLET**  
[#76] *Centre d'Etudes Nucleaires de Cadarache, Association EURATOM-CEA, France*  
Light and metallic impurity identification in the 225-302 Å range from the SURVIE spectrometer in the WEST tokamak  
*With Corinne DESGRANGES*
- 11:50 – 12:10 **Conor PERKS**  
[#112] *Plasma Science and Fusion Center, Massachusetts Institute of Technology, USA*  
SPARC x-ray crystal spectroscopy for ion temperature and toroidal rotation measurements
- 12:10 – 12:30 **Erik FLOM**  
[#66] *University of Wisconsin-Madison, USA*  
Improved uncertainty modeling for the helium collisional-radiative model used for line-ratio spectroscopy on Wendelstein 7-X

- 
- 12:30 – 14:00 Lunch
- 14:00 – 15:00 **Yuri RALCHENKO**  
[T1] *National Institute of Standards and Technology, USA*  
Atomic processes in plasmas  
*Tutorial Lecture*
- 15:00 – 15:30 Coffee Break

## Session 2: Magnetic Confinement Fusion Plasmas II

*Chair: Rémy GUIRLET*

- 15:30 – 16:00 **Curtis JOHNSON**  
[#111] *Oak Ridge National Laboratory, USA*  
Time-dependent collisional radiative modeling and  
ultra-violet spectroscopy of neutral tungsten for erosion  
diagnosis  
*Invited Presentation*
- 16:00 – 16:20 **Ling ZHANG**  
[#107] *Institute of Plasma Physics, Chinese Academy of Sciences  
(ASIPP), China*  
Further requirement of tungsten atomic data for tungsten  
influx estimation at EAST plasma edge
- 16:20 – 16:40 **Yves PEYSSON**  
[#71] *CEA/IRFM, France*  
A unified atomic description for high-Z impurities  
modelling in tokamak plasmas
- 16:40 – 17:00 **P. Bharathi MAGESH**  
[#62] *Institute for Plasma Research, Ahmedabad, India*  
Overview of Doppler shift spectroscopy diagnostics  
technique used in neutral beam injectors: challenges and  
limitations
- 17:00 – 17:20 **Kajal SHAH**  
[#69] *Pandit Deendayal Energy University, India*  
Estimation of argon impurity transport in Aditya-U ohmic  
discharges using Be-like, B-like and Cl-like argon spectral  
line emissions

---

## Tuesday, 16 May 2023

- 09:00 – 09:30 **Connor BALLANCE**  
[T2a] *Queen's University Belfast, United Kingdom*  
A non-perturbative R-matrix tutorial for single photon ionization of atoms and ions  
*Tutorial Lecture*
- 09:30 – 10:00 **Christopher J. FONTES**  
[T2b] *Los Alamos National Laboratory, USA*  
Atomic cross-section calculations  
*Tutorial Lecture*

### Session 3: High Energy Density Plasmas and Powerful Light Sources I

*Chair: Hae Ja LEE*

- 10:00 – 10:30 **Beata ZIAJA-MOTYKA**  
[#22] *Centre for Free-Electron Laser Science - Deutsches Elektronen-Synchrotron (CFEL-DESY), Germany*  
Modelling the evolution of X-ray free-electron-laser irradiated solids towards warm-dense-matter state  
*Invited Presentation*
- 10:30 – 10:50 **Mike MACDONALD**  
[#117] *Lawrence Livermore National Laboratory, USA*  
Investigation of opacity effects on optically thick lines for diagnosing plasma conditions in buried layer targets for x-ray opacity studies
- 10:50 – 11:20 Coffee Break
- 11:20 – 11:40 **Sofia BALUGANI**  
[#25] *European Synchrotron Radiation Facility (ESRF), France*  
Laser-driven shock compression of Fe up to 250 GPa probed by X-ray Absorption Spectroscopy

- 
- 11:40 – 12:00 **David BISHEL**  
[#90] *University of Rochester, USA*  
Measurement of line absorption at Gbar pressures
- 12:00 – 12:20 **Joseph NILSEN**  
[#52] *Lawrence Livermore National Laboratory, USA*  
Using K-shell S line ratios to measure the plasma temperature in a transient FeS plasma
- 12:20 – 12:40 **Marta GALBIATI**  
[#104] *Polytechnic University of Milan, Italy*  
Numerical investigation of bremsstrahlung in laser-plasma interaction with double-layer targets
- 12:40 – 14:00 Lunch
- 14:00 – 15:00 **Ming Feng GU**  
[T3] *University of California, Berkeley, USA*  
FAC for intermediate users  
*Tutorial Lecture*

#### **Session 4: Poster Session**

- 15:00 – 17:00 Posters outside Board Room A

---

## Wednesday, 17 May 2023

### Session 5: Fundamental Data and Modelling I

*Chairs: Yuri RALCHENKO and Catherine RAMSBOTTOM*

- 09:00 – 09:30 **Alisher KADYROV**  
[#21] *Faculty of Science and Engineering, Curtin University, Australia*  
Energy and angular distributions of electrons emitted in ion collisions with atomic and molecular targets  
*Invited Presentation*
- 09:30 – 09:50 **Marek PAJEK**  
[#116] *Jan Kochanowski University, Kielce, Poland*  
X-ray studies of atomic processes involving highly charged ions at EBIT/S
- 09:50 – 10:10 **Valdas JONAUSKAS**  
[#75] *Vilnius University, Lithuania*  
Multiple photoionization for the Fe<sup>+</sup> 2p subshell  
*With Aušra KYNIENĖ.*
- 10:10 – 10:30 **Christine STOLLBERG**  
[#68] *École Polytechnique Fédérale de Lausanne (EPFL), Switzerland*  
An LCIF diagnostic to test fusion relevant atomic data in RAID
- 10:30 – 11:00 Coffee Break
- 11:00 – 11:20 **Pedro AMARO**  
[#106] *Faculty of Science and Technology, Nova University of Lisbon, Portugal*  
Benchmark of the 2p line formation in O VII near the collisional excitation threshold
- 11:20 – 11:40 **Endre TAKACS**  
[#100] *Clemson University, USA*  
Influence of metastable levels on the charge-state distribution of highly charged ions in EBIT plasma





- 
- 15:50 – 16:20 **David HOARTY**  
[#23] *Atomic Weapons Establishment, United Kingdom*  
Radiation burn-through measurements to infer opacity at conditions close to the solar radiative zone-convective zone boundary  
*Invited Presentation*
- 16:20 – 16:40 **Taisuke NAGAYAMA**  
[#29] *Sandia National Laboratories, USA*  
Updates on iron opacity measurements at solar interior temperature
- 16:40 – 17:00 **Yang YANG**  
[#70] *Fudan University, China*  
First laboratory measurement of magnetic-field-induced transition effect in Fe X at different magnetic fields
- 17:00 – 18:00 **Stephanie HANSEN**  
[T4] *Sandia National Laboratories, USA*  
Density effects on plasmas  
*Tutorial Lecture*

---

## Thursday, 18 May 2023

09:00 – 10:00 **Mourad TELMINI**  
[T5] *University of Tunis El Manar, Tunisia*  
Electron-molecule collisions  
*Tutorial Lecture*

### Session 7: High Energy Density Plasmas and Powerful Light Sources II

*Chair: Bob NAGLER*

10:00 – 10:30 **Byoung-Ick CHO**  
[#78] *Gwangju Institute of Science and Technology, South Korea*  
Non-equilibrium dynamics during warm dense matter  
formation  
*Invited Presentation*

10:30 – 10:50 **Alina KONONOV**  
[#92] *Sandia National Laboratories, USA*  
Improving warm dense matter models with accurate  
first-principles benchmarks

10:50 – 11:20 Coffee Break

11:20 – 11:50 **Jianmin YUAN**  
[#35] *Atomic and Molecular Physics Group, National University  
of Defense Technology, China*  
A self-consistent model of ionization potential depression of  
ions in hot and dense plasmas with local field correction  
*Invited Presentation*

11:50 – 12:20 **Suxing HU**  
[#128] *University of Rochester, USA*  
Probing extreme atomic physics in super-dense plasmas  
*Invited Presentation*

12:20 – 12:40 **Michal ŠMÍD**  
[#109] *Helmholtz-Zentrum Dresden-Rossendorf, Germany*  
Raman shifts and plasma screening in Warm Dense Copper

---

12:40 – 14:00 Lunch

### Session 8: High Energy Density Plasmas and Powerful Light Sources III

Chair: Beata ZIAJA-MOTYKA

- 14:00 – 14:30 **Annette CALISTI**  
[#4] *Physique des Interactions Ioniques et Moléculaires (PIIM), Aix-Marseille Université (AMU), France*  
Ionization Potential Depression and dense plasma collisional properties  
*Invited Presentation*
- 14:30 – 14:50 **Ibtissem HANNACHI**  
[#6] *University of Batna 1, Algeria*  
Stark spectroscopy in the presence of Langmuir waves in non-equilibrium plasma
- 14:50 – 15:10 **Brian Edward MARRÉ**  
[#40] *Helmholtz-Zentrum Dresden-Rossendorf, Germany*  
Atomic population kinetics for Particle in Cell
- 15:10 – 15:30 **Howard SCOTT**  
[#61] *Lawrence Livermore National Laboratory, USA*  
Expanded application of the Linear Response Method

15:30 – 16:00 Coffee Break

### Session 9: Fundamental Data and Modelling II

Chair: Lalita SHARMA

- 16:00 – 16:20 **Dmitry FURSA**  
[#129] *Faculty of Science and Engineering, Curtin University, Australia*  
Elastic scattering and rotational excitation of H<sub>2</sub> by electron impact

- 
- 16:20 – 16:50 **Keisuke FUJII**  
[#58] *Oak Ridge National Laboratory, USA*  
Simple explanation for the observed power law distribution  
of line intensity in complex many-electron atoms and heavy  
nuclei  
*Invited Presentation*
- 16:50 – 17:10 **Kalyan Kumar CHAKRABARTI**  
[#26] *Scottish Church College, India*  
Electron collision studies on some molecules and molecular  
ions in plasmas

---

## Friday, 19 May 2023

09:00 – 10:00 **Nina ROHRINGER**  
[T6] *Deutsches Elektronen-Synchrotron (DESY), Germany*  
X-ray lasers  
*Tutorial Lecture*

### Session 10: Atmospheric and Medical Plasmas

*Chair: Christian HILL*

10:00 – 10:30 **Marquidia PACHECO**  
[#50] *Instituto Nacional de Investigaciones Nucleares, Mexico*  
Plasma technology to mitigate climate crisis: Usefulness of  
OES as processes optimization  
*Invited Presentation*

10:30 – 10:50 **Vladimir SCHOLTZ**  
[#103] *University of Chemistry and Technology, Prague, Czechia*  
Bio-applications of non-thermal plasma

10:50 – 11:20 Coffee Break

### Session 11: High Energy Density Plasmas and Powerful Light Sources IV

*Chairs: Annette CALISTI and Howard SCOTT*

11:20 – 11:50 **Sam VINKO**  
[#127] *Oxford University, United Kingdom*  
Non-thermal evolution of dense plasmas driven by intense  
x-ray fields  
*Invited Presentation*

11:50 – 12:10 **Robin PIRON**  
[#89] *CEA / DAM / DIF, France*  
A variational atomic model of plasma accounting for ion  
radial correlations and electronic structure of ions  
(VAMPIRES)

- 
- 12:10 – 12:30 **Maylis DOZIÈRES**  
[#82] *General Atomics, USA*  
Integrated reflectivity inferred from crystal response measurement for several NIF X-ray spectrometers
- 12:30 – 14:00 Lunch
- 14:00 – 14:20 **Pedro VELARDE**  
[#137] *Universidad Politécnica de Madrid, Spain*  
Time-dependent radiation emission from an X-ray laser-produced plasma
- 14:20 – 14:40 **Evgeny STAMBULCHIK**  
[#95] *Weizmann Institute, Israel*  
Progress in modeling of krypton He-beta lineshape for diagnostics of high-energy-density plasmas
- 14:40 – 15:00 **Michael KRUSE**  
[#99] *Lawrence Livermore National Laboratory, USA*  
Two-photon processes and their minor contribution to the Sandia Z-pinch Iron opacity experiments
- 15:00 – 15:20 Meeting Close

# **PRESENTATIONS**





## **Ionization potential depression and dense plasma collisional properties.**

**Annette Calisti<sup>1</sup>, Sandrine Ferri<sup>2</sup>, Jean-Christophe Pain<sup>3</sup>, Djamel Benredjem<sup>4</sup>**

<sup>1</sup>*CNRS*

<sup>2</sup>*Aix Marseille University, CNRS, PIIM*

<sup>3</sup>*CEA, DAM, DIF*

<sup>4</sup>*Université Paris-Saclay, CNRS, Laboratoire Aimé Cotton*

The radiative properties of an atom or an ion surrounded by a plasma, are modified through various mechanisms. Depending on plasma conditions the electrons supposedly occupying the upper quantum levels of radiators no longer exist as they belong to the plasma free electron population. All the charges present in the radiator environment, electrons and ions, contribute to the lowering of the energy required to free an electron in the fundamental state. This mechanism is known as ionization potential depression (IPD). The knowledge of IPD is fundamental as it affects both the radiative properties of the various ionic states and their populations. Its evaluation deals with highly complex n-body coupled systems, involving particles with different dynamics and attractive ion-electron forces. Two distinct models, namely the Stewart–Pyatt (SP) [1] and Ecker–Kröll (EK) [2] models, are widely used to estimate the IPD.

More recently, an approach based on classical molecular dynamics simulation has been developed providing an alternative way to calculate the IPD [3]. Ions and electrons are treated as classical particles and a minimum of quantum properties are taken into account through a regularized potential allowing to model collisional ionization and recombination processes. The related numerical code, BinGo-TCP, has been designed to describe neutral mixtures composed of ions of the same atom with different charge states, and electrons. Within the limits of classical mechanics, all charge-charge interactions are accounted for in the particle motion.

In this work, after a brief reminder of the modeling basis, the importance of the choice of the IPD modelling will be emphasized through a study of the influence of the IPD on the magnitude of the cross-section of ionization by free-electron impacts in the high-density domain [4]. Additionally, we will discuss the ionization energy distributions obtained with BinGo-TCP due to the fluctuating environment of the ions.

---

## References

1. Stewart J C and Pyatt K D 1966, *Astrophys. J.* 144, 1203.
2. Ecker G and Kröll W 1963, *Phys. Fluids* 6, 62.
3. Calisti A, Ferri S and Talin B 2015, *J. Phys. B: At. Mol. Opt. Phys.* 48, 224003.
4. Benredjem D, Pain J.-C, Calisti A and Ferri S 2022, *J. Phys. B: At. Mol. Opt. Phys.* 55, 105001.

## Stark spectroscopy in the presence of Langmuir waves in non-equilibrium plasma

**Ibtissem Hannachi<sup>1</sup>, Roland Stamm<sup>2</sup>, Joël Rosato<sup>2</sup>, Yannick Marandet<sup>2</sup>**

<sup>1</sup>*Université de Batna 1, PRIMALAB, Algeria*

<sup>2</sup>*Aix Marseille Université, CNRS, PIIM, France*

The collective behavior of a plasma is favored by the long range of electric and magnetic fields, and is well known to be able to excite waves with an oscillating electric field. For example, Langmuir waves are ubiquitous in many types of laboratory, fusion, and astrophysical plasmas. By using a classical equipartition theorem for a plasma in equilibrium, one can attribute half of the energy of the wave to the oscillating field, and the other half to kinetic energy, and one can then estimate that the modulus of the electric field of the wave is an order of magnitude smaller than the mean plasma microfield, for example, in a plasma with a temperature  $T = 1$  eV, and a density  $N = 10^{21} \text{ m}^{-3}$ . In a non-thermal plasma, however, the waves can be amplified by an instability, which allows the modulus of the oscillating electric field to reach values greater than the mean plasma microfield.

We here study the spectroscopic signature of an oscillating field  $E_L^+ = E_W^+ \cos(\omega_p t + \phi)$ , where  $\omega_p = \sqrt{Ne^2/(m\epsilon_0)}$  is the electronic plasma frequency, with  $e$  and  $m$  being the charge and the mass of the electron, and  $\epsilon_0$  the permittivity of free space. We calculate the first Lyman and Balmer lines of hydrogen for densities between  $10^{19} \text{ m}^{-3}$  and  $10^{23} \text{ m}^{-3}$ , and a temperature of  $10^4$  K, conditions for which the ion dynamics affect the central part of the spectral lines. Our aim is the simultaneous diagnostic of the plasma and Langmuir wave parameters. By treating the electron contribution with a constant collision operator, we calculate the simultaneous effect of ion dynamics and an oscillating electric field using a numerical simulation of ion motion, coupled with a numerical integration of the Schrödinger equation. For intense electric field calculations, we show how the dynamic fields transfer the intensity of the central part of the line to an increasing number of satellites at multiples of the plasma frequency.

## Atomic data and opacity calculations in niobium and silver ions for kilonova spectral analyses

**Sirine Ben Nasr<sup>1</sup>, Helena Carvajal Gallego<sup>1</sup>, Jérôme Deprince<sup>1</sup>, Patrick Palmeri<sup>1</sup>, Pascal Quinet<sup>1,2</sup>**

<sup>1</sup>*Atomic physics and Astrophysics, Mons university – UMONS, B-7000 Mons, Belgium*

<sup>2</sup>*Atomic physics and Astrophysics, Mons university IPNAS, Université de Liège, Sart Tilman, B-4000 Liège, Belgium – UMONS, B-7000 Mons, Belgium*

Neutron star (NS) mergers are at the origin of gravitational waves (GW) detected by LIGO/Virgo interferometers. Such events produce a large amount of elements heavier than iron by a rapid neutron capture (r-process) nucleosynthesis. Among these elements, those belonging to the fifth row of the periodic table, in particular from Zr ( $Z = 40$ ) and Cd ( $Z = 48$ ), are the greatest contributors to the opacity affecting the kilonovae, after the lanthanides and actinides. In the present work, new atomic structures and radiative parameters (wavelengths and oscillator strengths) are reported for a large number of spectral lines in two selected elements, namely Nb ( $Z = 41$ ) and Ag ( $Z = 47$ ) from neutral to triply ionized states. These results were obtained through large-scale atomic structure calculations using the pseudo-relativistic Hartree–Fock method implemented in Cowan code. The results obtained were used to calculate the expansion opacities characterizing the kilonova signal observed resulting from the collision of two NS, for typical conditions corresponding to time after the merger  $t = 1$  day, the temperature in the ejecta  $T \leq 15000$  K, and a density of  $\rho = 10^{-13}$  g.cm<sup>-3</sup>. Comparisons with previously published experimental and theoretical studies have shown a good agreement. In terms of quantity and quality, the results presented in this work are the most complete currently available, concerning the atomic data and monochromatic opacities for niobium and silver and are useful for astrophysicists to interpret kilonova spectra.

## Energy and angular distributions of electrons emitted in ion collisions with atomic and molecular targets

Alisher Kadyrov<sup>1</sup>

<sup>1</sup>*Curtin University, Australia*

A detailed understanding of the principles underlying ion-atom and ion-molecule collisions is essential for plasma modelling and diagnostics. Recent advances in experimental techniques have resulted in detailed and highly accurate kinematically complete measurements. However, theory lags far behind and cannot describe the experiments on differential ionisation. In particular, the description of experimental data on energy and angular distributions of electrons produced in intermediate-energy ion collisions with simple atomic and molecular targets has remained an insurmountable problem for over five decades. We have developed a coupled-channel method that provides the first accurate solution to the problem. The method is based on an expansion of the total scattering wave function using a two-centre pseudostate basis. This allows one to take into account all underlying interdependent processes, namely, direct scattering and ionisation, and electron capture into bound and continuum states of the projectile. Wave packets are used to discretise the continuous spectrum of the target and projectile. The method is applied to calculate the doubly differential cross section as a function of the energy and angle of electrons emitted in proton-induced ionisation of H, He and H<sub>2</sub>. Excellent agreement between the obtained results and the experimental data is found. This paves the way for an accurate description of the recent kinematically complete experiments.

## Modelling the evolution of X-ray free-electron-laser irradiated solids towards warm-dense-matter state

**Beata Ziaja-Motyka**<sup>1</sup>

<sup>1</sup>*Center for Free-Electron Laser Science CFEL, Deutsches Elektronen Synchrotron DESY, Germany*

Structural transitions in solids induced by intense femtosecond pulses from X-ray free-electron lasers are in the focus of this talk. Depending on the dose absorbed, the irradiation can trigger an ultrafast electronic or structural transition in these materials. For very high doses, transition from the solid to warm-dense-matter or to plasma state follows. Dedicated theoretical modeling tools reveal complex multistage evolution of the irradiated systems, confirmed by experimental measurements performed at X-ray free-electron-laser facilities. Challenges remaining for the modeling and possible further model developments are discussed.

## Radiation burn-through measurements to infer opacity at conditions close to the solar radiative zone-convective zone boundary

David Hoarty<sup>1</sup>, John Morton<sup>1</sup>, Jonathan Rougier<sup>1</sup>, Michael Rubery<sup>2</sup>, Damon Swatton<sup>1</sup>, Kyle McLean<sup>3</sup>, Robert Heeter<sup>2</sup>, Scott Richardson<sup>1</sup>, Steven Rose<sup>3</sup>, Ted Perry<sup>4</sup>, Yekaterina Opachich<sup>2</sup>, Bruce Remington<sup>2</sup>

<sup>1</sup>*Atomic Weapons Establishment, UK*

<sup>2</sup>*Lawrence Livermore National Laboratory, USA*

<sup>3</sup>*Imperial College London, UK*

<sup>4</sup>*Los Alamos National Laboratory, USA*

Recent measurements at the Sandia National Laboratory of the x-ray transmission of iron plasma much higher than predicted by theory have cast doubt on modelling of iron x-ray radiative opacity at conditions close to the solar convective zone-radiative zone boundary. An increased radiative opacity of the solar mixture, in particular iron, is a possible explanation for the disagreement in the position of the solar convection zone-radiative zone boundary as measured by helioseismology and predicted by modelling using the currently accepted elemental composition based on photosphere analysis. Here we present data from radiation burn-through experiments which do not support a large increase in the opacity of iron at conditions close to the base of the solar convection zone and provide a constraint on the possible values of both the mean opacity and the opacity in the x-ray range of the Sandia experiments.

## Laser-driven shock compression of Fe up to 250 GPa probed by X-ray absorption spectroscopy

Sofia Balugani<sup>1</sup>, Alessandra Ravasio<sup>2</sup>, Hugo Doyle<sup>3</sup>, Jean-Alexis Hernandez<sup>1</sup>, Nicolas Sevelin-Radiguet<sup>1</sup>, Daniel Eakins<sup>4</sup>, Olivier Mathon<sup>1</sup>, Raffaella Torchio<sup>1</sup>

<sup>1</sup>*European Synchrotron Radiation Facility, France*

<sup>2</sup>*Ecole Polytechnique de Paris, France*

<sup>3</sup>*First Light Fusion, UK*

<sup>4</sup>*Oxford University, UK*

Laser-driven shock compression coupled to brilliant X-rays probes opens new research opportunities in the field of matter at extreme conditions allowing to answer questions relevant for planetary science. At beamline ID24 at ESRF (Grenoble, France) a High-Power laser was coupled to time-resolved X-ray Absorption Spectroscopy (XAS)[1]. The unique advantage represented by coupling XAS together with a High-Power laser is the ability to microscopically probe a sample regardless its state. This because, XAS technique-besides being element selective- is sensitive to short-range order and to the electronic configuration. We present here the laser-driven shock compressed XAS data of iron collected at ID24 up to 250 GPa and 4000K along the Hugoniot curve and of liquid iron measured during the shock release, that means probing at later times after the shock was out of the Fe layer. We were able to locate our shocked Fe measurements on the phase diagram by anchoring the VISAR interferometer outputs to ESTHER hydrodynamic simulation code. The acquired XAS range was long enough to retrieve the first coordination shell radius and to so retrieve its volume. The laser energy upgrade foreseen in 2023, will allow to reach and microscopically probe WDM states and thus provide an experimental constrain to theoretical models.

### References

1. Sevelin-Radiguet, N., Torchio, R., Berruyer, G., Gonzalez, H., Pasternak, S., Perrin, F., Occelli, F., Pepin, C., Sollier, A., Kraus, D., Schuster, A., Voigt, K., Zhang, M., Amouretti, A., Boury, A., Fiquet, G., Guyot, F., Harmand, M., Borri, M., Groves, J., Helsby, W., Branly, S., Norby, J., Pascarelli, S. & Mathon, O. (2022). *J. Synchrotron Rad.* 29, 167-179.



## Electron collision studies on some molecules and molecular ions in plasmas

**Kalyan Chakrabarti<sup>1</sup>, Nilanjan Mukherjee<sup>1</sup>, Raju Ghosh<sup>2</sup>, Ioan F. Schneider<sup>3</sup>, Zsolt J. Mezei<sup>4</sup>, Jonathan Tennyson<sup>5</sup>,**

<sup>1</sup>*Department of Mathematics, Scottish Church College, Kolkata, India*

<sup>2</sup>*Department of Mathematics, Sukumar Sengupta Mahavidyalaya, Keshpur, India*

<sup>3</sup>*Université Le Havre Normandie, France*

<sup>4</sup>*Institute for Nuclear Research (ATOMKI), Hungary*

<sup>5</sup>*University College London, UK*

Electron collision processes with molecules and molecular ions play a very important role in plasmas. The collision processes lead to new species in the plasma and hence the cross sections (or equivalently, the rate coefficients) for these processes are necessary for modeling the plasma characteristics and to understand release of neutral atoms.

For several years we have been engaged in studying electron collision with molecules and molecular ions that are relevant in plasmas occurring in astrophysics, industry and fusion. Our studies, using the R-matrix method, have produced significant fundamental data on electron induced processes that can be used for plasma modeling and understanding release of neutral atoms by collision processes. In addition, these studies have also produced molecular data on bound states, neutral and anionic resonant states and corresponding resonance widths which are useful for initiating studies on many other electron induced processes such as dissociative recombination and dissociative electron attachment.

In this work we present our recent results on electron collision with the molecular ions  $\text{CH}_2^+$ ,  $\text{NH}^+$  [1,2] (relevant in fusion and astrophysics) and the neutral molecules BeO [3] and BeN [4] (both significant for fusion). We have provided cross sections for elastic collision, electronic excitation, electron impact dissociation and compared with experiments wherever available. Differential and momentum transfer cross sections are also provided when possible.

---

## References

1. K. Chakrabarti, J. Zs. Mezei, I. F. Schneider and J. Tennyson, *Electron collision studies on the  $CH_2^+$  molecular ion*, J. Phys. B: At. Mol. Opt. Phys. **55** (2022) 095201.
2. R. Ghosh, K. Chakrabarti and B. S. Choudhury, *Electron impact studies on the imidogen ( $NH^+$ ) molecular ion*, Plasma Sources Sci. Technol. **31** (2022) 065005.
3. N. Mukherjee and K. Chakrabarti, *Theoretical study of low energy electron collisions with the BeO molecule*, J. Phys. B:At. Mol. Opt. Phys. **56** (2023) 015202.
4. K. Chakrabarti and S. Dinda, *Calculated cross sections for electron collisions with the BeN molecule*, Plasma Phys. Control. Fusion (2023) **Submitted**

## **Updates on iron opacity measurements at solar interior temperature**

**Taisuke Nagayama**<sup>1</sup>

<sup>1</sup>*Sandia National Laboratories, USA*

Since solar abundance was renewed in 2005, solar models and helioseismology disagree. One hypothesis is that calculated iron opacity used in the solar model is underestimated. In 2015, we measured Fe opacity at solar interior temperatures using Z machine at Sandia National Laboratories and revealed significant disagreement with calculated opacities. If true, it can partially resolve the discrepancy, but the more-than-expected disagreement aroused a controversy in the community. Since then, we performed more than 20 experiments and refined the analysis methods to improve the accuracy of the result. We will present how the iron opacity and its uncertainty changed with the analysis refinements and the increased number of experiments and discuss its impact on the solar problem.

## **XRISM and atomic processes in plasmas**

**Timothy Kallman**<sup>1</sup>

<sup>1</sup>*NASA Goddard Space Flight Center, USA*

The X-ray Imaging and Spectroscopy Mission (XRISM) is a Collaborative Mission jointly developed by NASA and the Japanese Space Agency (JAXA), with the European Space Agency (ESA) participation. It will have Two instruments: Resolve: a soft X-ray (0.3–12 keV) spectrometer providing non-dispersive high-resolution X-ray spectroscopy; and Xtend: a 40 arcminute field of view soft X-ray imager. XRISM is scheduled to launch from Japan in May of 2023. The mission is to recover science lost with the demise of Hitomi in 2016. After a 9-month calibration and performance verification phase, the rest of the mission lifetime will be for General Observers worldwide. In this talk I will review the capabilities of XRISM, and some of the science goals for the observations to be carried out during the performance verification phase. I will highlight the fundamental atomic physics knowledge needed in order to interpret XRISM observational data, and also how this impacts the XRISM science.

## Exploring hyperfine structures of many-electron ions using laser spectroscopy

Naoki Kimura<sup>1</sup>, Priti<sup>2</sup>, Keigo Soutome<sup>3</sup>, Naoki Numadate<sup>4</sup>, Nobuyuki Nakamura<sup>3</sup>, Pipatpakorn Pativate<sup>3</sup>, Susumu Kuma<sup>1</sup>, Toshiyuki Azuma<sup>1</sup>, Yasutaka Kono<sup>3</sup>

<sup>1</sup>*Atomic, Molecular and Optical Physics Laboratory, RIKEN, Japan*

<sup>2</sup>*National Institute for Fusion Science, Gifu, Japan*

<sup>3</sup>*Institute for Laser Science, The University of Electro-Communications, Japan*

<sup>4</sup>*Komaba Institute for Science, The University of Tokyo*

The study of hyperfine structures in many-electron highly charged ions (HCIs) can provide a deeper understanding of strongly correlated electrons and serve as a benchmark for advanced theoretical calculations. Additionally, the possibility of using HCIs as atomic clock candidates emphasizes the importance of hyperfine structures in many-electron HCIs [1]. However, there has been limited progress in hyperfine spectroscopy of many-electron HCIs due to experimental challenges. We successfully performed hyperfine-structure resolved laser spectroscopy of HCIs in an electron beam ion trap plasma. In the meeting, we present the hyperfine structures in the  $4d^9 5s^1$  metastable states of Pd-like  $^{127}\text{I}^{7+}$  by laser-induced fluorescence (LIF) spectroscopy of magnetic-dipole (M1) transitions along with the detailed modeling and theoretical hyperfine structure calculations [2].

### References

1. Kozlov M et al 2018 Rev. Mod. Phys. 90 045005
2. Kimura, N., Priti, Kono, Y. et al. 2023 Commun Phys 6, 8.

## A self-consistent model of ionization potential depression of ions in hot and dense plasmas with local field correction

**Jianmin Yuan<sup>1</sup>, Jiaolong Zeng<sup>2</sup>**

<sup>1</sup>*Graduate School of China Academy of Engineering Physics*

<sup>2</sup>*College of Science, Zhejiang University of Technology, China*

We propose a consistent approach to determine the screening potential in dense plasmas with inhomogenous free electron micro-space distribution. Based on a local density and temperature-dependent ion-sphere model, the Saha equation approach is extended to the regime of strongly coupled plasmas by taking the free-electron-ion interaction, free-free-electron-interaction, inhomogenous free-electron micro-space distribution, and free-electron quantum partial degeneracy into account, in the free energy calculation. The ionization balance is determined by solving an extended Saha equation. All the quantities, including the bound orbitals with ionization potential depression, free-electron distribution, and bound and free-electron partition function contributions, are calculated self-consistently in the theoretical formalism. It has been shown that the ionization equilibrium is evidently modified by considering the above non-ideal characteristics of the free electrons [1].

To explicitly taking the exchange-correlation effect of free electrons into account, we incorporate the effective static approximation of local field correction (LFC) within our IPD framework through the connection of dynamical structure factor. The effective static approximation poses an accurate description for the asymptotic large wave number behavior with the recently developed machine learning representation of static LFC induced from the path-integral Monte Carlo data. Our calculation shows that the introduction of static LFC through dynamical structure factor brings a nontrivial influence on IPD at warm/hot dense matter conditions. The correlation effect within static LFC could provide up to 20% correction to free-electron contribution of IPD in the strong coupling and degeneracy regime. Furthermore, a new screening factor is obtained from the inhomogenous density distribution of free electrons calculated within the self-consistent model, with which excellent agreements are observed with other methods and experiments at warm/hot dense matter conditions[2].

---

## References

1. Jiaolong Zeng, Yongjun Li, Yong Hou, and Jianmin Yuan, Non-ideal effect of free electrons on ionization equilibrium and radiative properties in dense plasmas. *Phys. Rev. E* to be published.
2. Xiaolei Zan, Chengliang Lin, Yong Hou, and Jianmin Yuan, Local field correction to ionization potential depression of ions in warm or hot dense matter. *Phys. Rev. E* 104, 025203 (2021).

## Atomic population kinetics for Particle in Cell

**Brian Edward Marré<sup>1</sup>, Axel Huebl<sup>2</sup>, Ulrich Schramm<sup>1</sup>, Michael Bussmann<sup>1</sup>,  
Thomas Kluge<sup>1</sup>, Thomas Cowan<sup>1</sup>, René Widera<sup>1</sup>, Sergei Bastrakov<sup>1</sup>**

<sup>1</sup>*Helmholtz Zentrum Dresden Rossendorf, Germany*

<sup>2</sup>*Lawrence Berkeley National Laboratory, USA*

Standard atomic physics models in PIC simulation either neglect excited states, predict atomic state population in post processing only, or assume quasi-thermal plasma conditions.

This is no longer sufficient for high-intensity short-pulse laser generated plasmas, due to their non-equilibrium, transient and non-thermal plasma conditions, which are now becoming accessible in XFEL experiments at HIBEF (EuropeanXFEL), SACLA (Japan) or at MEC(LCLS/SLAC).

To remedy this, we have developed a new extension for our PIC simulation framework PIconGPU to allow us to model atomic population kinetics in-situ in PIC-Simulations, in transient plasmas and without assuming any temperatures.

This extension is based on a reduced atomic state model, which is directly coupled to the existing PIC-simulation and for which the atomic rate equation is solved explicitly in time, depending on local interaction spectra and with feedback to the host simulation. This allows us to model de-/excitation and ionization of ions in transient plasma conditions, as typically encountered in laser accelerator plasmas.

This new approach to atomic physics modelling will be very useful in plasma emission prediction, plasma condition probing with XFELs and better understanding of isochoric heating processes, since all of these rely on an accurate prediction of atomic state populations inside transient plasmas.



---

## Simulation of Doppler-free spectra using the Collisional Radiative Model

**Joseph John Simons<sup>1</sup>, Motoshi Goto<sup>2</sup>**

<sup>1</sup>*Department of Fusion Science, The Graduate University for Advanced Studies, SO-KENDAI, Japan*

<sup>2</sup>*National Institute for Fusion Science, Japan*

Saturated absorption spectroscopy is a tool that can be used to suppress the Doppler broadening of observed atomic and molecular transition lines in order to measure their precise wavelengths. Obtaining a saturated absorption condition by laser excitation is an essential technique for use in saturated absorption spectroscopy. We are introducing the laser excitation process into the collisional radiative model of hydrogen atoms to uncover how much saturation can be achieved under realistic plasma conditions and laser power density. Results show that the simulated spectra were able to successfully model Lamb dips and peaks utilizing this method, with the simulated plasma and laser parameters showing good agreement with the ones used in the experiment. This model has additionally helped to give further insight into how plasma parameters can affect the spectral characteristics of Lamb dips and peaks by noting the dependence of the simulated spectral saturation on these parameters.

## Plasma technology to mitigate climate crisis: Usefulness of OES as processes optimization

Marquidia Josseline Pacheco Pacheco<sup>1</sup>, Joel Pacheco Sotelo<sup>1</sup>, Ricardo Valdivia Barrientos<sup>1</sup>

<sup>1</sup>*Instituto Nacional de Investigaciones Nucleares, Mexico*

Plasma technologies are a promising route in a wide range of applications concerning negative impacts of climate crisis (e.g. stress conditions on seeds inhibiting germination or normal growth of plants, epidemic proliferation) and even, for the conversion of greenhouse gases (GHG) into energetic gases.

In this work, an overview of plasma technologies currently applied to ameliorate our environment would be depicted; followed by projects developed at our Laboratory where optical emission spectroscopy (OES) resulted in an useful tool to better understand and optimize these techniques. Specifically, rotational and electronic temperatures and key chemical species (e.g.  $O^{\bullet}$ ,  $O(^1D)$ ,  $\bullet OH$ ,  $e^-$ ) are here described.

Particularly, four affordable and green plasma applications would be depicted: the use of non-thermal plasma to improve the germination and growth of endangered Mexican maize specie, the deactivation of virus type, the synthesis of carbon nanoparticles with thermal plasmas to construct environmental friendly supercapatteries and, finally, the treatment of toxic gases and the conversion of GHG into syngas.

---

## Using K-shell S line ratios to measure the plasma temperature in a transient FeS plasma

**Joseph Nilsen<sup>1</sup>, Alejandro MesaDame<sup>1</sup>, Francisco Rilloraza<sup>1</sup>, Madison Martin<sup>1</sup>,  
Richard London<sup>1</sup>**

<sup>1</sup>*Lawrence Livermore National Laboratory, USA*

This talk describes how the steady state atomic kinetics approximation can underestimate the electron temperature determined from K-shell lines in ps-time-scale transient plasmas. In particular we model the inferred temperature evolution of solid FeS targets used in opacity experiments at the Orion laser facility determined from the ratio of the sulfur He-alpha to Ly-alpha lines. Initially we model the constant density steady state scenario and then expand this to include the time dependent density effects. The Orion experiments use short-pulse lasers to heat a thin microdot of FeS buried in a plastic target to temperatures of more than 1 keV and densities of approximately  $1 - 2 \text{ g/cm}^3$  after the FeS quickly equilibrates with the density of plastic. Using atomic kinetics calculations based on the temperature and density history from a radiation hydrodynamic simulation of the target evolution, we show how the peak temperature inferred from the sulfur line ratios is both lower and temporally lags the input temperature history. We then discuss how opacity effects impact the analysis and consider whether other materials may be optimal temperature diagnostic for different temperature ranges.

## Evaluation of extreme ultraviolet spectral models for mid-charged tungsten ions with LHD experiments

Izumi Murakami<sup>1</sup>, Akira Sasaki<sup>2</sup>, Daiji Kato<sup>1</sup>, Hiroyuki A. Sakaue<sup>1</sup>, Motoshi Goto<sup>1</sup>, Tetsutarou Oishi<sup>3</sup>, Tomoko Kawate<sup>1</sup>, Yasuko Kawamoto<sup>1</sup>

<sup>1</sup>*National Institute for Fusion Science, Japan*

<sup>2</sup>*National Institute for Quantum Science and Technology, Japan*

<sup>3</sup>*Tohoku University, Japan*

The behavior of tungsten impurity in fusion plasmas is one of the important issues to be studied to achieve high-temperature plasmas for fusion reactions since tungsten used as plasma-facing material is sputtered by plasma particles and is expected to reduce electron temperature due to large radiation power. Many studies have been done to examine atomic properties and spectral models for tungsten ions, however, tungsten ions with 4f open subshells are not well studied yet due to the complexity of the atomic structure. Extreme ultraviolet (EUV) spectra of tungsten ions have been measured in various fusion devices and electron beam ion traps (e.g. [1,2]), and examined by comparison of theoretically calculated spectra by collisional-radiative (CR) models (e.g. [3,4]). The unresolved transition array (UTA) measured at 4.5–7 nm wavelength region for plasma with electron temperature  $\sim 1$  keV is produced by numerous overlapped 4d-4f and 4p-4d transitions of tungsten ions. The wide two-peak feature of the UTA profile is not fully understood yet, even though recombination processes are included in the CR models [4,5] for  $W^{q+}$  with  $q = 25 - 39$ . On the other hand, the peaks measured at 2-4nm are well understood and are produced by many  $n = 4 - 5$  and  $n = 4 - 6$  transitions of  $W^{q+}$  with  $q = 22 - 30$ . They are useful to estimate charge state distributions [4,5]. For ions with  $q < 22$ , no peaks are found in this region and we need some identifier for such lower charged ions. We extend our study to EUV spectra at 10–30 nm where  $n = 5 - 5$  transitions are found for mid-charged tungsten ions by CR model calculations. We have performed plasma experiments to measure tungsten spectra by pellet injection with Large Helical Device (LHD) for wide wavelength regions. Measured spectra at 10-30 nm can be used to evaluate calculated spectra by CR models for mid-charged tungsten ions. Details of the comparison will be presented at the conference.

### References

1. R. Neu et al., Plasma Phys. Control. Fusion 38, A165 (1996)
2. H. A. Sakaue et al., AIP Conf. Proc. 1438, 91 (2012)
3. T. Putterich, R. Neu, R. Dux et al., Plasma Phys. Control. Fusion 50, 085016. (2008)
4. I. Murakami, H. A. Sakaue, C. Suzuki et al., Nucl. Fusion 55, 093016 (2015)
5. I. Murakami, D. Kato, T. Oishi et al., Nucl. Mater. Energy 26, 100923 (2021)

## Simple explanation for the observed power law distribution of line intensity in complex many-electron atoms and heavy nuclei

**Keisuke Fujii<sup>1</sup>, Julian Berengut<sup>2</sup>**

<sup>1</sup>*Oak Ridge National Laboratory, USA*

<sup>2</sup>*School of Physics, University of New South Wales, Australia*

It has long been observed that the number of weak lines from many-electron atoms follows a power law distribution of intensity. While computer simulations have reproduced this dependence, its origin has not yet been clarified. Here we report that the combination of two statistical models—an exponential increase in the level density of many-electron atoms and local thermal equilibrium of the excited state population—produces a surprisingly simple analytical explanation for this power law dependence. We find that the exponent of the power law is proportional to the electron temperature. This dependence may provide a useful diagnostic tool to extract the temperature of plasmas of complex atoms without the need to assign lines.

Because of the generality of this statistical model, a similar principle may apply to other quantum complex system. Indeed, we find for the first time that the gamma-ray emission from heavy nuclei also satisfy a similar power-law intensity distribution. For the nuclei, the power-law exponent is always unity and the intensity parameter of the distribution is independent from nuclear property. We confirm these properties from the experimental results registered in a nuclear database.

---

## Expanded application of the Linear Response Method

**Howard Scott<sup>1</sup>, Hai Le<sup>1</sup>**

<sup>1</sup>*Lawrence Livermore National Laboratory, USA*

The Linear Response Method (LRM) uses tabulated data obtained with a small number of radiation fields to replace inline steady-state non-local thermodynamic equilibrium (NLTE) collisional-radiative calculations for (nearly) arbitrary radiation fields. The tabulated data includes first-order derivatives with respect to the frequency-dependent radiation, i.e. linear response coefficients. Straightforward application of the LRM provides radiative properties and equation-of-state information as a function of plasma conditions and radiation field as required for radiation-hydrodynamics calculations. This approach has successfully been used in simulations of inertial confinement fusion hohlraums and other high energy density applications.

The response coefficients themselves contain information which can improve simulations in other ways. One approach provides a simple quantitative measure of how far a given set of conditions is from LTE. This allows a code to transition between LTE and NLTE data and numerical treatments at the most appropriate time. A more far-reaching improvement comes from integrating the response coefficients into radiation transport calculations, making them implicit and consistent with both the material temperature and the radiation field. We discuss these improvements and their implementations.

### Acknowledgements

This work performed under the auspices of U.S. Department of Energy by Lawrence Livermore National Laboratory under Contract DE-AC52-07NA27344.

## Overview of Doppler shift spectroscopy diagnostics technique used in neutral beam injectors: challenges and limitations

P Bharathi Magesh<sup>1</sup>, Arnab Deka<sup>2</sup>, Arun Chakraborty<sup>1</sup>, Bhargav Choksi<sup>1</sup>, Kaushal Pandya<sup>1</sup>, Mahendrajit Singh<sup>3</sup>, Mainak Bandhopadhyay<sup>1</sup>, Manas Bhuyan<sup>3</sup>, V. Prahlad<sup>1</sup>, Sanjeev Sharma<sup>1</sup>, Ujjwal Baruah<sup>3</sup>

<sup>1</sup>*Institute for Plasma Research, Ahmedabad, India*

<sup>2</sup>*Homi Bhabha National Institute (HBNI), Mumbai, India*

<sup>3</sup>*ITER-India, Institute For Plasma Research*

The Doppler Shift Spectroscopy (DSS) diagnostics, since its inception as a diagnostics technique in Neutral Beam Injectors (NBI), has proved to be an indispensable tool for characterizing positive and negative ion beams and optimising the ion sources performance [1-2]. For positive ion beams, beam parameters such as beam energy, beam species mix, beam impurity fractions, beam divergence and injected power fraction are routinely estimated using this technique [3-5]. In case of negative ion beams, this technique is primarily used to assess the beam inhomogeneity and beam stripping fractions which are very important parameters for understanding the negative ion source performance [2,6].

In positive ion beams, the ion source plasma discharge contains multi specie ions:  $H^+$ ,  $H_2^+$  and  $H_3^+$  which are accelerated to the same energy ( $E$ ) during extraction of beam. During neutralization phase, they undergo variety of collisions such as charge exchange, dissociative charge exchange, dissociative ionization etc with the background  $H_2$  gas to form positive, neutral and negative ion species at different energies. Some of these species are also be formed in excited state, whose emissions are recorded and analysed in this technique. The beam or ion species mix is usually obtained from the ratios of the observed intensities corresponding to each energy group of excited neutrals which are correlated to various production processes via an extensive emission model. Similar technique are also used for DSS analysis of negative ion beams for the applications mentioned above. It may be noted that the present modelling efforts consider the uncertainties related to the available measured cross section database for both positive and fast negative ion beams.

Further in both positive and negative ion beams, the beam divergence is estimated using a rigorous line profile analysis [1,6-7]. In our recent study, it is observed that the conventional deconvolution techniques when applied to a low divergent large focal length beams (e.g. ITER-HNB/DNB, JET NBI etc.) yielded errors larger than 30%. A novel line profile method has been developed to account for such errors.

In this presentation, the details of a comprehensive collisional radiative modelling applicable to positive and negative ion beams and the line profile method developed for

---

estimating divergence of low divergent large focal length beams are presented and discussed. The challenges and limitations of this technique are highlighted.

## References

1. W. F. Burrell C F, Cooper W S, Steele, “Doppler Shift Spectroscopy of powerful neutral beams”, Rev. Sci. Instrum, 51, 1451 (1980).
2. G Serianni, P Agostinetti, M Agostini, V Antoni, D Aprile, C Baltador, et al, New Journal of Physics 19, 045003,2017.
3. R. Uhlemann, R. S. Hemsworth, G. Wang, and H. Euringer, Rev. Sci. Instrum., 64, 974, 1993.
4. P. Bharathi and V. Prahlad, J. Appl. Phys., 107, 1, 2010.
5. P. Bharathi, A.J. Deka, M. Bandyopadhyay, M. Bhuyan et al , Nuclear Fusion, 60, 046008,2020.
6. A. J. Deka, P. Bharathi, K. Pandya, M. Bandyopadhyay, M. Bhuyan et al , J. Appl. Phys., 43307, 123, 2018.
7. A. J. Deka, P. Bharathi, M. Bandyopadhyay, M. J. Singh, and A. K. Chakraborty, Fusion Eng. Des., 161, 112005, 2020.



## Production of singly charged Sn ions by charge exchange in H<sub>2</sub> gas

**Luc Assink<sup>1,2</sup>, Klaas Bijlsma<sup>1,2</sup>, Lucas Poirier<sup>2,3</sup>, Emiel de Wit<sup>1</sup>, Subam Rai<sup>1,2</sup>, Ismanuel Rabadán<sup>4</sup>, Luis Méndez<sup>4</sup>, John Sheil<sup>2,3</sup>, Oscar Versolato<sup>2,3</sup>, Ronnie Hoekstra<sup>1,2</sup>**

<sup>1</sup>*Zernike Institute for Advanced Materials, University of Groningen, Groningen, The Netherlands*

<sup>2</sup>*Advanced Research Center for Nanolithography (ARCNL), Amsterdam, The Netherlands*

<sup>3</sup>*Department of Physics and Astronomy, and LaserLaB, Vrije Universiteit, Amsterdam, The Netherlands*

<sup>4</sup>*Laboratorio Asociado al CIEMAT de Física Atómica y Molecular en Plasmas de Fusión, Departamento de Química, Universidad Autónoma de Madrid, Madrid, Spain*

The evolution of charge-state-resolved kinetic energy spectra of Sn ions ejected from a laser-produced plasma (LPP) of Sn as a function of the density of the H<sub>2</sub> buffer gas surrounding the LPP is investigated. Without a H<sub>2</sub> buffer gas, energetic 1 - 5 keV Sn ions in charge states of 4+ up to 8+ are detected. In this keV regime, lower Sn charge states, i.e., below 4+ are absent. When H<sub>2</sub> is introduced into the system, low-charged energetic Sn ions can be produced by a series of consecutive electron capture processes. However, as electron capture by Sn<sup>2+</sup> ions from H<sub>2</sub> is endothermic, no significant population of singly charged Sn ions is expected in the keV regime. At H<sub>2</sub> pressures of 6x10<sup>-4</sup> mbar and higher, however, we only detect Sn<sup>2+</sup> and Sn<sup>+</sup> ions.

To explain the production of keV Sn<sup>+</sup> ions, electron capture by metastable Sn<sup>2+\*</sup> ions has been proposed [1]. Semi-classical calculations on Sn<sup>3+</sup>- H<sub>2</sub> collisions [2] indicate that one-electron capture by Sn<sup>3+</sup> ions populates Sn<sup>2+</sup> ions in metastable states. Model simulations (using theoretical 2-state Landau-Zener cross sections to account for capture by each of the three metastable <sup>3</sup>P<sub>J</sub> levels) to track the charge states of Sn ions while traversing the H<sub>2</sub> gas agree with our measured data. This underpins the key role of metastable Sn<sup>2+\*</sup> ions as a gateway to the production of Sn<sup>+</sup> ions. From an LPP-based EUV source perspective, the production of energetic Sn<sup>+</sup> ions in the buffer gas is of high relevance, as it shifts the charge state balance from Sn<sup>2+</sup> towards Sn<sup>+</sup> ions, which have a larger stopping cross section than Sn<sup>2+</sup> ions [3].

---

## References

1. Rai et al., 2023 to appear in Plasma Sources Sci. Techn.
2. Rai et al., 2022, Phys. Rev. A. **106**, 012804
3. Abramenko et al., 2018, Appl. Phys. Lett. **112**, 164102

## Improved uncertainty modeling for the helium collisional-radiative model used for line-ratio spectroscopy on Wendelstein 7-X

**Erik Flom<sup>1</sup>, Tullio Barbui<sup>2</sup>, Oliver Schmitz<sup>1</sup>, Allison Harris<sup>3</sup>, Ralf Koenig<sup>4</sup>, Sehyun Kwak<sup>4</sup>, Jakob Svensson<sup>4</sup>, Stuart Loch<sup>5</sup>**

<sup>1</sup>*University of Wisconsin-Madison, USA*

<sup>2</sup>*Princeton Plasma Physics Laboratory, USA*

<sup>3</sup>*Illinois State University, USA*

<sup>4</sup>*IPP-Greifswald, Germany*

<sup>5</sup>*Auburn University, USA*

Understanding the basic plasma parameters of temperature and density, as well as their gradients in the scrape-off layer (SOL), is a topic critical for providing information about the performance of a divertor concept. The stellarator Wendelstein 7-X features a novel resonant island divertor with an adjustable rotational transform of  $\iota = 2\pi(5/6, \dots, 5/4)$ . In order to study the performance of this divertor concept, an active spectroscopy system on a thermal helium beam [1] was developed and installed on the device [2]. The system consists of four identical Czerny-Turner spectrometers imaging two stellarator-symmetric upper and lower divertor modules, allowing for tomographic reconstruction of impurity radiation in the island divertor region. The helium beam diagnostic operates using the technique of line ratio spectroscopy, applying a collisional-radiative model (CRM) to relate the observed line radiation to the underlying plasma parameters [3]. Despite successful operation during previous experiments, there have been systematic disagreements observed between the helium beam and other edge diagnostics. In order to investigate the uncertainties of the helium beam diagnostic and the vulnerabilities of the underlying atomic data set, a complete Bayesian treatment has been undertaken with the Minerva Bayesian modeling framework [4]. First, it has been shown through a sensitivity study that the diagnostic method is robust against random measurement errors and systematic calibration errors on the scales achievable with the current diagnostic setup. From this, it is concluded that the majority of the uncertainty in the reconstructed temperature and density arises from systematic uncertainties in the underlying CRM rather than from measurement errors, and that a narrow subset of these processes is disproportionately responsible for plasma profile reconstruction uncertainties [5]. A new R-matrix data set for helium has been calculated and its differences from previous data sets will be discussed, as well as the implications on plasma parameter reconstructions. Finally, corrections for finite magnetic field effects are discussed and the relevant regimes for neglecting these effects are shown.

---

## References

1. B. Schweer, et al., *J. Nucl. Mater.* 196–198 174–8
2. T. Barbui, et al. *Nuclear Fusion* 60.10 (2020): 106014
3. J. M. Muñoz Burgos et al. 2012 *Phys. Plasmas* 19 012501
4. Svensson, J., and A. Werner 2007 *IEEE*, 2007.
5. Flom, E. et al. *Nuclear Mat. & Eng.* 2023.

## Acknowledgements

This work was funded in part by the U.S. Department of Energy under grant DE-SC00014210 and DE-SC00013911. This work has been carried out within the framework of the EUROfusion Consortium, funded by the European Union via the Euratom Research and Training Programme (Grant Agreement No 101052200 — EUROfusion). Views and opinions expressed are however those of the author(s) only and do not necessarily reflect those of the European Union or the European Commission. Neither the European Union nor the European Commission can be held responsible for them.

## An LCIF diagnostic to test fusion relevant atomic data in RAID

**Christine Stollberg<sup>1</sup>, Ivo Furno<sup>2</sup>, Lyes Kadi<sup>2</sup>, Marcelo Baquero-Ruiz<sup>2</sup>, Philippe Guittienne<sup>2</sup>, Renat Karimov<sup>2</sup>, Rémy Jacquier<sup>2</sup>**

<sup>1</sup>*École Polytechnique Fédérale de Lausanne (EPFL), Switzerland*

<sup>2</sup>*EPFL - Swiss Plasma Center*

Collisional cross sections and collisional-radiative (CR) models are of utmost importance for plasma diagnostics in the entire community, from low-temperature atmospheric pressure plasmas and fusion applications to astrophysical studies. Large efforts have been undertaken to provide collisional data by experiments, simulations, and analytic calculations. However, the validation of collisional data and CR models is very challenging and requires high-quality spectroscopic measurements and complex data analysis methods [1-2]. Here, we present our effort to validate collisional data relevant for fusion applications by modeling the results of fast spectroscopic diagnostics in a highly reproducible plasma experiment.

The Resonant Antenna Ion Device (RAID) [3], operated at EPFL, Switzerland, is a linear plasma device that produces a steady-state Helicon discharge, sustaining electron densities  $n_e$  of few  $10^{17}$  to  $10^{19}$   $\text{m}^{-3}$  and temperatures  $T_e$  of 1 to 10 eV in hydrogen (deuterium), helium, and argon. The plasma is highly reproducible and well diagnosed by means of Langmuir (LP) and B-dot probes, as well as optical emission spectroscopy (OES), Thomson scattering (TS), laser induced fluorescence (LIF), and two photon absorption LIF (TaLIF).

A Laser Collisional Induced Fluorescence (LCIF) diagnostic in helium plasmas [4] that enables simultaneous monitoring of various ( $> 10$ ) optical transitions ( $n = 3$  and  $4 \rightarrow n = 2$ ), was recently developed at RAID [5]. The local pumping of the  $1s3s$   $1D$  level hereby minimizes the effect of integration along the line of sight. In the future, we suggest to utilize a tunable ps-laser pulse (28 ps, 193 nm to 2300 nm) which will allow us to pump different He levels with high temporal resolution. An absolute calibration of the detection system can directly yield the (combined direct and cascade) apparent population rate of the probed levels (except  $1P$ ) resulting from the pumping process, while the measurement of the fluorescence life time enables quantitative inference about the opacity of the plasma and the (collisional) quenching in various plasma conditions. Comparison of the experimental results with predictions from a CR model allows understanding the role of complex (de)population processes like opacity. Ultimately, we intend to develop a method that allows simultaneous fitting of the experimental spectra obtained from different pumping schemes, while varying the reaction rates for the dominant collision processes by using a probabilistic approach based on Bayesian data analysis, similar to [1-2]. With the extensive spectral data sets provided by the LCIF diagnostics and the independently obtained plasma parameters from TS and LIF, we will push this analysis

---

to a level that will enable us to put experimental constraints on the collisional cross sections for helium to improve present-day plasma diagnostics in the fusion community.

## References

1. D. Dodt et al., 2010 *New J. Phys.* 12, 073018
2. E. Flom et al., 2022 *Nuclear Materials and Energy* 33, 101269
3. I. Furno et al., 2017 *EPJ Web Conf.* 157, 03014
4. E V Barnat and K Frederickson, 2010 *Plasma Sources Sci. Technol.* 19, 055015
5. M. Baquero-Ruiz et al., 25th Europhysics Conference on the Atomic and Molecular Physics of Ionized Gases (ESCAMPIG), 2022

## Acknowledgements

This work was partially supported by the Swiss National Fund grant No 200020\_204983.

## Estimation of argon impurity transport in Aditya-U Ohmic discharges using Be-like, B-like and Cl-like argon spectral line emissions

Kajal Shah<sup>1</sup>, Sharvil Patel<sup>2</sup>, Malay Chowdhuri<sup>3</sup>, Kumarpal Sinh Jadeja<sup>3</sup>, Gaurav Shukla<sup>4</sup>, Tanmay Macwan<sup>5</sup>, Ankit Kumar<sup>3</sup>, Suman Dolui<sup>3</sup>, Kaushlender Singh<sup>3</sup>, Rakesh Tanna<sup>3</sup>, Kaushal Patel<sup>3</sup>, Ritu Dey<sup>3</sup>, Ranjana Manchanda<sup>3</sup>, Nilam Ramaiya<sup>3</sup>, Rohit Kumar<sup>3</sup>, Suman Aich<sup>3</sup>, Nandini Yadava<sup>6</sup>, Shishir Purohit<sup>3</sup>, Manoj Kumar Gupta<sup>3</sup>, Umesh Nagora<sup>3</sup>, Suryakumar Pathak<sup>3</sup>, Praveen Atrey<sup>3</sup>, Balamurali Krishna Mayya Kolake<sup>2</sup>, Joydeep Ghosh<sup>3</sup>

<sup>1</sup>*Pandit Deendayal Petroleum University, India*

<sup>2</sup>*Pandit Deendayal Energy University, India*

<sup>3</sup>*Institute for Plasma Research, India*

<sup>4</sup>*ITER-India, Institute for Plasma Research*

<sup>5</sup>*University of California, Los Angeles, USA*

<sup>6</sup>*Nirma University, India*

Argon seeding in a tokamak has several benefits such as, achieving lower-H-mode thresholds [1, 2], reducing heatloads on plasma-peripherals through radiative power dissipation at the plasma boundary [3] etc. Trace argon is also injected for diagnostic purposes [4, 5]. Nonetheless, argon accumulation in the core and its high radiation through line and continuum emissions result in confinement degradation and fuel dilution and it is an important concern for the present and future tokamaks such as ITER [3]. Therefore, it is important to understand argon impurity dynamics in fusion plasmas thereby controlling argon concentration and accumulation inside the plasma column.

Vacuum Ultraviolet (VUV) and visible line emissions from partially ionized argon impurity ions are simultaneously observed in the Aditya-U [6] ohmically heated plasma with trace argon impurity injection ( $\approx 1017$  particles) during the current flat top phase of the discharge. These line emissions, observed using absolutely calibrated high resolution visible and VUV spectrometer systems are used to understand argon impurity dynamics in the plasma [7]. Argon transport coefficients (diffusivity and convective velocity) are calculated from the integrated use of these two spectroscopic diagnostics and the 1D impurity transport code STRAHL.

During the experiments, space resolved visible line emissions of Cl-like argon ions and line integrated VUV line emissions from Be-like and B-like argon ions have been observed. The  $\text{Ar}^+$  line emissions in the visible range at 472.68 nm ( $3p^4 4s^2 P_{3/2} - 3p^4 4p^2 D_{3/2}$ ), 473.59 nm ( $3p^4 4s^4 P_{5/2} - 3p^4 4p^4 P_{3/2}$ ), 476.48 nm ( $3p^4 4s^2 P_{1/2} - 3p^4 4p^2 P_{3/2}$ ), 480.60 nm ( $3p^4 4s^4 P_{2/5} - 3p^4 4p^4 P_{2/5}$ ) and VUV emissions of  $\text{Ar}^{13+}$  at 18.79 nm ( $2s^2 2p^2 P_{3/2} - 2s 2p^2 P_{3/2}$ ) and  $\text{Ar}^{14+}$  at 22.11 nm ( $2s^{21} S_0 - 2s 2p^1 P_1$ ) are identified using NIST database. From the experiments, radial emissivity profile of  $\text{Ar}^+$  spectral emission and brightness

---

ratio of  $\text{Ar}^{13+}$  and  $\text{Ar}^{14+}$  ions have been calculated simultaneously. In order to estimate the argon impurity transport coefficients, the experimental emissivity profile and brightness ratio need to be simultaneously compared with those simulated using the impurity transport code, STRAHL. Since the photon emissivity coefficients (PEC), required to obtain the emissivity profiles of the observed transitions, are not directly available, they have been generated using NIST and ADAS databases. For all the observed transitions of  $\text{Ar}^+$ ,  $\text{Ar}^{13+}$  and  $\text{Ar}^{14+}$  ions used in the study the appropriate fundamental data related to electron impact excitation rate coefficients are obtained from the ADAS database, by properly matching the energy levels between NIST and ADAS database. These data were then used in ADAS generalised collisional-radiative (GCR) data production routine which provided the required PECs for the range of electron density and temperature. The calculated PECs were then used in STRAHL code to simulate the emissivity profile of  $\text{Ar}^+$  spectral emission and brightness ratio of  $\text{Ar}^{13+}$  and  $\text{Ar}^{14+}$  ions and compared with experimental values to estimate argon transport coefficients. Argon diffusivity  $\approx 12 \text{ m}^2/\text{s}$  in the edge ( $\rho_i 0.85$ ) and  $\approx 0.3 \text{ m}^2/\text{s}$  in the core region have been observed. The diffusivity values in the edge and core are found to be higher than the neo-classical values, which suggests that the argon transport is mainly anomalous in the Aditya-U tokamak. Moreover, it has been observed that an inward pinch of  $\approx 10 \text{ m/s}$  is required to match the experimental and simulated data. The measured peaked profile of total argon density suggests impurity accumulation in these discharges. The detailed results on experimental measurements, calculation of PEC profiles and argon transport coefficients will be discussed in the paper.

## References

1. Ongena J., et al 2001 Plasma Phys. Control. Fusion 43, A11.
2. Reinke M. L. et al 2011 Journal of Nuclear Materials 415, S340–S344.
3. I. Ivanova-Stanik et al 2016 Fusion Eng. Des. 109-111, 342.
4. Hong J. et al 2015 Nucl. Fusion 55 063016.
5. Krupin V. A. et al 2018 Plasma Phys. Control. Fusion 60 115003.
6. Tanna R. L. et al 2022 Nucl. Fusion 62 042017.
7. Shah K. et al 2021 Rev. Sci. Instrum. 92, 053548.



## First laboratory measurement of magnetic-field-induced transition effect in Fe X at different magnetic fields

Guoqin Xu<sup>1</sup>, Chenglong Yan<sup>1</sup>, Yang Yang<sup>1</sup>, Hui Tian<sup>2</sup>, Wenxian Li<sup>3</sup>, Xianyong Bai<sup>3</sup>

<sup>1</sup>*Fudan University, China*

<sup>2</sup>*Peking University, China*

<sup>3</sup>*National Astronomical Observatories, Chinese Academy of Sciences*

The magnetic field is extremely important for understanding the properties of the solar corona. However, there are still difficulties in the direct measurement of the coronal magnetic field. The magnetic-field-induced transition (MIT) in Fe X, appearing in coronal spectra, was discovered to have prospective applications in coronal magnetic field measurements. In this work, we obtained the extreme ultraviolet spectra of Fe X in the wavelength range of 174 – 267 Å in the Shanghai High-temperature Superconducting Electron Beam Ion Trap, and examined the effect of MIT in Fe X by measuring the line ratios between 257.262 Å and the reference line of 226.31 Å (257/226) at different magnetic field strengths for the first time. The electron density that may affect the 257/226 value was also obtained experimentally and verified by comparing the density-sensitive line ratio (175.266 Å/174.534 Å) measurements with the theoretical predictions, and there was good agreement between them. The energy separation between the two levels of  $3s^23p^43d^4 D_{5/2}$  and  $^4D_{7/2}$ , one of the most critical parameters for determining the MIT rate, was obtained by analyzing the simulated line ratios of 257/226 with the experimental values at the given electron densities and magnetic fields. Possible reasons that may have led to the difference between the obtained energy splitting and the recommended value in previous works are discussed. Magnetic field response curves for the 257/226 value were calculated and compared to the experimental results, which is necessary for future MIT diagnostics.

## A unified atomic description for high- $Z$ impurities modelling in tokamak plasmas

Yves Peysson<sup>1</sup>, Axel Jardin<sup>2</sup>, Didier Mazon<sup>3</sup>, Dominik Dworak<sup>2</sup>, Jakub Bielecki<sup>2</sup>, Jedrzej Walkowiak<sup>2</sup>, Marek Scholz<sup>2</sup>

<sup>1</sup>*CEA, France*

<sup>2</sup>*IFJ-PAN, France*

<sup>3</sup>*CEA Cadarache, France*

Most of the realistic kinetic calculations for tokamak plasmas require now to incorporate the effect of partially ionized high- $Z$  elements, arising either from uncontrolled influxes of metallic impurities like tungsten in high input power regimes or from mitigation by massive gas injection of runaway electrons generated after plasma disruptions [1,2]. The usual electron-ion Fokker-Planck collision operator must be therefore modified, according to the atomic physics, as well as the cross-sections for some synthetic diagnostics, like bremsstrahlung, whose importance for characterizing the plasma state is considerable [3]. This represents a challenge, in order to perform fast but also accurate calculations, regardless the types of elements present in the plasma and their local level of ionization, while covering a wide range of electron energies in a consistent way, from thermal to highly relativistic limits. In this context, a unified modelling of the atomic physics has been developed, based on a multi-Yukawa potential representation calibrated against advanced quantum relativistic calculations [4]. Besides the possibility of an accurate description of inner and outer atomic shells, it is possible to derive analytical formulations for elastic and inelastic scattering which can be easily incorporated in kinetic codes [3,5-7]. The impact of the number of exponentials in the description of the atomic potential is discussed, and compared with the Thomas-Fermi or Thomas-Fermi-like atomic models.

### References

1. V. Ostuni, et al., Nucl. Fusion, 62 (2022) 106034
2. L. Hesslow, et al., Phys. Rev. Letter, 118 (2017) 255001
3. Y. Peysson, et al., in proceedings of IAEA FEC 2020 - The 28th IAEA Fusion Energy Conference, 10-15 May 2021, Nice (E-Conference), France
4. F. Salvat, et al., Phys. Rev. A, 36(2) (1987) 467
5. X. Garbet, et al., J. Appl. Phys., 61 (1987) 907
6. J. Linhard and M. Scharff, Dan. Mat. Fys. Medd., 27(15) (1953)
7. J. Walkowiak, et al., Phys. Plasmas 29 (2022) 022501

---

## **Acknowledgements**

This work was partially funded by National Science Centre, Poland (NCN) grant HARMONIA 10 no. 2018/30/M/ST2/00799.

## Multiple photoionization for the $\text{Fe}^+$ $2p$ subshell

Aušra Kynienė<sup>1</sup>, Sigitas Kučas<sup>1</sup>, Šarūnas Masys<sup>1</sup>, Valdas Jonauskas<sup>1</sup>

<sup>1</sup>*Institute of Theoretical Physics and Astronomy, Vilnius University, Lithuania*

Photoionization plays a key role in the production of highly charged ions in active galactic nuclei (AGNs). The inner shell photoionization leads to highly excited states that are the subject of radiative and Auger cascade. An electron from a higher shell fills the inner-shell vacancy while simultaneously causing the removal of another electron from the atomic system during the Auger decay. As a result of the Auger cascade, the produced ions have higher charge states than the initial ion. However, the final ion population eventually stabilizes in states that are below the ionization threshold of the corresponding ion.

The aim of the current work is to study multiple photoionization of the  $2p$  subshell of the  $\text{Fe}^+$   $3d^64s$  configuration. The investigation of multiple photoionization for the iron atom and ions was the subject of our earlier work [1, 2], and this study represents a continuation of that research. The  $\text{Fe}^+$  ion is an important diagnostic tool for the study of AGNs. The  $\text{Fe}^+$  emission is thought to arise from gas in the broad line region. On the other hand, the higher ionization stages of Fe were observed in spectra from AGNs [3].

Multiple photoionization cross sections are studied for all 63 energy levels of the  $\text{Fe}^+$   $3d^64s$  configuration. The study also includes partial photoionization cross sections to the configurations of produced ions. The photoionization of the  $2p$  subshell of the  $\text{Fe}^+$   $3d^64s$  configuration leads to the autoionizing  $\text{Fe}^{2+}$   $2p^53d^64s$  configuration which has 360 energy levels.

Decay of the  $\text{Fe}^{2+}$   $2p^53d^64s$  configuration through a cascade of radiative and Auger transitions produces 9 final configurations which population exceeds 0.01%:  $\text{Fe}^{2+}$   $3d^54s$ ,  $\text{Fe}^{3+}$   $3d^5$ ,  $\text{Fe}^{3+}$   $3d^44s$ ,  $\text{Fe}^{4+}$   $3d^4$ ,  $\text{Fe}^{4+}$   $3d^34s$ ,  $\text{Fe}^{4+}$   $3p^53d^5$ ,  $\text{Fe}^{5+}$   $3d^3$ ,  $\text{Fe}^{5+}$   $3d^24s$ ,  $\text{Fe}^{5+}$   $3p^53d^4$ . The study of the cascade includes only electric dipole transitions. The produced configurations can lead to further decay through radiative transitions of higher multipoles.

The main populations of the cascade decay reside in states of the  $\text{Fe}^{4+}$  and  $\text{Fe}^{5+}$  ions. The yield of the  $\text{Fe}^{6+}$  ion is lower than 0.01% for all levels of the  $\text{Fe}^{2+}$   $2p^53d^64s$  configuration from which the cascade starts. It has to be noted that the largest ion yields depend on the level of the  $\text{Fe}^{2+}$   $2p^53d^64s$  configuration. The largest population of the  $\text{Fe}^{4+}$  ion amounts to  $\sim 72\%$  for the lowest level of the  $\text{Fe}^{2+}$   $2p^53d^64s$  configuration. The lowest ion yield of  $\sim 30\%$  corresponds to the highest levels of the initial configuration of the cascade. On the other hand, the largest population of  $\sim 57\%$  for the  $\text{Fe}^{5+}$  ion is produced from the level with index 160 while the lowest population of  $\sim 24\%$  is a result of cascade decay from the level with index 9. What is more, the yield of the  $\text{Fe}^{3+}$  ion varies from  $\sim 1.7\%$  (index 1) to  $\sim 24.6\%$  (index 137).

---

## References

1. S. Kučas *et al.*, *Astron. Astrophys.* **643**, A46 (2020).
2. S. Kučas *et al.*, *Astron. Astrophys.* **654**, A74 (2021).
3. F.C. Cerqueira-Campos *et al.*, *Mon. Not. R. Astron. Soc.* **500**, 2666 (2020).

## Light and metallic impurity identification in the 225 – 302 Å range from the SURVIE spectrometer in the WEST tokamak

Corinne Desgranges<sup>1</sup>, Rémy Guirlet<sup>1</sup>, Jean-Louis Schwob<sup>2</sup>, Nicolas Fedorczyk<sup>1</sup>, Olivier Peyrusse<sup>4</sup>, Pierre Manas<sup>1</sup>, Pierre Mandelbaum<sup>3</sup>, Yaakoub Boumendjel<sup>1</sup> and the WEST team<sup>\*</sup>

<sup>1</sup>CEA, IRFM, F-13108 Saint-Paul-lez-Durance, France

<sup>2</sup>Racah Institute of Physics, The Hebrew University, 91904 Jerusalem, Israel

<sup>3</sup>Azrieli College of Engineering, 91035 Jerusalem, Israel

<sup>4</sup>Aix-Marseille Université, CNRS, Laboratoire LP3, UMR7341, F-13288 Marseille, France

<sup>\*</sup><http://west.cea.fr/WESTteam>

The WEST tokamak aims at testing actively cooled solid W monoblock Plasma Facing Units mounted in shape of a flat crown forming the lower divertor. These tests aim at long plasma discharges, with thermal loads of the same order of magnitude as those expected for the ITER vertical part of the lower divertor (10 MW/m<sup>2</sup>). This solid W actively cooled lower divertor has been under test since December 2022. More than 60 seconds stable L-mode X-point plasma discharges have already been realised. The main gas used for WEST plasmas is deuterium. The plasma impurity content must be as low as possible because it dilutes the fuel and more importantly cools the plasma, decreasing its performances.

Two VUV spectrometers are used to characterise plasma contamination due to impurities coming from plasma facing components. One is equipped with two mobile detectors and dedicated to physics studies, the other one (called SURVIE) is a survey spectrometer equipped with a single fixed detector. Here the focus will be put on this latter spectrometer. Its spectral range is 225 – 302 Å. Its fixed line of sight crosses the plasma centre almost in the midplane

A thorough line identification of the VUV spectra has been performed since 2018 in various configurations : ohmic, with LHCD heating, with ICRH heating, with both LHCD and ICRH heating. These lines are identified mainly from the Kelly tables [1] and the NIST database [2].

At the start of the experimental campaigns, during ohmic phase, Chlorine (Cl XII to Cl XIV) as well as Oxygen (O IV), Titanium (Ti X, XVIII and XX), Nitrogen (N IV and V) and Boron (B V) lines dominate the spectra. Chlorine comes from a plastic plate which fell down behind a vacuum vessel protection panel and was never completely eliminated in the subsequent campaigns. The presence of Nitrogen and Titanium is due to a number of limiter tiles made of BN fixed to the limiter frame by titanium rings. When the plasma leans on these tiles, consequently B, N and Ti lines appear.

---

An ohmic plasma including a large Argon injection allowed identification of Argon lines (Ar XIII, XIV and XV).

Then during plasmas heated by LH power only, it is observed that Copper (Cu XIII, XVIII and XIX) is dominant and lines from W VII-VIII to W XLV appear and increase with LHCD power.

In the case of ICRH power alone, silver lines (Ag XVI, XVIII and XIX) appear and increase with ICRH power. Silver is due to the Silver coating of ICRH antennae front face.

The lower ionisation stages of impurities give indications on the plasma edge temperature and sources, the higher ones on the impurity content of plasma core. From these two types of information, impurity transport can be evaluated.

Furthermore this line identification helps on the one hand to determine the impurity production processes and consequently to adapt the plasma's magnetic equilibrium; on the other hand it helps to assess the plasma conditioning state and performance.

## References

1. R. L. Kelly, Journal of Physical and Chemical Reference Data Vol. 16 (1997) supplement N°1
2. <https://www.nist.gov/pml/atomic-spectra-database>

## Non-equilibrium dynamics during warm dense matter formation

**Byoung-Ick Cho**<sup>1</sup>

<sup>1</sup>*Gwangju Institute of Science and Technology, Republic of Korea*

The ultrafast absorption of laser energy in condensed matter results in strongly out-of-equilibrium material conditions, which evolve into warm dense matter (WDM). Understanding the fundamental processes of ultrafast energy relaxation and structural evolution in these extreme systems is crucial for a wide range of fields, from laser nano-surgery to laser-fusion research.

The generally accepted concept for the response of systems irradiated by femtosecond laser pulses is that the optical pulse directly excites electrons, which quickly thermalize, establishing a finite electronic temperature in a few tens of femtoseconds, while the lattice remains cold. The two subsystems then equilibrate through electron-phonon coupling, which is the basic premise of the two-temperature model (TTM). This framework has been widely applied to calculate optical and thermophysical properties of laser-irradiated matter, develop advanced models for thermal and nonthermal melting, and interpret data from various experiments. However, the electronic system's detailed dynamics might be more complex than described by the simple TTM.

This contribution presents measurements of XFEL absorption of WDCu, and the optical reflectivity of WDAu irradiated with femtosecond laser pulses. The measurements for the WD noble metals ( $\approx 1$  eV/atom) reveal the rich dynamical features of nonthermal electrons and vacancies and their interactions with the lattice. The improved modeling of electron dynamics, which includes the recombination of nonthermal electrons and the dynamic shift of the excited valence band, successfully reproduces the key features observed in the measurements. These findings shed light on improving our understanding of the ultrafast population balance between conduction and localized electrons in materials and related transport properties under extreme temperature and pressure conditions.

### Acknowledgements

This work received support from the National Research Foundation of Korea (NRF2019R1A2C2002864, NRF-2020K1A3A7A09080397).



## Integrated reflectivity inferred from crystal response measurement for several NIF X-ray spectrometers

Maylis Dozières<sup>1</sup>, Christine Krauland<sup>1</sup>, Jeremy Huckins<sup>2</sup>, John Seely<sup>3</sup>, Joshua Tabimina<sup>2</sup>, Mai Beach<sup>2</sup>, Marilyn B. Schneider<sup>2</sup>, Nathaniel Thompson<sup>2</sup>, Stanislav Stoupin<sup>2</sup>

<sup>1</sup>*General Atomics, USA*

<sup>2</sup>*Lawrence Livermore National Laboratory, USA*

<sup>3</sup>*Syntek Technologies Inc., USA*

The spectrometer calibration station at LLNL is used to characterize and calibrate the many crystals used in the various geometries of the x-ray spectrometers regularly used at the National Ignition Facility (NIF). Such absolute calibration is essential for every experiment in order to extract meaningful results and properly diagnose the plasmas. We present the calibration of three NIF spectrometers, the Imaging Spectroscopy Snout (ISS) used at magnification of 12X, its homologue dedicated to low magnification (ISS-LM) and the NIF X-ray Spectrometer (NXS).

The ISS can be equipped with up to four different transmission Quartz crystals in Cauchois geometry, each offering different energy ranges from  $\approx 7.5$  keV to  $\approx 12$  keV with high spectral resolutions while the ISS-LM is using Silicon transmission crystals. Meanwhile, the NXS utilizes different crystal materials in an elliptical Bragg-reflection geometry allowing for a choice in spectral range  $\approx 1.5$  keV to  $\approx 20$  keV, each with a wide bandwidth and low spectral resolution. This work will present and compare the measurements of crystal's responses in  $\text{eV}\cdot\mu\text{sr}/\text{mm}^2$  for Qz(100) and Si(111) in both ISS and NXS geometries as well as results for PET (002) in NXS configuration. The inferred integrated reflectivity will also be presented and compared, in some cases, to theoretical calculations made with pyTTE program.

### Acknowledgements

This work performed under the auspices of the U.S. Department of Energy by General Atomics under Contract 89233119CNA000063 and by Lawrence Livermore National Laboratory under Contract DE-AC52-07NA27344.

LLNL-ABS-840130.

---

## A variational atomic model of plasma accounting for ion radial correlations and electronic structure of ions (VAM-PIRES)

Thomas Blenski<sup>1</sup>, Robin Piron<sup>2</sup>

<sup>1</sup>*Laboratoire “Interactions, Dynamiques et Lasers”, UMR 9222, CEA-CNRS-Universite Paris-Saclay, France*

<sup>2</sup>*CEA, DAM, DIF, France*

We propose a model of ion-electron plasma (or nucleus-electron plasma) that accounts for the electronic structure around nuclei (i.e. ion structure) as well as for ion-ion correlations. The model equations are obtained through the minimization of an approximate free-energy functional, and it is shown that the model fulfills the virial theorem. The main hypotheses of this model are 1) nuclei are treated as classical indistinguishable particles 2) electronic density is seen as a superposition of a uniform background and spherically-symmetric distributions around each nucleus (system of ions in a plasma) 3) free energy is approached using a cluster expansion 4) resulting ion fluid is modeled through an approximate integral equation.

In this presentation we will describe the set of hypotheses of this model, sketch the derivation of the model equations and comment on them. We will show how this model fulfills the virial theorem, allowing a sound definition of the related thermodynamic quantities. Finally, we will show results from numerical calculations, comparison with other models such as VAAQP or INFERNO, and discuss the limitations of the model.

---

## Measurement of line absorption at Gbar pressures

**David Bishel<sup>1</sup>, Igor Golovkin<sup>2</sup>, David Chin<sup>1</sup>, Ethan Smith<sup>1</sup>, Gilbert Collins<sup>1</sup>, John Ruby<sup>3</sup>, Phil Nilson<sup>1</sup>, Reuben Epstein<sup>1</sup>, Ryan Rygg<sup>1</sup>, Suxing Hu<sup>1</sup>**

<sup>1</sup>*Laboratory for Laser Energetics, University of Rochester, USA*

<sup>2</sup>*Prism Computational Sciences, USA*

<sup>3</sup>*Department of Physics and Astronomy, University of Rochester, USA*

Atomic structure profoundly impacts the material and radiative properties of dense plasmas. Accurate atomic models are critical to understanding the structure and evolution of stellar interiors, inertial fusion plasmas, and traditional and nuclear explosives. Even at a few times solid density, however, interactions between neighboring ions in a plasma may substantially modify the atomic wavefunctions. Calculations of these many-body quantum interactions are exceedingly difficult, requiring approximations to be made in most atomic structure models, yet few datasets exist to verify their accuracy. We present inner-shell x-ray absorption spectra of mid- $Z$  witness layers in a laser-driven spherical implosion compressed to Gbar pressures. We map the energy shift of inner-shell transitions during disassembly and the relationship to the evolving thermodynamic conditions. Impacts on atomic structure models are discussed.

---

## Improving warm dense matter models with accurate first-principles benchmarks

**Alina Kononov<sup>1</sup>, Thomas Hentschel<sup>2</sup>, Stephanie Hansen<sup>1</sup>, Andrew Baczewski<sup>1</sup>**

<sup>1</sup>*Sandia National Laboratories, USA*

<sup>2</sup>*Cornell University, USA*

Quantum degeneracy and thermal effects challenge atomic models of warm dense matter (WDM), a regime where partial ionization, interatomic bonding, and band structure can modify plasma response properties. We use real-time time-dependent density functional theory (TDDFT), a multi-center first-principles approach, to benchmark the predictions of an improved average-atom (AA) framework for WDM. Our comparisons of dynamic structure factors in warm dense deuterium, carbon, and aluminum help constrain models of electron-ion collision frequencies that broaden and shift the plasmon feature often analyzed in x-ray scattering diagnostics. However, TDDFT also predicts other effects that remain difficult for AA to capture. First, we find that collective behavior in warm dense iron blue shifts transitions into thermally depleted  $d$  states. Also, we uncover subtle signatures of atomic order in isochorically heated aluminum arising from non-idealities in the density of states. But despite its higher accuracy relative to AA, TDDFT still relies on some poorly characterized and difficult to improve approximations. We will conclude with a preview of some potential advantages that emerging quantum computing technologies may offer for modeling atomic processes in plasmas. This work has important implications for WDM modeling and characterization, most immediately the possibility of novel diagnostic techniques for high temperatures and/or systems out of thermal equilibrium.

## Progress in modeling of krypton He-beta lineshape for diagnostics of high-energy-density plasmas

**Evgeny Stambulchik<sup>1</sup>, Ramy Doron<sup>1</sup>, Yitzhak Maron<sup>1</sup>, Manfred Bitter<sup>2</sup>, Hui Chen<sup>3</sup>, Arati Dasgupta<sup>4</sup>, Philip Efthimion<sup>2</sup>, Lan Gao<sup>2</sup>, Kenneth Hill<sup>2</sup>, Carlos Iglesias<sup>3</sup>, Bob Kauffman<sup>3</sup>, Frances Kraus<sup>5</sup>, Brandon Lahmann<sup>6</sup>, Duane A. Liedahl<sup>3</sup>, Mike MacDonald<sup>3</sup>, Andrew MacPhee<sup>3</sup>, Novimir Pablant, Marilyn B. Schneider<sup>3</sup>, Howard Scott<sup>3</sup>, Stanislav Stoupin<sup>3</sup>, Daniel B. Thorn<sup>3</sup>**

<sup>1</sup>*Weizmann Institute of Science, Israel*

<sup>2</sup>*Princeton Plasma Physics Laboratory, USA*

<sup>3</sup>*Lawrence Livermore National Laboratory, USA*

<sup>4</sup>*Naval Research Laboratory, USA*

<sup>5</sup>*Princeton University, USA*

<sup>6</sup>*Massachusetts Institute of Technology, USA*

K-shell transitions of He-like species have been widely used to diagnose high-energy-density plasmas, including those in the inertial-confinement fusion experiments. Recently, Stark broadening of the krypton He-beta line was used for inferring the electron density in NIF compressed capsules [1,2] and suggested for diagnostics in Laser Mega-Joule experiments [3]. Here, we report on the Stark lineshape modeling of Kr He-beta based on computer simulations that include electron penetration effects [4], resulting, in particular, in the consistent evaluation of the plasma polarization shift. Measuring the latter can serve as an independent method of plasma density diagnostics. Furthermore, Li-like satellites, contributing to the overall shape of the He-beta complex, were also calculated.

### References

1. L. Gao *et al.*, <https://doi.org/10.1103/PhysRevLett.128.185002>
2. K. W. Hill *et al.*, <https://doi.org/10.1088/1361-6587/ac9017>
3. G. Pérez-Callejo *et al.*, <https://doi.org/10.1103/PhysRevE.106.035206>
4. E. Stambulchik and C. A. Iglesias, <https://doi.org/10.1103/PhysRevE.105.055210>

---

## Two-photon processes and their minor contribution to the Sandia Z-pinch iron opacity experiments

Michael Kruse<sup>1</sup>, Carlos Iglesias<sup>1</sup>

<sup>1</sup>*Lawrence Livermore National Laboratory, USA*

The discrepancies between theoretically calculated and experimentally measured Iron opacities at the Sandia National Laboratory Z-pinch machine are hitherto still unexplained even after nearly a decade of effort. Theoretical opacities have neglected higher-order processes such as two-photon processes, i.e., two-photon ionization or Raleigh and Raman scattering and thus could be a potential additional source of opacity that may lessen the disagreement with experimental measurements. We will present a summary of our two-photon ionization calculations in which we conclude that two-photon absorption cannot explain the bound-free discrepancy between experiment and theory, and then move on to show previously unreported calculations for the elastic (Raleigh) and inelastic (Raman) scattering contributions for the measured 2-4 Ne-like Iron lines.

### Acknowledgements

This work was performed under the auspices of the U.S. Department of Energy by Lawrence Livermore National Laboratory under contract DE-AC52-07NA27344. LLNL-ABS-XXXXX

## Influence of metastable levels on the charge-state distribution of highly charged ions in EBIT plasma

**Endre Takacs<sup>1</sup>, Dipti<sup>2</sup>, Adam Hosier<sup>1</sup>, Timothy Burke<sup>1</sup>, Galen C. O'Neil<sup>3</sup>, Joan P. Marler<sup>1</sup>, Yuri Ralchenko<sup>3</sup>**

<sup>1</sup>*Department of Physics and Astronomy, Clemson University, USA*

<sup>2</sup>*Atomic and Molecular Data Unit, International Atomic Energy Agency*

<sup>3</sup>*National Institute of Standards and Technology, USA*

In an electron beam ion trap (EBIT) the ion plasma is confined in a spatially narrow region centered around the electron beam compressed to about  $10^{10}$ - $10^{12}$  cm<sup>-3</sup> densities. The ion cloud in its equilibrium generally consists of a narrow distribution of charge states. This can be finely tuned by adjusting the electron beam energy and current, the axial magnetic field, and the amount of neutral atoms in the trap region. The almost mono-energetic electrons are responsible for electron impact ionization and recombination processes and contribute to the confinement of the ions.

In the EBIT of the National Institute of Standards and Technology (NIST) the non-Maxwellian plasma has been modeled by collisional-radiative calculations [1] to reliably predict the spectral emission of the ion cloud [2-3]. In recent experiments we have found that in some cases, the charge state distribution of the ions is strongly affected by metastable energy levels that accumulate considerable ion population. Ag-like and Ni-like heavy ions are examples of such systems, where the lowest excited states are highly metastable. The effect strongly depends on the density of the electrons; therefore, it can serve as a sensitive diagnostic of plasmas where metastable ions are present. Measured spectral features and details of model calculations will be presented.

### References

1. Y. Ralchenko and Y. Maron, *J. Quant. Spec. and Rad. Trans.* **71** (2001) 609
2. R. Silwal, Dipti, E. Takacs, J.M. Dreiling, S.C. Sanders, A.C. Gall, B.H. Rudramadevi, J.D. Gillaspay, Y. Ralchenko, *J. Phys. B. At. Mol. and Opt. Phys.* **54** (2021) 245001
3. C. Suzuki, Dipti, Y. Yang, A.C. Gall, R. Silwal, S. Sanders, A. Naing, J.N. Tan, E. Takacs, Y. Ralchenko, *J. Phys. B. At. Mol. and Opt. Phys.* **54** (2020) 015001

## **Bio-applications of non-thermal plasma**

**Vladimir Scholtz<sup>1</sup>, Josef Khun<sup>1</sup>, Jana Jiresova<sup>1</sup>, Ladislav Fiser<sup>1</sup>, Myron Klenivskyi<sup>1</sup>, Zuzana Racova<sup>1</sup>, Eva Vankova<sup>1</sup>, Eliska Lokajova<sup>1</sup>, Anna Machkova<sup>1</sup>, Jan Hrudka<sup>1</sup>, Michal Jankovsky<sup>1</sup>, Anna Hodziova<sup>1</sup>, Jaroslav Julak<sup>1</sup>**

<sup>1</sup>*Department of Physics and Measurements, University of Chemistry and Technology, Prague, Czechia*

Non-thermal plasma (NTP) possesses useful properties for interacting with biomaterials. Our NTP laboratory group focuses mainly on the study and generation of NTP and the explanation of its interactions with biological objects. For NTP generation, we mainly use the corona and related discharges. The NTP quality and intensity depend on the set up of electrode arrangement, power supply and can be adjusted to specific applications. Our devices range from very weak sources based on point-to-ring discharge, to relatively strong ones based on transient spark discharge. Additionally, we are developing portable, affordable and user-friendly NTP generation devices for practical applications in medicine, food production, or agriculture. Our laboratory investigates the interactions of NTP with biological materials, with a focus on microbial decontamination of sensitive materials such as the face masks and food products (improving food shelf life), treatment of infections such as onychomycosis (fungal nail infection), enhancement of seed quality and early plant growth, and modification of biosurfaces through the activation of biomolecular films.



## Numerical investigation of bremsstrahlung in laser-plasma interaction with double-layer targets

Marta Galbiati<sup>1</sup>, Arianna Formenti<sup>1</sup>, Francesco Mirani<sup>1</sup>, Alessandro Maffini<sup>1</sup>, Matteo Passoni<sup>1</sup>

<sup>1</sup>*Department of Energy, Politecnico di Milano, Italy*

When an ultra-intense ( $> 10^{18}$  W/cm<sup>2</sup>) laser pulse interacts with a suitable target in the plasma state, relativistic electrons are accelerated. These electrons can emit high-energy photons (keV–MeV energy range) mainly through bremsstrahlung [1,2], mediated by the atoms and ions inside the target, and through synchrotron-like emission [3]. These emission processes can be exploited for diagnostics in experiments and for developing laser-based high-energy photon sources. These sources could complement conventional ones by providing unique properties like compactness, ultrafast duration, small source size, high energy and high flux. Advanced targets, like a double-layer target (DLT), can enhance the number and energy of relativistic electrons produced in the interaction and consequently boost emission. Specifically, a DLT is made of a solid substrate covered with a low-density layer which favours the laser-plasma coupling [4]. This contribution presents the results of numerical simulations investigating, in particular, bremsstrahlung in laser interaction with DLTs. The modelling of this atomic emission process in laser-plasma interaction needs proper investigation and discussion of the cross-section choice and use. Indeed, particle-in-cell codes, widely used tools to study laser-plasma interaction, can be coupled in different ways with Monte Carlo approaches [5,6] to simulate bremsstrahlung. After considering the rationale and criticalities of some of these simulation approaches based on open-source codes, we use these tools with the support of analytical models to study the leading processes and properties of bremsstrahlung in DLTs [7]. We look at the impact of the DLT and laser parameters on the emission properties. We also consider the competition with synchrotron-like emission and the effect of including other atomic processes, like target ionization, in the simulations. Our 2D and 3D simulations show how DLTs can enhance the number of high-energy emitted photons and tune emission according to their properties (thickness, density, atomic number). These results make bremsstrahlung in DLTs worthy of investigation in future experimental campaigns and potential applications like photon activation analysis [8] and laser-driven tomography.

### References

1. J.D. Kmetec et al. Physical Review Letters 68, 1527 (1992)
2. F. Albert et al. Plasma Physics and Controlled Fusion 58, 103001 (2016)
3. A. Di Piazza et al. Reviews of Modern Physics 84, 1177 (2012)

- 
4. L. Fedeli et al. *Scientific Reports* 8, 3834 (2018)
  5. C.D. Chen et al. *Physics of Plasmas* 20, 052703 (2013)
  6. B. Martinez et al. *Physics of Plasmas* 26, 103109 (2019)
  7. A. Formenti et al. *Plasma Physics and Controlled Fusion* 64, 044009 (2022)
  8. F. Mirani et al. *Communications Physics* 4, 185 (2021)

## Benchmark of the $2p$ line formation in OVII near the collisional excitation threshold

**Pedro Amaro**<sup>1</sup>,

<sup>1</sup>*Faculdade de Ciências e Tecnologia da Universidade Nova de Lisboa (FCT, Nova University of Lisbon), Portugal*

Emission lines from He-like ions are an essential diagnostics tool of high-resolution X-ray spectra from satellite missions, such as Chandra and XMM-Newton. Due to the simplest close-shell structure of these ions, observable spectra contains the strongest and easiest identifiable emission lines in a variety of astrophysical objects. The physical insight of these lines can be used to probe the dynamics of hot coronal plasmas, cool photo-ionized plasmas, as well as out-of-equilibrium-plasmas like ones present in the winds of X-ray binaries, and supernova remnants. Recently, the Perseus cluster's X-ray spectrum was analyzed using Hitomi's Soft X-ray Spectrometer micro-calorimeter to measure turbulent motion at its center. The broadening and Doppler shift of He-like lines of FeXXVIII was used in this regard. However, obstacles emerged in the analysis due to inaccuracies in atomic data employed in standard plasma modelling codes. This motivates not only a careful analysis of the theoretical methods, but also an experimental benchmark of the line formation mechanisms.

X-ray measurements of He-like OVII were carried out at the FLASH- Electron Beam Ion Trap (EBIT), Heidelberg. The decay of the forbidden  $z$  line population was directly observed with an electron beam energy scheme defined by a triangular wave. We observed the He-like dielectronic recombination (DR) KLn structure, as well as resonant excitations (RE) superimposed to collisional excitations (CE) of H-like and He-like ions at the collisional excitation threshold. The  $2p$  line emission ( $x + y + w$ ) was isolated with a sufficient fast scan that makes the  $z$  emission constant, allowing its subtraction from the overall emission. The experimental method was verified with a home-made collisional-radiative code. Results of the line formation are compared with calculations of FAC, based on isolated-resonant approximation, and R-matrix method, as well as current state-of-the art R-matrix calculations.

## Further requirement of tungsten atomic data for tungsten influx estimation at EAST plasma edge

Ling Zhang<sup>1</sup>, Ailan Hu<sup>1</sup>, Fengling Zhang<sup>1</sup>, Haiqing Liu<sup>1</sup>, Ke Yao<sup>1</sup>, Shigeru Morita<sup>1</sup>, Wenmin Zhang<sup>1</sup>, Xiaobin Ding<sup>1</sup>, Yang Yang<sup>1</sup>, Yunxin Cheng<sup>1</sup>,

<sup>1</sup>*Institute of Plasma Physics, Chinese Academy of Sciences*

Upper and lower graphite divertor in EAST tokamak have been updated to tungsten divertors in 2014 and 2021 respectively to investigate the tungsten divertor operation and to realize high-performance long pulse discharge. Therefore, studies on the tungsten behavior are crucially important for improving the plasma performance. For the purpose four fast-time-response [1,2] and four space-resolved [3,4] extreme ultraviolet (EUV) spectrometers have been installed on EAST to observe line emissions from tungsten ions and their intensity radial profiles in wavelength ranges of 5 – 520 Å.

Photon emission coefficient (PEC) data for W<sup>45+</sup> at 62.336 and 126.998 Å, W<sup>43+</sup> at 61.334 and 126.29 Å have been used to estimate density profiles of W<sup>45+</sup> and W<sup>43+</sup> ions in the bulk plasma [3,5]. Tungsten unresolved transition arrays (W-UTA) in the long wavelength range of 168 – 225 Å, 225 – 268 Å and 278 – 332 Å observed from typical EAST ELMy H-mode plasmas are analyzed for the study of edge tungsten behaviors. As a result, three lines of 186.28 Å, 190.48 Å and 192.02 Å with relatively strong intensities emitted from W<sup>8+</sup> ions could be confirmed by comparing with the time behaviors of well-known line emissions from W<sup>6+</sup> at 216.219 and 261.387 Å [6,7], W<sup>7+</sup> at 200.367 Å and 200.483 Å [8] and W<sup>27+</sup> at 49.403 Å [1-4]. Therefore, the ionization per photon coefficients, S/XB, for the lines from weakly ionized ions are therefore required to estimate the tungsten influx at plasma edge. Additionally, visible spectrometer with spatial viewing range covering the whole EAST poloidal cross section have been newly developed for the attempt of investigating the radial profile of line emissions of M1 transitions from W<sup>26+</sup>–W<sup>28+</sup> and W<sup>8+</sup>–W<sup>12+</sup> ions which have been observed in LHD [9] and EBIT [10] respectively. Calculation of full radial profiles of impurity density and influx will be attempted using the PEC and S/XB data of the observable lines.

### References

1. L. Zhang et al., Rev. Sci. Instrum. 86 (2015) 123509
2. Z. Xu et al., Nucl. Instrum. Meth. A 1010 (2021) 165545
3. L. Zhang et al., Nucl. Instrum. Meth. A 916 (2019) 169
4. Y.X Cheng et al., Rev. Sci. Instrum. 93 (2022) 123501
5. Y.X Cheng et al., IEEE T Plasma Sci. 50(2022):691-699
6. J. Clementson et al., J. Phys. B 43 (2010) 144009
7. C.F. Dong et al., Nucl. Fusion 59 (2019) 016020

- 
8. D. Kato et al., Nucl. Fusion 61 (2021) 116008
  9. Q. Lu et al. Phys. Rev. A 103 (2021) 022808

## Acknowledgements

This work was supported by the National MCF Energy R&D Program (Grant No. 2022YFE03180400) and Chinese Academy of Sciences President's International Fellowship Initiative (PIFI) (Grant No. 2020VMA0001).

## Raman shifts and plasma screening in warm dense copper

Michal Šmíd<sup>1</sup>

<sup>1</sup>*Helmholtz Zentrum Dresden Rossendorf, Germany*

We show data and first analysis of a recent (Feb 2022) experiment on the spectroscopic investigation of XFEL-heated Cu foil targets. Cu foils were irradiated by the tightly focused XFEL beam ( $\approx 1 \mu\text{m}$  focus, up till 300  $\mu\text{J}$  in energy, European XFEL), which heats the target to approximately 100 eV during its duration ( $\approx 25$  fs). The XFEL photon energy was varied in the range 8.8 – 9.8 keV to scan resonances and K edges of various charge states; three spectrometers were observing the emission  $K\alpha$  and  $K\beta$  lines and their satellites. The experimental data are compared to the SCFly simulations and the details are analyzed by using the FAC atomic code.

First of the many interesting phenomena, the shift of the  $K\alpha$  satellite lines is discussed. Each of the  $K\alpha$  lines from ions with different occupancy of the L shell is shifting both due to the charge state of the emitting ion (i.e. number of electrons in M shell) and due to electron temperature via plasma screening. Both these shifts are experimentally observed and well described by using the FAC calculations. The observed shifts of the absorption K edges are also observed and agrees well to the Stewart-Pyatt model newly included in the FAC code, when the temperature parameter is adjusted to account for the strongly non-thermal electron distribution.

## Time-dependent collisional radiative modeling and ultraviolet spectroscopy of neutral tungsten for erosion diagnosis

**Curtis Johnson<sup>1</sup>, Connor Ballance<sup>2</sup>, David Ennis<sup>3</sup>, David Maurer<sup>3</sup>, Gregory Hartwell<sup>3</sup>, Stuart Loch<sup>3</sup>,**

<sup>1</sup>*Oak Ridge National Laboratory, USA*

<sup>2</sup>*Queen's University Belfast, UK*

<sup>3</sup>*Auburn University, USA*

High- $Z$  materials such as tungsten and molybdenum have become leading solutions for plasma-facing materials. There are uncertainties in both erosion and transport of these elements requiring further research. The spectral emission of these high- $Z$  species in combination with Collisional Radiative (CR) modeling can provide necessary information for plasma transport modeling. The Python program, ColRadPy, has been developed to solve collisional-radiative and ionization balance equations which can be applied to fusion, laboratory, and astrophysical plasmas [1]. The program provides generalized coefficients that can be used in existing plasma modeling codes and spectral diagnostics.

A spectral survey of tungsten emission in the ultraviolet region was conducted in two experiments, DIII-D tokamak and Compact Toroidal Hybrid (CTH) torsatron, to assess the potential benefits of UV emission for tungsten erosion diagnosis. A total of 53 neutral tungsten spectral lines were observed, including 32 lines not previously reported at fusion conditions [2]. Metastable level populations of neutral tungsten can impact both emission and erosion measurements, which can be significant at ITER relevant divertor electron densities. Observation of spectral lines in the UV region allows for relative metastable fractions and electron temperature to be diagnosed at the erosion location. The observed neutral tungsten emission lines can be used to measure gross tungsten erosion. The simultaneous observation of neutral tungsten and singly charge tungsten lines can estimate net erosion and the fraction of tungsten that is re-deposited.

Spin-changing collisional rate coefficients for metastable levels allow for the detailed exploration of the dynamics of metastable levels [3]. Long-lived metastable states in neutral tungsten can impact erosion measurements, so time-dependent collisional radiative modeling is used to analyze their role in tungsten emission and ionization. The large number of non-quasistatic atomic states in neutral tungsten can take milliseconds to reach equilibrium, affecting erosion measurements, so a scheme for measuring relative metastable fractions is proposed through simultaneous observation of multiple ultraviolet spectral lines of neutral tungsten. The Chodura sheath is a region of low electron density produced by magnetic fields impinging on plasma facing surfaces at shallow angles. The Chodura sheath also is important due to its potential impact on time-dependent neutral tungsten [4]. A simple model is developed to account for the effects of the Chodura sheath on the time-dependence of neutral tungsten. The study provides a roadmap for

---

modeling the spectral emission from complex species like tungsten and yields accurate tungsten erosion.

## References

1. C. A. Johnson et al. 2019 Nucl. Mater. Energy 20 100579
2. C. A. Johnson et al. 2019 PPCF 61 095006
3. R. T. Smyth et al. 2018 Phys. Rev. A 97 052705
4. C. A. Johnson et al (2020, November 9–13) Diagnosing metastable populations in fusion edge plasmas using collisional-radiative modeling constrained by experimental observations 62nd Annual Meeting of the APS Division of Plasma Physics



## SPARC x-ray crystal spectroscopy for ion temperature and toroidal rotation measurements

**Conor Perks<sup>1</sup>, Matthew Reinke<sup>2</sup>, John Rice<sup>1</sup>, Didier Vezinet<sup>2</sup>**

<sup>1</sup>*MIT Plasma Science and Fusion Center, USA*

<sup>2</sup>*Commonwealth Fusion Systems, USA*

High-resolution X-ray crystal spectroscopy has been a workhorse on numerous tokamaks to measure the ion temperature and toroidal rotation profiles from the Doppler broadening and shift, respectively, of intrinsic or seeded impurity line radiation emission. SPARC will be a first-of-its-kind tokamak that will similarly employ this diagnostic. The unique high electron temperature and high neutron flux environment of SPARC has been driving factors for the engineering design. Presented is the performance of the envisaged system of spectrometers optimized to view the Ne-like Xe 3D line ( $\lambda \approx 2.7 \text{ \AA}$ ) for low-temperature operations ( $T_{e0} \approx 4 - 10 \text{ keV}$ ) and the He-like Kr w resonance line ( $\lambda \approx 0.94 \text{ \AA}$ ) for high-temperature operations ( $T_{e0} > 10 \text{ keV}$ ). The Flexible Atomic Code (FAC) has been utilized to calculate line intensities, including satellites and polluting tungsten lines. The throughput has been calculated ensuring integration times on the order of the expected energy confinement time,  $\approx 100 \text{ ms}$ . This workflow has been validated against measured spectra from an absolutely calibrated von Hamos as well as a Johann spectrometer installed on Alcator C-Mod to good agreement. While the number of lines-of-sight is highly constrained, the staged installation of beamlines over the first campaigns minimizes error in calculated fusion power from the reconstructed profiles.

## X-ray studies of atomic processes involving highly charged ions at EBIT/S

Marek Pajek<sup>1</sup>, Dariusz Banaś<sup>1</sup>, Łukasz Jabłoński<sup>1</sup>

<sup>1</sup>*Institute of Physics, Jan Kochanowski University, 25-406 Kielce, Poland*

The electron beam ion traps and sources (EBIT/S) producing highly charged ions (HCI) offer unique experimental conditions to study various atomic processes [1], including electron impact ionization/excitation, recombination and radiative and nonradiative deexcitation of trapped and extracted HCI from EBITs. Here the experiments on X-ray emission from EBIT plasma involving highly charged  $\text{Xe}^{q+}$  ( $q$  up to 40) ions are discussed, in particular, in context of radiative (RR) and dielectronic (DR) recombination of ions with electrons (see Fig. 1). In experiments with extracted slow  $\text{Xe}^{q+}$  ions interacting with metallic beryllium the relaxation of Rydberg hollow atoms (RHA) [2], formed at a surface, was studied. We demonstrate experimentally that in ultrafast relaxation of RHA the two-electron processes, such as interatomic Coulombic decay (ICD) [3,4] and internal dielectronic excitation (IDE) [5], play important role. The present results clearly demonstrate that that x-ray spectroscopy, applied to measure the radiation emitted from HCI produced at, allows to reveal fine details of various atomic processes involving highly excited heavy ions.

### References

1. H. Winter and F. Aumayr, J. Phys. B 32, R39 (1999).
2. J.P. Briand et al., Phys. Rev. Lett. 65, 159 (1990).
3. L.S. Cederbaum et al. Phys. Rev. Lett. 79, 4778 (1997).
4. R.A. Wilhelm et al., Phys. Rev. Lett. 119, 103401 (2017).
5. R. Schuch et al., Phys. Rev. Lett. 70, 1073 (1993).

## Investigation of opacity effects on optically thick lines for diagnosing plasma conditions in buried layer targets for x-ray opacity studies

Mike MacDonald<sup>1</sup> Greg Brown<sup>1</sup>, Dylan Cliche<sup>1</sup>, Mark Foord<sup>1</sup>, Bob Heeter<sup>1</sup>, David Hoarty<sup>2</sup>, Duane A. Liedahl<sup>1</sup>, Rich London<sup>1</sup>, Madison Martin<sup>1</sup>, Joe Nilsen<sup>1</sup>, Mehul Patel<sup>1</sup>, Howard Scott<sup>1</sup>, Ronnie Shepherd<sup>1</sup>, Heather Whitley<sup>1</sup>, Klaus Widmann<sup>1</sup>

<sup>1</sup>*Lawrence Livermore National Laboratory, USA*

<sup>2</sup>*AWE, UK*

K-shell x-ray emission spectroscopy is a standard tool used to diagnose the plasma conditions created in high-energy-density physics experiments such as short-pulse heated buried microdot targets. In the simplest approach, the emissivity-weighted average temperature of the plasma can be extracted by fitting an emission spectrum to a single temperature condition. Recent work has shown that temperature distributions resulting from spatial gradients and the time evolution of the sample can be extracted from time-integrated x-ray spectra [1], however the intensity of the optically thick emission lines needed to be modified to fit the experimental spectra. In this work, we explore the effects of various treatments of optically thick emission lines in the analysis of buried layer microdot targets including escape factors and full radiation transport calculations. In doing so, we aim to identify the origin of the multipliers required to fit such experimental spectra and improve the characterization of the plasma conditions in the buried layer targets used for x-ray opacity studies.

### Reference

1. M. J. MacDonald et al., *Rev. Sci. Instrum.* **93**, 093517 (2022).

### Acknowledgements

This work was performed under the auspices of the U.S. Department of Energy by Lawrence Livermore National Laboratory under Contract No. DE-AC52-07NA27344.

## Tracking of internal states in collisional-radiative models employed in the transport codes

**Dmitriy Borodin<sup>1</sup>, F. Cianfrani<sup>1</sup>, B. Küppers<sup>1</sup>, J. Romazanov<sup>1</sup>, M. Groth<sup>2</sup>, P. Boerner<sup>1</sup>, S. Brezinsek<sup>1</sup>, Y. Marandet<sup>3</sup>**

<sup>1</sup>*Forschungszentrum Jülich GmbH, Institut für Energie- und Klimaforschung IEK-4: Plasmaphysik, Germany*

<sup>2</sup>*Aalto University, Finland*

<sup>3</sup>*Physique des Interactions Ioniques et Moléculaires, Aix-Marseille Université, France*

The collisional-radiative models (CRMs) play a significant role in the Monte-Carlo (MC) transport codes used for edge and divertor plasma in fusion relevant devices. In turn, the codes like the impurity transport code ERO [1] or the more oriented on the main plasma species EIRENE [2] are indispensable for the understanding of the interplay of various processes in edge and divertor plasmas of fusion devices also in relation with the plasma-wall interaction and power exhaust. The study of detachment phenomenon including the dominating atomic and molecular (A&M) processes is of particular interest. EIRENE needs iterations with a fluid plasma codes like for instance Edge2D or B2.5 (making up the SOLPS-ITER package [3]) to produce a self-consistent simulations which are often used as a background plasma input for ERO. Therefore it is of great value to unify the CRMs in all the deeply interconnected codes. Both main plasma species containing hydrogen isotopes H/D/T including molecular neutrals and ions and main impurities like beryllium, tungsten, argon, etc. are to be included into simulations, thus in CRMs, including related spectroscopy as well as impact on particle, momentum and energy balance. Recently a large effort [4] is put into the improvement of the EIRENE code which includes restructuring and extension of the CRMs associated with it. This includes development of the PLOUTOS tool for A&M data pre-processing for EIRENE (allowing flexible setting of various model assumptions), which however also contains a stand-alone (SA) solver for CRM. Another SA CRM used is YACORA [5] containing a very established and up-to-date A&M data collection. It was shown multiple times that despite standalone CRMs neglect most part of transport effects they can produce insights into the physics and even practically useful simulation results [6].

The systematic challenges for any CRM employed inside the transport codes are a) the variety and amount, thus controllability of the data and b) decrease of the code performance. Both issues are addressed to a certain extent by the code structure in EIRENE providing much of the data preparation before entering the main loop – rates are pre-calculated for every volume cell inside which the plasma parameters (often taken from the fluid code) are fixed. The reaction data structure was further optimised to reduce the branching by the reaction types. Nonetheless, the upcoming dramatic increase of the data due to necessity to consider rovibrational states in molecules or simply very complex elements like tungsten (W) requires tracking the internal state of the species.

---

This, however must not necessarily be the full-detailed CRM, but can be a reduced essence of it. Earlier, the ERO code has demonstrated the tracking of the internal states in beryllium (Be): just 2 BeI states (the ground and the metastable ones) allowing to capture mostly the population dynamics provided by the whole CRM - these are different options provided in ADAS [7]. Similar effort was provided for WI with various number and bundling assumptions of the tracked states. In case of 2 states tracked a fully analytical approach can be used for solution of the time-dependent evolution of the populations; for more states matrix exponent based solution is applied. The present work suggests how this approach can be used for molecular species. Tracking the vibrational states as independent species is demonstrated by Edge2D-EIRENE, however this leads to enormous CPU time demands if a decent MC statistic for each vibrostate is provided. Tracking of state populations as internal variables will remedy that on a price of negligible numerical bias error in case the ionisation and other processes impacting the specie transport are little dependent on its particular vibrational state. It is of importance to provide a flexible link and data pre-processing procedure between the SA CRM like PLOUTOS and the internal tracker inside the main loop of EIRENE.

The presentation is aimed to overview the already developed parts on the internal state (e.g. metastable) tracking with few illustrations for BeI and WI spectroscopy in edge plasma and to present a concept of how this experience can be used in EIRENE with PLOUTOS for molecules.

## References

1. J. Romazanov et al., Phys. Scr. 2017 014018 (2017)
2. D. Reiter et al., Fusion Sci. Technol. 47 172–86 (2005)
3. S. Wiesen et al., J. Nucl. Mat. 463, pp 480-484 (2015)
4. D. V. Borodin et al., Nucl. Fusion 62 086051 (2022)
5. D. Wunderlich et al., J. Quant. Spectrosc. Radiat. Transfer 240, 106695 (2020)
6. F. Cianfrani et al., 48th EPS conf., P2a.105 (2022)
7. H. P. Summers (2004) The ADAS User Manual, version 2.6, <http://www.adas.ac.uk>

## Emission spectroscopy of dense iron plasma created at LCLS

**Bob Nagler**<sup>1</sup>

<sup>1</sup>*SLAC National Accelerator Laboratory, USA*

I will present the results of experiments at LCLS where we created and diagnosed iron plasma at temperature exceeding 1keV, and at solid iron (atomic) densities, with bulk electron densities greater than  $2 \times 10^{24} \text{ cm}^{-3}$ . Using photon energies between 7100 eV and 9000 eV and pulse lengths less than 100 femtoseconds, we focussed the LCLS beam to a 120 nm focal spot. A 2 micron thin iron sample was placed in this focus and irradiated with intensities in excess of  $10^{20} \text{ W/cm}^2$ .

In this way, the heated iron foil reaches conditions (i.e. electron density and temperature) comparable to the stellar core condition in stars on the main sequence between 0.1 and 100 solar masses. The temperature we reached are relevant to emission seen from Galaxy clusters.

We compare the x-ray emission from the iron sample with atomic-kinetic calculation (i.e. SC-FLY). The analysis confirm the charges states and temperatures reached, and give a measure of the Ionization Potential Depression and collision rates in these dense plasmas.

## Non-thermal evolution of dense plasmas driven by intense x-ray fields

Hyun-Kyung Chung<sup>1</sup>, Shenyuan Ren<sup>2</sup>, Yuanfeng Shi<sup>2</sup>, Sam Vinko<sup>2</sup>, Justin Wark<sup>2</sup>

<sup>1</sup>*National Fusion Research Institute, Republic of Korea*

<sup>2</sup>*Department of Physics, University of Oxford, UK*

The advent of x-ray free-electron lasers (XFELs) has enabled a range of new experimental investigations into the properties of matter driven to extreme conditions via intense x-ray-matter interactions. The femtosecond timescales of these interactions lead to the creation of transient high-energy-density plasmas, where both electrons and ions may be far from local thermodynamic equilibrium (LTE). Predictive modelling of such systems remains challenging because of the substantially different timescales on which electrons and ions thermalize, and because of the vast number of atomic configurations that are required to describe the resulting highly-ionized plasmas. Here we present work discussing the evolution of systems driven to high energy densities using CCFLY, a non-LTE, Fokker-Planck collisional-radiative code. We use CCFLY to investigate the evolution dynamics of a solid-density plasma driven by an XFEL, and explore the relaxation of the plasma to local thermodynamic equilibrium on femtosecond timescales in terms of the charge state distribution, electron density, and temperature.

### Reference

1. S. Ren, Y. Shi, Q.Y. van den Berg, M. Firmansyah, H.-K. Chung, E.V. Fernandez-Tello, P. Velarde, J.S. Wark, S.M. Vinko, arXiv:2208.00573 (2023).

## Probing extreme atomic physics in super-dense plasmas

**Suxing Hu**<sup>1</sup>

<sup>1</sup>*Laboratory for Laser Energetics, University of Rochester, USA*

Matter under extreme high-energy-density (HED) conditions (e.g. at superhigh pressures from billions to trillions of atmospheres) are often encountered in stars and inertial confinement fusion targets. Such extreme HED matter can now be created on energetic laser/XFEL facilities and pulsed-power machines in laboratories. Accurate knowledge of extreme HED matter is essential to better understanding planetary science and astrophysics, as well as reliably designing fusion energy targets. Over the past decade, research has revealed that traditional plasma-physics models often fail to describe the physics of matter under HED conditions since strong coupling and electron degeneracy play a crucial role in such quantum many-body systems.

Probing HED matters in an experiment mostly relies on x rays since it is one of the possible sources that can penetrate dense matters. X-ray-induced fluorescence and/or absorption are often used to infer what happens inside extreme HED matter. On the theoretical/computational side, *ab initio* methods such as density functional theory (DFT) and time-dependent DFT [1] can provide a self-consistent way to predict the properties of HED matter (with systematic improvement possible). Combining both x-ray spectroscopy experiments and *ab initio* calculations, we have investigated some new HED physics phenomena over the past few years, which include the *Fermi-surface rising* in warm dense matter [2] and *interspecies radiative transition* in super-dense matter [3]. To understand these precision x-ray spectroscopy measurements, we have derived a DFT-based kinetic model to explore the extreme atomic physics of HED matters at Gbar pressures [4], which enables us to eliminate the controversial continuum-lowering models for dense plasmas. In this talk, I will share what we have learned so far in exploring HED matter, as well as what we are still struggling to understand.



---

## References

1. Y. H. Ding *et al.*, Phys. Rev. Lett. **121**, 145001 (2018).
2. S. X. Hu, Phys. Rev. Lett. **119**, 065001 (2017).
3. S. X. Hu *et al.*, Nature Communications **11**, 1989 (2020).
4. S. X. Hu *et al.*, Nature Communications **13**, 6780 (2022).

## Elastic scattering and rotational excitation of H<sub>2</sub> by electron impact

Dmitry Fursa<sup>1</sup>, Igor Bray<sup>1</sup>, Liam Scarlett<sup>1</sup>, M. S. Zammit<sup>2</sup>, N. A. Mori<sup>1</sup>, U. S. Rehill<sup>1</sup>

<sup>1</sup>*Curtin University, Australia*

<sup>2</sup>*Los Alamos National Laboratory, USA*

The problem of low-energy electron-impact rotational excitation of H<sub>2</sub> has been studied in great detail over the last 60 years, due to its importance in low-temperature hydrogen plasmas and gases. Below 10 eV, rotational excitation comprises up to 20% of the total cross section, and below the  $v = 0 \rightarrow 1$  threshold ( $\approx 0.5$  eV) it is the dominant contribution to electron energy loss. Accurate cross sections for the rotational transitions of H<sub>2</sub> are vital for modelling the emission spectra of astrophysical clouds, or for constructing collisional-radiative (CR) models of fusion-relevant plasmas. Up to 0.5 eV, the  $N = 0 \rightarrow 2$  and  $1 \rightarrow 3$  rotational excitation cross sections are well known, with good agreement between the results of electron swarm experiments, which are reproduced by several calculations. At higher energies, however, the situation is less ideal, with substantial disagreement between various measurements and calculations.

The theoretical techniques applied to this problem in the past have utilised a variety of approximations to the treatment of coupling between rovibrational levels, from the adiabatic-nuclei (AN) approximation in which the coupling is neglected, to the most accurate rovibrational close-coupling approach. However, the common factor in all previous studies is the use of model potentials in place of coupling to the closed electronically-inelastic channels. The various choices of potential can lead to differences in the calculated cross sections far more significant than the errors introduced by the AN approximation, particularly since the greatest discrepancies are at energies more than 10 times the threshold energy, where the AN approximation is accurate. What is missing from the literature are theoretical studies of low-energy rotational excitation in which the coupling to closed electronic channels is accounted for rigorously. Within the AN approximation this is feasible provided one can solve the electronic scattering problem accurately. Here we apply the molecular convergent close-coupling (MCCC) method, which in recent years has been shown to completely solve the electronic scattering problem for H<sub>2</sub> [1]. The results presented here are available online [2].

### References

1. Zammit *et al.* 2016 *Phys. Rev. Lett* 116 233201
2. mccc-db.org
3. Lane N F and Geltman S 1967 *Phys. Rev.* **160** 53

- 
4. Henry R J W and Lane N F 1969 *Phys.Rev.* 183 221
  5. Hara S 1969 *J. Phys. Soc. Japan* **27** 1592
  6. Morrison M A et al. 1984 *Phys. Rev. A* **29** 2518
  7. Morrison M A et al. 1987 *Aust. J. Phys.* **40** 239
  8. Trail W K et al. 1990 *Phys. Rev. A* **41** 4868
  9. Ehrhardt H and Linder F 1968 *Phys. Rev. Lett.* **21** 419
  10. Gibson D K 1970 *Aust. J. Phys.* **23** 683
  11. Linder F and Schmidt H 1971 *Zeitschrift für Naturforschung* **26** 1603
  12. England J P *et al.* 1988 *Aust. J. Phys.* **41** 573

## Time-dependent radiation emission from an X-ray laser-produced plasma

Pedro Velarde<sup>1,2</sup>, Manuel Cotelo<sup>1,2</sup>, Alberto G. de la Varga<sup>1</sup>, Elisa Vázquez<sup>1,2</sup>, Eduardo Oliva<sup>1,2</sup>

<sup>1</sup>*Instituto de Fusión Nuclear Guillermo Velarde, Universidad Politécnica de Madrid, Spain*

<sup>2</sup>*Departamento de Ingeniería Energética, Universidad Politécnica de Madrid, Spain*

With new ultra-intense lasers, such as the XFEL, the effects of non-thermal electronic distributions (EDF) are important. This deviation from the thermal distribution comes from the time dependence of the EDF and atomic populations. To study this problem, it is necessary to couple the time evolution of the atomic populations with the time evolution of the EDF and of the radiation energy distribution. We have studied the change in the radiation emission due to the time evolution of the EDF in dense plasmas, initially a Fermi-Dirac distribution, generated by XFEL. To numerically simulate this process, we coupled the time evolution equations of the atomic populations with the Fokker-Planck time equation for electrons with degeneracy. This implies recalculating at each instant all atomic process rates, as well as the coefficients and independent terms of the FP equation.

A signature of non-equilibrium processes is the emission of radiation differentiated from that of equilibrium. We present and explain the differences between such emissions with and without time dependence, pointing out the possibility of measuring the time effects of the EDF. To study these time-dependent phenomena, we used the atomic physics code BigBarT which has been validated for the calculation of spectral opacities for plasmas in equilibrium. In the figure below we show the time-integrated emission spectrum for thermal and non-thermal EDF. Two low-intensity signals are seen in the non-thermal case that are missing with thermal EDF. This opens the possibility of measuring non-thermal effects in dense plasmas. Furthermore, we will present results for the transmission of XUV electromagnetic radiation in time-varying refraction index of a dense plasma generated by XFEL.

---

## References

1. Q. Y. van den Berg et al., Clocking Femtosecond Collisional Dynamics via Resonant X-Ray Spectroscopy, *Phys. Rev. Lett.* **120**, 055002 (2018)
2. Alberto G. de la Varga, Non-maxwellian electron distributions in time-dependent simulations of low-z materials illuminated by a high-intensity x-ray laser, *High Energy Density Phys.* **9**:542–547, 2013.



## **POSTERS**





## Impact of using realistic partition functions to calculate kilonova opacities

Helena Carvajal Gallego<sup>1</sup>

<sup>1</sup>*Atomic physics and Astrophysics, Mons university, B-7000 Mons, Belgium*

On August 17, 2017, the LIGO-VIRGO collaboration observed a neutron star merger thanks to the first detection of gravitational waves. They also detected an explosion of hot and radioactive matter called a kilonova [1]. In the latter, there are nuclear reactions that form heavy nuclei (heavier than iron) such as lanthanides ( $Z = 57 - 71$ ) which play a particular role. In fact, given their rich spectra, they strongly contribute to the opacity affecting radiation emission [2]. In order to interpret the spectrum of a kilonova, it is therefore crucial to precisely know the radiative parameters characterizing these elements. Over the past few years, several studies have been carried out (see e.g. [3-4]), for the first degrees of ionisation (up to 3+) but almost all these investigations were limited to the analysis of kilonovae in a temperature range below 20 000 K. To extend the study to early phases of kilonovae (i.e.  $T > 20\,000$  K), it is essential to know the radiative parameters of lanthanide ions in higher charge stages (see e.g. [5-7]). Thanks to the calculation of lanthanides' atomic data for different degrees of ionization, we can calculate the expansion opacities using the expansion formalism [8-10].

In all of the works mentioned (except in [7]) the partition function,  $U(T)$ , was approximated to the statistical weight of the ground level,  $g_0$ , for the computation of the Sobolev optical depth. This approximation has a significant impact on the computed opacities. The main goal of this present work is to show how it can affect the expansion opacity for a couple of lanthanide examples, namely for samarium (Sm) in the case of early-phase kilonova conditions ( $t = 0.1$  day after the merger), which is associated with moderately-charged species (Sm V - XI) and for neodymium (Nd) in the case of plausible conditions in the kilonova ejecta that should take place about 1 day after the neutron star merger (NSM), corresponding to the presence of lowly-ionized elements in the ejecta (Nd II - IV) [11].

### References

1. B. Abbott et al., Phys. Rev. Lett. 119, 161101 (2017)
2. D. Kasen et al., Nature 551, 80 (2017)
3. Gaigalas G., Kato D., Rynkun P., Radziute L., Tanaka M., ApJS , 240, 29, (2019)
4. Tanaka M., Kato D., Gaigalas G., Kawaguchi K., MNRAS , 496, 1369, (2020)
5. Carvajal Gallego H., Berengut J. C., Palmeri P., Quinet P., MNRAS, 509,6138, (2022)
6. Carvajal Gallego H., Berengut J. C., Palmeri P., Quinet P., MNRAS, 513,2302, (2022)

- 
7. Carvajal Gallego H., Deprince, J., Berengut J. C., Palmeri P., Quinet P., MNRAS, 518, 332-352, (2023)
  8. Karp H., Lasher G., Chan K. L., Salpeter E. E., ApJ , 214, 161, 1977
  9. Eastman R. G., Pinto P. A., ApJ, 412, 731, 1993
  10. Kasen D., Thomas R. C., Nugent P., ApJ, 651, 366, 2006
  11. Carvajal Gallego H., Deprince, J., Godefroid, M., Goriely, S., Palmeri P., Quinet P., Eur. Phys. J. D, submitted (2023)

**Atomic data calculations for electric dipole transitions in doubly-, trebly- and quadruply-charged rhenium ions (Re III–V) of interest to nuclear fusion research****Maxime Brasseur<sup>1</sup>, Sébastien Gamrath<sup>1</sup>, Pascal Quinet<sup>1</sup>**<sup>1</sup>*Université de Mons, Belgium*

It is now well established that tungsten will be one of the main divertor components of the ITER nuclear fusion reactor. When D-T fusion takes place, very energetic neutrons will strike the walls of the reactor and cause the transmutation of tungsten atoms by irradiation. The primary transmutation products for tungsten are rhenium, osmium and tantalum. In particular, the calculations revealed that, after 5-year irradiation under first wall fusion power-plant conditions in ITER, Re, Os and Ta would reach concentrations of 3.8, 1.4, and 0.8 atomic percentage, respectively. As with tungsten, during fusion operations, these atoms, and more particularly rhenium atoms, will be torn from the reactor wall and enter the plasma where they will constitute impurities contributing to the energy loss by radiation but can also be used for plasma temperature and density diagnostics from the analysis of their spectra in all ionization stages. Therefore the radiative properties of these ions have potential important applications in this field. The purpose of the present work is to provide a new set of atomic data (oscillator strengths and transition probabilities) for electric dipole lines in rhenium ions, from Re III to Re V, obtained using two independent theoretical approaches, i.e. the pseudo-relativistic Hartree-Fock (HFR) and the fully relativistic Dirac-Hartree-Fock (MCDHF) methods.

## Lanthanide and actinide opacity computations for kilonova modeling

Jérôme Deprince<sup>1</sup>

<sup>1</sup>*Université Libre de Bruxelles, Belgium*

Gravitational waves from the neutron star merger GW170817 were detected for the first time in August 2017 [1]. Such an astrophysical event also provokes the ejection of hot and radioactive matter which powers an electromagnetic signal known as kilonova. This first observation also provided evidences that rapid neutron-capture process (or r-process) of nucleosynthesis responsible for heavy element production takes place during these events. The luminosity and spectra of such radiative emission depend significantly on the ejecta opacity, which is dominated by millions of lines from f-shell elements newly created by r-process, i.e. lanthanides and actinides [2]. Atomic data and opacities for these elements are thus sorely needed to model and interpret kilonova light curves and spectra.

In this context, the present work focusses on atomic data and opacity computations for lanthanides and actinides. More specifically, since the observations of the kilonova AT2017gfo (the GW170817 electromagnetic counterpart) have been recorded about one day after the neutron star merger happened, the kilonova temperature and density are such that only the first ionization stages of the ejected elements (from the neutral to three-time ionized species) are expected to be present in the ejecta [3].

In this contribution, we plan to discuss our new computations of atomic data and expansion opacities for all the weakly-ionized lanthanides and actinides and compare them with previously reported studies (e.g., [3-6]). In order to do so, we use the pseudo-relativistic Hartree-Fock (HFR) method as implemented in Cowan's code [7], in which the choice of the interaction configuration model is of crucial importance.

### References

1. Abbott B. et al., Phys. Rev. Lett. 119, 161101 (2017).
2. Just O. et al., Mon. Not. Roy. Astr. Soc. 510, 2820 (2022).
3. Tanaka M. et al., Mon. Not. Roy. Astron. Soc. 496, 2 (2020).
4. Gaigalas G. et al., Astrophys. J. Suppl. Ser. 240, 29 (2019).
5. Silva R.F. et al., Atoms 2022, 10-18 (2022).
6. Fontes C.J. et al., Mon. Not. Roy. Astr. Soc. stac2792. arXiv:2209.12759v1 (2022).
7. R.D. Cowan, The Theory of Atomic Structure and Spectra (University of California Press, Berkeley, 1981).

## Hyperfine structure splitting and the Zeeman effect of $^{83}\text{Kr}$ in laser absorption spectroscopy investigated at the linear plasma device PSI-2

Marc Sackers<sup>1</sup>, Oleksandr Marchuk<sup>1</sup>, Dipti<sup>2</sup>, Stephan Ertmer<sup>1</sup>, Yuri Ralchenko<sup>3</sup>, Arkadi Kreter<sup>1</sup>

<sup>1</sup>*Forschungszentrum Jülich, Germany*

<sup>2</sup>*International Atomic Energy Agency*

<sup>3</sup>*National Institute of Standards and Technology, USA*

Magnetic-field-induced transitions have recently seen an enormous increase in interest. They arise due to the mixing of magnetic sublevels that start to occur in the non-linear region of the Zeeman effect. Especially concerning highly charged ions, the modeling is based on MCDHF calculations that are perturbed by the diagonalization of the full Zeeman interaction matrix [1].

However, this is not the only approach since, in the early days of quantum mechanics, C. G. Darwin correctly modeled the line splitting and line intensities of fine structure atoms from the weak field through the Paschen-Back regime [2]. Goudsmit and Bacher extended this model to hyperfine structure (HFS) atoms [3].

In this talk, laser absorption spectra measured at the linear plasma device PSI-2 from the metastable Kr I  $5s$  levels are investigated using both methods. The magnetic field strength (20 mT to 90 mT) provides different conditions for the isotopes of krypton. Regarding the even-numbered isotopes, the magnetic field is just a small perturbation on top of the fine structure. However,  $^{83}\text{Kr}$  has a much finer level splitting (HFS) due to its non-zero nuclear spin generating substantial magnetic sublevel mixing. The corresponding analysis reveals the non-linear dependency of the magnetic sublevel splitting on the field strength and a substantially changing relative intensity distribution of the magnetic subtransitions.

### References

1. W. Li et al., Hfszeeman95—A program for computing weak and intermediate magnetic-field- and hyperfine-induced transition rates, *Comput. Phys. Commun.* 2020, **253**, 107211.
2. C. G. Darwin, The Zeeman effect and spherical harmonics, *Proc. R. Soc. Lond.* 1927, A **115**, 1-19.
3. S. Goudsmit and R. F. Bacher, The Paschen-Back Effect of Hyperfine Structure, *Phys. Rev.* 1929, **34**, 1499-1500.

## **The effect of toroidal magnetic field strength on the energy of runaway electrons in Damavand tokamak**

**Banafsheh Pourshahab<sup>1</sup>**

<sup>1</sup>*School of Plasma Physics and Nuclear Fusion, Nuclear Science and Technology Research Institute, AEOI, Iran*

In addition to the ohmic heating of the plasma, toroidal electric field in tokamaks which crosses a critical limit, leads to the acceleration of plasma electrons to relativistic energies. Due to the inability of the tokamak magnetic fields to confine them, these energetic electrons escape from the plasma column and collide with the vacuum chamber wall and the plasma facing components. As a result of the collision of these electrons with the target, hard X-rays are produced due to the bremsstrahlung process, and these radiations, in addition to causing serious damage to the wall materials, can carry information about their generating electrons.

In this research, the spectrum of hard X-rays emitted from Damavand tokamak at different times of discharge has been studied. Also, the effect of toroidal magnetic field intensity on the energy spectrum of runaway electrons and their confinement quality in Damavand tokamak was investigated. The results showed that the presence of stronger toroidal magnetic fields causes more confinement of the runaway electrons in the discharge column and thus increases their average energy. According to these results, it can be expected that tokamaks with stronger toroidal magnetic fields are subject to more damage by runaway electrons.

## Study of radiative properties of helium isoelectronic sequence

**Haikel Jelassi**<sup>1</sup>

<sup>1</sup>*National Centre for Nuclear Sciences and Technologies, Tunisia*

The heavy elements with high  $Z$  are of potential interest in controlled thermonuclear fusion and astrophysics. Indeed, they could be used in plasma-facing materials such as the divertors in tokamaks and/or could be generated by neutron-induced transmutations of divertor's materials. Therefore, extensive spectroscopic studies, both experimental and theoretical, have been performed in the last years in order to estimate the power loss from the impurities in the forthcoming fusion reactors [1].

In this work, two independent theoretical atomic structure computational approaches have been considered, i.e. the ab initio multiconfiguration Dirac-Hartree-Fock with subsequent relativistic configuration interaction method (MCDHF-RCI) implemented in the code GRASP2018 [2] and the Dirac-Fock-Slater (DFS) implemented in the code FAC (Flexible Atomic Code) [3]. The relativistic configuration interaction method was applied to estimate the electron correlation effects.

The radiative properties of ions ( $Z = 2 - 53$ ) belonging to the helium isoelectronic sequence are reported. Energy levels for the ground state and the lowest  $1s2l$  singly excited states are considered. The effects of correlation effects are studied for the selected ions by increasing the active set (AS). Relativistic effects such as the Breit interaction and the QED corrections are also computed. The transition probabilities and the oscillator strengths have been calculated for E1, E2, M1 and M2 transitions spanning the spectral range from UV to IR regions. Our results are compared with available experimental and other theoretical values. Good agreement was found for the majority of cases. Lifetimes are also considered in this work, first to check the accuracy of calculated results of transitions rates and second, to complete the databases by a complete and accurate values of lifetimes. This can help future works by experimentalists to compare their results with those results calculated theoretically.

Finally, this study underlines the importance of relativistic corrections especially for the heavy atomic ions. This computational approach enables us to present a consistent and improved data set of all-important atomic data of the helium isoelectronic sequence, which are useful for identifying transition lines in further investigations.

### References

1. A. J. H. Donne et al., Nucl. Fusion 47 (2007) S337.
2. C. Froese Fischer, G. Gaigalas, P. Jönsson, and J. Bieroń, Comput. Phys. Commun., 237 (2019) 184.
3. M. F. Gu, Can. J. Phys. 86 (2008) 675-689.

## Electron-impact single ionization for $N^+$ ion

Valdas Jonauskas<sup>1</sup>

<sup>1</sup>*Institute of Theoretical Physics and Astronomy, Vilnius University, Lithuania*

Impurities of the low- and medium- $Z$  elements injected into the fusion reactors are used to control the heat load from the hydrogen plasma. The radiative cooling from the injected impurities depends on the charge state distribution of ions. Radiative recombination and electron-impact ionization define the charge state distribution in the fusion plasma. Nitrogen is one of the elements that can be used to protect plasma-facing components in fusion reactors.

The aim of the current work is to analyze single ionization for the  $N^+$  ion by including both direct and indirect processes from the levels ( $^3P_0$ ,  $^3P_1$ ,  $^3P_2$ ,  $^1D_2$ ,  $^1S_0$ ) of the ground configuration. The indirect process being investigated is electron impact excitations to autoionizing states followed by Auger transitions. The indirect process includes the excitations from the  $2s$  subshell up to shells with the principal quantum numbers  $n \leq 10$ . The excitations from the  $2p$  subshell lead to configurations below the single ionization threshold. The direct ionization is analyzed from the  $2s$  and  $2p$  subshells of the ground configuration of the  $N^+$  ion.

The scaled distorted wave (SDW) [1] cross sections are employed to analyze experimental data for the  $N^+$  ion [2, 3] since the distorted wave calculations strongly overestimate measurements. Contribution of the indirect process to the total ionization cross sections is  $\sim 10\%$  at its maximum for levels of the ground configuration. It should be noted that previous studies [2, 3] did not take into account the contribution from the indirect process in determining the total ionization cross sections.

The SDW cross sections for the ground term match well with measurements [3] taken at energies starting from the ionization threshold and extending up to near peak energy. The peak cross sections are  $\sim 4\%$  lower than the measured ones. Difference between the theoretical and experimental values indicates the presence of metastable states in the ion beam.

Modeling shows that population of the excited terms does not exceed  $\sim 50\%$  for the latest experimental data [3]. However, the larger population of the excited states is obtained in the previous measurements [2]. In addition, an onset of the cross sections below the ionization threshold in the experimental data [3] further supports the existence of metastable states in the measurements. It should be noted that the experimental data obtained using the crossed electron - ion beam technique [2] show a better agreement with the theoretical cross sections for the  $^1D_2$  level of the ground configuration.

### References

1. V. Jonauskas, *Astron. Astrophys.* **620**, A188 (2018).



- 
2. I. Yamada *et al.*, J. Phys. Soc. Jpn **58**, 1585 (1989).
  3. J. Lecointre *et al.*, J. Phys. B: At. Mol. Opt. Phys. **46**, 205201 (2013).

## Fe XVII line emission problem

**Chintan Shah**<sup>1,2</sup>

<sup>1</sup>*NASA Goddard Space Flight Center, US*

<sup>2</sup>*Max-Planck-Institute für Kernphysik, Heidelberg, Germany*

Iron, the most abundant heavy element in the universe, is essential for spectroscopic studies. X-ray astronomers use the emission lines from highly ionized iron states like Fe XVII to study properties of hot celestial plasmas. These emission lines, which result from atomic processes like electron-impact excitation, dielectronic recombination, resonance excitation, and charge exchange, allow researchers to diagnose electron temperature and density, elemental abundance, velocity turbulence, and opacity parameters of hot plasmas. However, for over four decades, the intensity ratio between two strong lines from 3d–2p transitions, 3C and 3D, has been low in lab experiments, differing from theoretical predictions of a high ratio. Similar discrepancies have also been observed in the ratio between line emission complexes 3d–2p and 3s–2p transitions. This has impacted the reliability of Fe XVII as a diagnostic tool in the astronomy and fusion communities. Here I will present targeted laboratory measurements [1–8] using electron beam ion traps and various spectrometers to measure individual line formation atomic processes that contribute to the overall line emission of Fe XVII. These measurements benchmark state-of-the-art atomic theories and improve atomic data in spectral plasma models, such as SPEX and AtomDB, which are crucial for achieving the scientific objectives of XRISM and Athena space missions.

### References

1. C. Shah et al., ApJ 881, 100, (2019).
2. S. Kühn, C. Shah et al., PRL 124, 225001 (2020).
3. F. Grilo, C. Shah et al., ApJ 913, 140 (2021).
4. G. J. Grell, M. A. Leutenegger, C. Shah, ApJ 917, 105 (2021).
5. L. Gu, et al., A&A 627, A51 (2019).
6. L. Gu, C. Shah et al., A&A 641, A93 (2020).
7. L. Gu, C. Shah et al., A&A 664, A62 (2022).
8. S. Kühn, et al., PRL 129, 245001 (2022).

**Collisional-radiative calculations and EUV emission of low-density tungsten plasmas in the temperature range 800 – 5000 eV****Olivier Peyrusse<sup>1</sup>**<sup>1</sup>*Aix-Marseille Université, CNRS, Laboratoire LP3, Marseille, France*

We present specific configuration-average (CA) collisional-modeling calculations of tungsten plasmas at low electron density  $N_e = 5 \times 10^{13} \text{ cm}^{-3}$  for electron temperatures in the range 0.8 to 5 keV. These conditions are relevant to current tokamaks. In this temperature range, the modeling of the ionization balance and of the spectra is a long-standing problem.

We discuss here the problem of ensuring completeness of the list of configurations included in the calculations. We also present comparisons of experimental measurements in the EUV range performed at tokamak WEST, with calculated spectra based on the use of the unresolved transition array (UTA) and of the spin-orbit split array (SOSA) formalisms.

A conclusion is that standard calculation methods used for the evaluation of the configuration-average collisional and radiative rates, are fine provided that a correct list of configurations is used in the calculations.

## Neutralisation of highly charged ions at surfaces

**Anna Niggas<sup>1</sup>, Matthias Werl<sup>1</sup>, Richard Wilhelm<sup>1</sup>**

<sup>1</sup>*Institute of Applied Physics, TU Wien, Austria*

Radiative and non-radiative decay are both important de-excitation mechanisms of ions. To study these processes, collisions including ions in very high charge states ( $q \geq 20$ ) are an ideal playground: When close to a surface, resonant electron transfer leads to a population of high- $n$  shells (with  $n \sim q$  [1]), initiating a de-excitation cascade of this – then neutral albeit still highly excited – projectile. X-ray emission is one of the de-excitation channels, however the measured yield drops with decreasing ion charge states [2,3]. To understand this behaviour it is crucial to consider also competing mechanisms, e.g. non-radiative Auger-like processes leading to the emission of electrons instead of photons.

We perform coincidence measurements to correlate the ion charge states after transmission through atomically thin samples [4] with electrons emitted during the interaction (energy and yield information) [5]. This allows us to disentangle de-excitation channels and identify participating processes in the neutralisation of highly charged ions upon interaction with a surface.

### References

1. J. Burgdörfer et. al., Phys. Rev. A, 44 5674 (1991).
2. J. Schwestka et al., Nucl. Instrum. Methods Phys. Res. B 422 63 (2018).
3. L. Jabłoński et al., J. Phys.: Conf. Ser. 1412 202002 (2020).
4. A. Niggas et al. Commun. Phys., 4 180 (2021).
5. A. Niggas et al. Phys. Rev. Lett., 129 086802 (2022).

## X-ray spectroscopy of Ne-like W in fusion plasmas

**Oleksandr Marchuk<sup>1</sup>**

<sup>1</sup>*Forschungszentrum Jülich, Germany*

Measurements of plasma parameters in the core of magnetic fusion devices represent a challenging task. Expected emission of x-ray lines of highly charged ions of W will be used in ITER or DEMO for derivation of electron and ion temperature, plasma rotation and finally the plasma control. In spite of considerable efforts to design the x-ray instruments operating in extreme harsh environment of future plasma devices [1], the accurate modelling of such spectra is still far from been complete [2].

The aim of this work is to provide the accurate effective rate coefficients for the lines in the spectral region of 1.35 Å to 1.5 Å of the contributing charged stages of W necessary in plasma modelling. The synthetic spectra are decomposed in contribution from Mg-, Na-, Ne-, F-, and O-like ions. This work provides probably the most complete set of atomic data for interpretation of the future X-ray spectra. Indeed, whereas the Ne-like ions are in general responsible for the line formation at the core of plasma devices, e.g., in the temperature range of 15 – 25 keV, the contribution from Na- and F-like ions remains considerable. We demonstrate here an overlooked impact of inner-shell ionization of Na-like W ions on the line formation of some of Ne-like lines. The intensity of some of the lines increase by up to 30 % which challenge the selection of the X-ray line to be measured in ITER or DEMO.

The calculations were performed with the collisional-radiative model NOMAD [3] using the FAC code [4] calculations of elementary atomic processes such as electron-impact rates, radiative and autoionization rates, etc. The model includes about 103 - 104 levels in each ion. We identified 51 lines in this interval which we describe in terms of effective rate coefficients of excitation  $Q^{\text{exc}}$ , recombination  $Q^{\text{rec}}$  and inner-shell ionization  $Q^{\text{ion}}$ :

$$I(T)\lambda \propto N_e N_{[\text{Ne}]} Q^{\text{exc}}(T) + N_e N_{[\text{Na}]} Q^{\text{ion}}(T) + N_e N_{[\text{F}]} Q^{\text{rec}}(T), \quad (1)$$

where  $T$  is the electron temperature,  $I$  is the line intensity,  $\lambda$ , is the wavelength corresponding to the specific bound-bound transition,  $N_{[\text{He}]}$ ,  $N_{[\text{Na}]}$  and  $N_{[\text{F}]}$  are the fractions of the Ne-, Na- and the F-like W ions, respectively. The tabulated values of fit results for the effective rate coefficients are presented. The errors of such decomposition remain on the order of 1 % and below in comparison to exact calculations and should provide a reliable basis for integrated plasma modelling of X-ray spectra from W ions.

### References

1. Cheng Z. et al, Review of Scientific Instruments 93 073502 (2022).
2. Beiersdorfer P. et al, J. Phys. B: At. Mol. Opt. Phys. 43 144008 (2010).

- 
3. Ralchenko Yu. V. and Maron Y J. *Quant. Spectrosc. Radiat. Transfer* 71 609 (2001).
  4. Gu, M. F. *ApJ*, 582, 1241 (2003).

---

## Progress of $Z$ -dependence analysis of soft X-ray spectra from highly charged heavy ions using high-temperature plasmas

**Chihiro Suzuki**<sup>1</sup>

<sup>1</sup>*National Institute for Fusion Science, Japan*

Soft X-ray emission spectra from highly charged heavy ions are of particular interest in nuclear fusion research, industrial light source applications as well as basic atomic physics. Though a number of experimental spectra have been recorded so far in tokamaks and electron beam ion traps (EBITs), the available data are still insufficient to complete the atomic number ( $Z$ ) dependencies for the elements in the 5th and higher periods. In the last decade, therefore, we have systematically recorded soft X-ray spectra from highly charged ions of various heavy elements using high-temperature plasmas produced in the Large Helical Device (LHD) at the National Institute for Fusion Science.

In this paper we present recent progress of  $Z$ -dependence analysis for the soft X-ray spectra from highly charged ions of the elements with  $Z$  from 57 to 74, based on the experimental data taken in the LHD. In particular, we focus on the isolated lines of Cu-, Zn-, Ga-like ions which have relatively simple spectral features. The measured wavelengths are compared with the other data taken in tokamaks and EBITs, as well as theoretical values calculated with a multi-configuration Dirac-Fock code. In addition, the  $Z$  dependencies are interpolated or extrapolated to assign unidentified lines. As a result, a number of lines have been experimentally identified for the first time. Some of the results clearly manifest large effects of configuration interaction and spin-orbit interaction, which are peculiar to highly charged heavy ions.

---

## Large scale atomic calculations for fluorescence yield determination

**Daniel Pinheiro<sup>1</sup>, Gonçalo Baptista<sup>1</sup>, André Fernandes<sup>1</sup>, César Godinho<sup>1</sup>, Jorge Machado<sup>1</sup>, Filipe Grilo<sup>1</sup>, Luís Sustelo<sup>1</sup>, Jorge M. Sampaio<sup>2</sup>, Pedro Amaro<sup>1</sup>, Roberta G. Leitão<sup>1</sup>, José P. Marques<sup>2,3</sup>, Fernando Parente<sup>1</sup>, Paul Indelicato<sup>5</sup>, Miguel de Avillez<sup>4,6</sup>, José Paulo Santos<sup>1</sup>, Mauro Guerra<sup>1</sup>**

<sup>1</sup>*Laboratory for Instrumentation, Biomedical Engineering and Radiation Physics (LIB-Phys), Portugal*

<sup>2</sup>*Laboratory of Instrumentation and Experimental Particle Physics, Portugal*

<sup>3</sup>*Faculty of Sciences of the University of Lisbon, Portugal*

<sup>4</sup>*Computational Astrophysics Group, Institute for Research and Advanced Training, University of Evora, Portugal*

<sup>5</sup>*Laboratoire Kastler Brossel, Sorbonne Université, CNRS, ENS-PSL Research University, Collège de France, France*

<sup>6</sup>*Zentrum für Astronomie und Astrophysik, Technische Universität Berlin, Germany*

When analysing and modeling the emissions of astrophysical events or plasmas an important quantity and benchmark is the fluorescence yield (FY). This will change according to the element, as well as the charge state we are modeling. These FYs can be calculated from first parameters, according to the atomic system, and can later be used in modeling codes to provide more accurate emitting models.

In this work, we discuss the computation requirements for the large scale calculation of FYs from first parameters. We will also explore how we presently calculate FYs using a state-of-the-art multiconfiguration Dirac-Fock approach. Additionally, we will give an example of recent K- and L- shell FY values for the full isonuclear sequence of Fe ions, which were found to be very similar up to the removal of 14 electrons.



---

## Single and double electron capture cross sections for $\text{Sn}^{3+}$ ions impacting on $\text{H}_2/\text{D}_2$ molecules in the energy range 50 eV – 50 keV

Klaas Bijlsma<sup>1</sup>

<sup>1</sup>*University of Groningen, Netherlands*

State-of-the-art nanolithography machines work with light in the extreme ultraviolet (EUV) regime. This light is generated by a laser-produced plasma (LPP) of Sn. Apart from the EUV photons, the LPP also emits highly charged Sn ions with up to several tens of keV of energy that may damage plasma-facing surfaces. Therefore, industry uses a buffer gas of  $\text{H}_2$  to slow these ions. In consecutive charge exchange reactions, the charge state of the Sn ions is reduced. Stopping cross sections are known to be charge-state dependent. Models used for optimization of industrial EUV sources therefore require accurate atomic data in the form of both charge exchange and stopping cross sections.

We have been working on generating this missing data at the ZERNIKELEIF facility where we can generate a beam of Sn ions of a pre-selected energy, charge state, and mass (isotope). At a high-voltage platform, we let the Sn ions traverse a jet of  $\text{H}_2$  gas and subsequently analyze the ion beam characteristics with a retarding field analyzer (RFA). By setting appropriate voltages on the RFA grid, we can separate and measure the different charge states that result from the charge exchange reactions. Using this new setup, we have measured the single electron capture cross section ( $\sigma_{32}$ ) for  $\text{Sn}^{3+}$  on  $\text{H}_2$  over the wide energy range of 50 eV to 50 keV. Moreover, by varying the pressure of  $\text{H}_2$  gas we obtained the double capture cross section  $\sigma_{31}$  as well. The single capture cross sections are found to peak at around 1 keV, whereas the double capture cross sections show a remarkable increase towards our lowest energies. On top of that, a large and unexpected difference between  $\text{H}_2$  and  $\text{D}_2$  is observed. We also calculate the cross sections using a semi-quantal framework.

We will present the experimental and theoretical data and discuss the possible origins of the observed behavior. In addition we will discuss the relevance of our data to state-of-the-art EUV nanolithography machines.

---

## Calculation of dielectronic recombination cross section For lithium-like Ni<sup>25+</sup> ion-system using Flexible Atomic Code (FAC)

**Mohammad Gharaibeh<sup>1</sup>, Eman Al-Mustafah<sup>2</sup>**

*<sup>1</sup>Physics Program, Department of Mathematics, Statistics and Physics, College of Arts and Sciences, Qatar University*

*<sup>2</sup>Physics Department, College of Science and Art, Jordan University of Science and Technology*

In this study we used FAC code method to study the dielectronic recombination for three electron system of Lithium-like Ni<sup>25+</sup>. The ground state configuration of Ni<sup>25+</sup> is (1s<sup>2</sup> 2s<sub>1/2</sub>). This configuration has been implemented in the scripts of FAC code that follow the *jj* coupling scheme. Comparison between our calculations and experimental results for ground states of Ni<sup>25+</sup> is made. Present calculations were performed for the energy of the resonances and their resonance strength in the excitation of 2s electron to 2p electron and with capturing the incident electron in shell with  $n \geq 13$  up to  $n = 19$ . The energy positions have shown a good agreement with the experimental values, where the resonance strength shows some discrepancies in some of the resonances.

## **Laser-induced double ionization of helium gas and pulse self-compression for table-top light sources**

**Devki Nandan Gupta**<sup>1</sup>

<sup>1</sup>*University of Delhi, India*

We investigate the spatiotemporal dynamics of a high-intensity laser pulse in a tunnel ionizing gas. We propose a way to compress the laser pulse using gas ionization in high-intensity regime. Transverse focusing and longitudinal compression are examined by characterizing the beam spot size in space and time, incorporating the gas ionization processes, relativistic mass variation, and ponderomotive effects. The results show that the inclusion of laser-induced double ionization of helium gas modifies the plasma density, which significantly affects the laser pulse evolution. For intense laser pulse, relativistic-ponderomotive nonlinearity enhances the pulse compression and consequently the self-focusing of the laser pulse. The compression mechanism and the localization of the pulse intensity both are boosted by the modified electron density via a dielectric function. Our results show the generation of 20 femtosecond laser pulses focused to 20 micrometer spot size. These results promise to be a method for the generation of table-top light sources for ultrafast high-field physics and advanced optics.

## Electron-impact excitation and dielectronic recombination cross-sections of tungsten ions

Neelam Shukla<sup>1</sup>

<sup>1</sup>*University of Nebraska Kearney, USA*

The study of electron-ion collisions always be a prime area of research as it provides the fundamental understanding of the dynamical behavior of different atomic processes in the high temperature plasma. During the collisions, the electrons can be recombined with ions through different reactions such as electron-impact excitation (EIE), dielectronic recombination (DR) and many more. In EIE process, the ions get excited through the collisions with highly energetic electrons followed by the radiative decay. This radiation loss affects the plasma ignition process and stability. Conversely, the DR usually occurs at lower electron energy compared to EIE and changes the charge state of the ions. Thus, it affects both the radiative energy losses and ionization balance in the plasma. An accurate information of these atomic processes thus plays a significant role in the diagnostics of plasma. The present work entails the calculation of EIE and DR cross-sections for Tungsten ions ( $W^{27+}$  to  $W^{29+}$ ) as they are being evaluated as prospective plasma-facing materials in magnetic confinement devices like the ITER tokamak [1–2]. These ions are selected from the recent experiment performed at NIFS Japan [3]. The calculations are performed using the relativistic method and the required wave functions are calculated using Multi-configuration Dirac-Fock method through GRASP2K, and Flexible Atomic Code (FAC). The accuracy of these wave functions is ascertained by comparing the transition energies and oscillator strengths with the previously reported measurements [3].

### References

1. N. Shukla, T. Das, and R. Srivastava, *J. Quant. Spectrosc. Radiat. Transf.* 222–223, 247 (2019).
2. N. Shukla, Priti, L. Sharma, and R. Srivastava, *Eur. Phys. J. D* 73, 109 (2019).
3. H. A. Sakaue, D. Kato, N. Yamamoto, N. Nakamura, and I. Murakami, *Phys. Rev. A* 92, 012504 (2015).

## Calculations of atomic structures and electron impact excitation cross sections of B-like Xe<sup>49+</sup>

**Lalita Sharma<sup>1</sup>, Shikha Rathi<sup>1</sup>, Aloka Kumar Sahoo<sup>1</sup>**

<sup>1</sup>*Indian Institute of Technology (IIT), Roorkee, India*

Atomic parameters of highly charged ions (HCI) are primely important for plasma control and diagnostics. A large amount of atomic data is needed to develop new spectral diagnostics for studying magnetic fusion plasma. Xenon, a rare gas, has been widely used in diagnosing tokamak fusion plasmas, for example, in ITER. The temperatures in these magnetic fusion devices can go up to 25 keV, producing all possible highly charged states of Xe ions, hence necessitating the atomic data for highly charged xenon ions.

Recently, studies on calculating the atomic parameters of various HCIs of xenon have been reported. However, there is a scarcity of extensive results for boron-like Xe. In fact, the NIST ASD has no results for energies and transition lines for boron-like Xe. Motivated by the significance of atomic data of various ions of Xe in plasma physics, we aim to carry out an extended calculation to provide atomic parameters for boron-like Xe ions.

In the present study, the energies, electric dipole (E1) transition parameters, hyperfine interaction constants, Lande  $g_J$  and isotope shift factors are calculated for the 213 levels of boron-like Xe ions using the multi-configuration Dirac-Hartree-Fock (MCDHF) theory. The levels under consideration include  $1s^22s^2nl$ ,  $1s^22p^2nl$ , and  $1s^22s2pnl$ , where  $n = 2 - 5$  and  $l = s, p, d$  and  $f$ , and are referred to as the multireference (MR) set. Calculations are done independently on even and odd states. A restrictive active space (AS) approach is used to monitor the convergence of the wave function. Active spaces (virtual orbitals) from  $n = 4$  to  $n = 9$ , with  $l = s, p, d$ , and  $f$  are considered. The effect of electron correlations is studied by performing two different calculations in core-core and core-valence correlations. The significance of including the QED (self-energy and vacuum polarization) effects and Breit interactions on the atomic structure parameters is also analyzed. Our results agree well with the previous theoretical and experimental results wherever available. Having established the accuracy of the ionic wavefunctions, we further study electron impact excitation of Xe<sup>49+</sup> using relativistic distorted wave approximation. The effective collision strengths are obtained from the calculated cross sections and assuming Maxwellian distribution of electrons' energy. Most of the present results are reported for the first time, and we hope these results will benefit plasma physics studies.

## Collisional-radiative modeling of the tungsten spectrum from the EBIT and EAST tokamak

Cunqiang Wu<sup>1</sup>, Lirong Lei<sup>1</sup>, Peng Yang<sup>1</sup>, Yile Liu<sup>1</sup>, Xiaobin Ding<sup>1</sup>, Fengling Zhang<sup>2</sup>, Ling Zhang<sup>2</sup>, Ke Yao<sup>3</sup>, Yang Yang<sup>3</sup>, Yunqing Fu<sup>3</sup>, Fumihiko Koike<sup>4</sup>, Izumi Murakami<sup>5</sup>, Daiji Kato<sup>5</sup>, Hiroyuki A. Sakaue<sup>5</sup>, Nobuyuki Nakamura<sup>6</sup>, Chenzhong Dong<sup>1</sup>

<sup>1</sup>*Northwest Normal University, China*

<sup>2</sup>*Institute of Plasma Physics, Chinese Academy of Sciences*

<sup>3</sup>*Fudan University, China*

<sup>4</sup>*Sophia University, Japan*

<sup>5</sup>*National Institute for Fusion Science, Japan*

<sup>6</sup>*Institute for Laser Science, The University of Electro- Communications, Japan*

The atomic structure, transition properties, kinetic processes, and emission spectra of tungsten ions are extremely important for diagnosing edge and impurity plasmas in the next-generation magnetic confined fusion reactors (such as ITER). For diagnostics, the accurate atomic data, such as the energy level, radiative transition rate, electron collisional excitation cross section, etc., and appropriate plasma model are required. Most of the atomic spectrum of the highly charged tungsten ions is measured from the electron beam ion trap (EBIT) and the fusion reactor such as JET, EAST Tokamak. These spectra need to be analyzed with the aid of the theoretical calculation on the atomic data and the collisional-radiative (CR) model.

The wavelength and transition rate of the  $5p - 5s$  transition of  $W^{13+} - W^{15+}$  ions have been calculated by the relativistic configuration interaction method with the implementation of the flexible atomic code (FAC). And reasonable CR model has been constructed to simulate these spectra observed in EBIT. The results are in reasonable agreement with the available experimental and theoretical data. The confusion on the assignment of the ionization stage to the spectrum is pointed out in the present work.

The wavelength and transition rates of  $W^{43+} - W^{45+}$  ions in the  $40 - 140 \text{ \AA}$  region have also been investigated to analyze the experimental spectrum from the EAST Tokamak. The result makes a reasonable agreement with the available experimental and theoretical data. The synthetic spectrum from the CR model agreed with the experimental spectrum. Some strong emission lines of the  $W^{43+} - W^{45+}$  ions are identified and assigned in the present work. Finally, according to the dependence of the intensity ratio on the electron temperature, some transition pairs are proposed as the diagnosis lines.

### References

1. R. Janev, *Contemp. Phys.*, 46, 121 (2005)
2. M. F. Gu, *Can. J. Phys.*, 86, 675 (2008)

- 
3. X.B. Ding et. al., Phys. Rev. A, 101, 042509 (2020)
  4. X.B. Ding et. al., Phys. Lett. A, 420, 127758 (2021)
  5. Y. L. Liu et. al., Phys. Lett. A, 454, 128500 (2022)

### **Acknowledgements**

This work was supported by the National Natural Science Foundation of China (Grant No.12274352).

## Study of $K\alpha$ X-ray source size based on high-intensity femtosecond laser-solid interaction

Mathieu Gambari<sup>1</sup>, Olivier Peyrusse<sup>1</sup>

<sup>1</sup>*Aix-Marseille Université, CNRS, Laboratoire LP3, Marseille, France*

Table-top plasma X-ray sources driven by high-peak power (fs) laser sources are of high applicative interest for imaging and material science [1,2] because of their capability to provide hard energetic, jitter-free point-source pulsed X-ray sources suitable for phase-contrast imaging or (time-resolved) X-ray diffraction. We thus study the characteristics (mainly here focusing on its size evolution) of a hard  $K\alpha$  Mo X-ray source ( $E_{K\alpha} = 17.48$  keV) produced by a high intensity femtosecond laser interacting with a solid molybdenum target for a wide range of laser intensity ( $I \sim 1 \times 10^{17} - 2.8 \times 10^{19}$  W/cm<sup>2</sup>) and for four values of the temporal Contrast Ratio ( $6.7 \times 10^7 < CR < 3.3 \times 10^{10}$ ). The temporal contrast ratio was varied by inserting or removing saturable absorbers between the different preamplifier stages of the laser chain [3]. Results demonstrate that increasing the laser intensity leads to enlargement of the X-ray source size and this phenomenon is emphasized when the temporal contrast of the laser driving pulse is deteriorated [4]. To explain these observations, we developed dedicated experiments and hydrodynamic simulations to estimate the impact of laser absorption mechanisms and hot electron scattering inside the solid on the evolution of both the X-ray source size and the  $K\alpha$  photon number. However, while bringing light on  $K\alpha$  photon number changes, they do not explain the increase of the X-ray source size. We finally deduce that the most probable mechanism leading to the broadening of the source size is linked to the creation of surface electromagnetic fields which confine the hot electrons at the solid surface [5]. This assumption is supported by experiments made with the highest contrast ratio and in which the evolution of the size enlargement of the X-ray source is studied as a function of the laser focal spot size.

### References

1. R. Schoenlein et al., Phil. Trans. R. Soc. A **377**: 20180384 (2019).
2. M. Gambari et al., Sci. Rep. **10**, 6766 (2020).
3. Y. Azamoum et al., Sci. Rep. **8**, 4119 (2018).
4. M. Gambari et al., Sci. Rep. **11**, 23318 (2021).
5. Y.T. Li et al., Phys. Rev. Lett. **96**, 165003 (2006).



## Computer simulation of Stark profiles accounting for oscillating electric fields

Roland Stamm<sup>1</sup>

<sup>1</sup>*Physique des Interactions Ioniques et Moléculaires, Aix-Marseille Université, France*

Oscillating electric fields are found in many kinds of plasmas. In laboratory and fusion plasmas, they are often generated by an external source, such as a laser or a microwave generator. In such plasmas and in astrophysical plasmas, oscillating fields can also be excited by a local fluctuation, and be amplified by a plasma instability, generating non-thermal plasma waves such as Langmuir waves. We here address the effect of oscillating electric fields on the line shapes emitted by hydrogen atoms in plasmas. This effect has long been studied, and the existence of satellites structures on the line shape has been observed and analyzed, e.g. [1]. In this work, we present new calculations simultaneously taking account of the plasma electric microfield and an oscillating electric field. Due in particular to ion dynamics, the atom is submitted to a complex dynamics difficult to take into account with an analytic approach. We propose the use of a computer simulation of the ion motion providing the ion electric microfield in addition to an oscillating electric field. The electronic field can also be simulated or included in the Hamiltonian by a collision operator. The total field is applied to an emitter for which we solve the Schrödinger equation in order to obtain the quantum evolution operator for one history of the total electric field. This evolution operator allows the calculation of the emitter dipole autocorrelation function once a large number of histories have been calculated. We present different hydrogen lines for plasma densities in the range  $10^{19}$  and  $10^{23} \text{ m}^{-3}$ , and temperatures between 1 and 10 eV.

### References

1. V. Lisitsa, *Atoms in plasmas*, Springer, Berlin, (1994).

---

## The effect of electron correlation on trielectronic recombination rate coefficients for Be-like ions

**Chunyu Zhang<sup>1</sup>, Chongyang Chen<sup>2</sup>, Nigel Badnell<sup>1</sup>**

<sup>1</sup>*Department of Physics, University of Strathclyde, UK*

<sup>2</sup>*Fudan University, China*

The merged-beam rate coefficients of dielectronic and trielectronic recombinations (DR and TR) for Be-like ions have been measured in many experiments. Meanwhile, theoretical data were also calculated with AUTOSTRUCTURE (AS) code for comparison with the measured resonance spectrum. However, TR resonance strengths were generally significantly underestimated by the AS calculations in most cases. In the present work, we find that the electron correlation between DR and TR resonance states with different captured electron principal quantum numbers  $n$  can lead to an obvious improvement in TR resonance strengths, which is cross-validated via the relativistic distorted-wave (RDW) approximation implemented in the Flexible Atomic Code (FAC) and the semi-relativistic distorted-wave (SRDW) approximation implemented in the AS code. Previous theoretical calculations for this system, however, did not include this form of electron correlation.

## **Electromagnetic and atomic processes for nuclear isomer excitation in optical laser-generated plasma**

**Simone Gargiulo**<sup>1</sup>

<sup>1</sup>*École Polytechnique Fédérale de Lausanne (EPFL), Switzerland*

Isomers, or long-lived nuclear excited states, are of significant interest in both fundamental and applied physics. For example, understanding the atomic and electromagnetic processes that lead to nuclear excitation is crucial from the study of nucleosynthesis in astrophysical plasmas to the development of high-density energy storage applications.

This study focuses on the design and implementation of an experimental setup for generating high-density plasma using a femtosecond pulsed laser. With this setup, we seek to investigate various atomic and electromagnetic processes that are expected to occur in such high-density plasma environments, some of which may have never been observed experimentally or have only been observed under specific conditions but not in a plasma scenario.

The experimental setup presented allows for the controlled and repeatable creation of high-density plasma from a solid metallic target, making it possible, in principle, to study the rate of occurrence of these processes.

## Non-LTE modeling of XFEL produced plasmas

Hai Le<sup>1</sup>, Howard Scott<sup>1</sup>

<sup>1</sup>*Lawrence Livermore National Laboratory, USA*

X-ray free electron lasers (XFEL) provide some unique capabilities in high energy density physics due to their ability to create solid density plasmas on very short time scales. The plasmas produced from these systems are typically far from LTE due to the large radiation field and short time scales. In recent years, collisional-radiative (CR) atomic kinetics codes have been adapted to handle these extreme conditions with promising results. Some of these modifications include extension of atomic data sets appropriate for solid density plasmas, treatment of continuum lowering and electron degeneracy. To reduce computational time, most models assume that the free electrons are instantaneously thermalized such that their distribution can be characterized by a Maxwellian or Fermi-Dirac distribution. This assumption breaks down for very short pulses and high XFEL photon energy, and an improved treatment of the electron distribution is required. We discuss the treatment of the electron distribution in the CR modeling framework and modifications to account for continuum lowering and degeneracy effects. We also show simulation results of an XFEL heated copper experiment.

### Acknowledgements

This work was performed under the auspices of the U.S. Department of Energy by Lawrence Livermore National Laboratory under contract DE-AC52-07NA27344. Lawrence Livermore National Security, LLC.

## Opacity calculations for various plasmas with the improved FLYCHK

**Jang Hyeob Sohn<sup>1</sup>, Hyun-Kyung Chung<sup>2</sup>, Byoung-Ick Cho<sup>1</sup>, Sang June Hahn<sup>3</sup>**

<sup>1</sup>*Gwangju Institute of Science and Technology, Republic of Korea*

<sup>2</sup>*Korea Institute of Fusion Energy, Republic of Korea*

<sup>3</sup>*Department of Physics, Chung-Ang University, Republic of Korea*

Opacity, which describes the extent to which the radiation is absorbed and scattered in the material, is essential in understanding the fundamental physical properties of high-energy-density(HED) and astrophysical plasmas. FLYCHK, a collisional-radiative code, has been used to calculate the opacities of HED plasmas under a wide range of conditions due to the simplicity and availability of the code [1,2]. However, it has been confirmed that the FLYCHK opacity has limitations in strongly coupled plasmas due to the problem of free-free opacity formalism [3,4]. In this research, we improve the free-free opacity calculation model of FLYCHK and generate opacities of various materials (Al, H, Au). The FLYCHK opacities are in good agreement with those obtained by the Los Alamos opacity code ATOMIC [5].

### References

1. H.-K. Chung et al., High Energy Density Physics, 1, 3-12 (2005).
2. H.-K. Chung, M. H. Chen, R. W. Lee., High Energy Density Physics, 3, 57-64 (2007).
3. M. S. Cho et al., Journal of Quantitative Spectroscopy and Radiative Transfer, 257, 107369 (2020).
4. M. S. Cho et al., Journal of the Korean Physical Society, 78, 1072-1083 (2021).§
5. J. Colgan et al., The Astrophysical Journal 817, 116 (2016): 116.

### Acknowledgements

This work was supported by the NRF of Korea (No. NRF-2019R1A2C2002864) and the Defense Research Laboratory Program of the Defense Acquisition Program Administration and the Agency for Defense Development of the Republic of Korea.

## Differential analysis of the ionization of hydrogen in Debye plasmas by light particle impact

Emiliano Acebal<sup>1</sup>, Sergio Hernán Martínez<sup>1</sup>, Agustina Cuenca<sup>2</sup>, Sebastian Otranto<sup>1</sup>

<sup>1</sup>*Instituto de Física del Sur (IFISUR), Argentina*

<sup>2</sup>*Instituto Angel H. Roffo, Comisión Nacional de Energía Atómica, Argentina*

In the present work, we calculate and analyze ionization total, singly differential and fully differential cross sections for hydrogen embedded in a weak plasma environment due to light particle impact. Calculations at the total and singly differential level, either in terms of the electron emission energy or the emission angle, are performed within the framework of the classical trajectory Monte Carlo method [1]. Fully differential cross sections (FDCS), on the other hand, are calculated by means of a Born-3DW model, in which distorted waves are used to represent the interactions among the three fragments resulting from the collision (projectile, target ion and emitted electron) [2,3]. This model can be considered the natural extension of the extensively used Born-3C model [4,5] for the case of screened interactions. In all cases, the interactions among particles were described by means of the Debye-Hückel potential.

The main focus of our study is placed on describing the sensitivity of the structures of the different cross sections with the degree of screening and tracing the physical origin of the changes they exhibit. While total cross sections are directly analyzed in terms of the projectile charge sign and the Debye screening length ( $r_D$ ) at a given impact energy, differential cross sections require the specification of the geometrical configuration resulting from the collision process. In addition, we show that a scaling law for the fully differential cross section in terms of the nuclear charge  $Z$ , proposed by Kornberg and Miraglia in the photo-double ionization context [6], also holds for the light particle impact ionization of hydrogenic ions in the present screened context.

### References

1. R. E. Olson, A. Salop, Phys. Rev. A 16, 531 (1977).
2. E. Acebal, A. Cuenca, S. Martínez, S. Otranto, Phys. Plasmas 28, 123510 (2021).
3. E. Acebal, S. Martínez, S. Otranto, Atoms 11, 15 (2023).
4. C. R. Garibotti, J. E. Miraglia, Phys. Rev. A 21, 572 (1980).
5. M. Brauner, J. S. Briggs, H. Klar, J. Phys. B 22, 2265 (1989).
6. M. A. Kornberg, J. E. Miraglia, Phys. Rev. A 49, 5120 (1994).

## Benchmarking model calculations of Fe XVII dielectronic recombination satellite line cross sections using an electron beam ion trap

**Gabriel Grell<sup>1,2,3</sup>, Chintan Shah<sup>1,4,5</sup>, Maurice Leutenegger<sup>1</sup>**

<sup>1</sup>*NASA Goddard Space Flight Center, USA*

<sup>2</sup>*University of Maryland College Park, USA*

<sup>3</sup>*Center for Research and Exploration in Space Science & Technology II, USA*

<sup>4</sup>*Max-Planck-Institut für Kernphysik, Heidelberg, Germany*

<sup>5</sup>*Lawrence Livermore National Laboratory, USA*

Dielectronic recombination (DR) is the dominant photorecombination channel for Fe XVII in hot astrophysical plasmas, producing strong satellite transitions seen in the 3s – 2p and 3d – 2p line formation channels of X-ray spectra from stellar coronae. Dielectronic resonances also contribute strongly to the collisional excitation of Fe XVII ions. Theoretical calculations of both DR and resonant excitation (RE) are effectively benchmarked by electron beam ion trap (EBIT) studies in which the electron beam energy is swept over the energy range of the resonances. Accurate interpretations of these DR channels are essential for accurate astrophysical plasma diagnostics.

We continue the work of Shah et al. (2019) and Grilo et al. (2021) by using the Flexible Atomic Code to calculate cross sections for the DR satellite lines of Fe XVII, with configurations including principal quantum numbers and orbital angular momentum quantum numbers up to  $n \leq 60$  and  $l \leq 8$  respectively. Calculations of the energies for the initial, intermediate, and final atomic states as well as their transition and autoionization rates were fed into the FAC line polarization module, in order to calculate the total line emissivities.

We benchmarked our theoretical predictions by converting the line emissivities to absolute cross sections, and compared these cross sections in all orders to experimental cross sections of Fe XVII resonances that were mono-energetically excited in FLASH-EBIT at the Max Planck Institute for Nuclear Physics (MPI-K) in Heidelberg, Germany. In particular, we extended the experimental benchmark of Shah et al. (2019) and Grilo et al. (2021) to all observable DR and RE channels, specifically the  $n = 4 - 2$  DR resonances of Fe XVII. Our theoretical calculations show a 20 – 25 % overestimation of the  $n = 4$  DR and DE absolute cross sections, but accurate overall agreement when broadening the cross sections with a Gaussian function to match the photon energy resolution of the FLASH-EBIT silicon drift detector.

---

## Ionization and charge exchange cross sections in collisions of singly charged lithium and sodium ions with helium and nitrogen atoms

**Károly Tőkési<sup>1</sup>**

<sup>1</sup>*Institute for Nuclear Research (ATOMKI), Hungary*

We present total and energy and angular differential cross sections for single-ionization and single charge exchange in a collision between singly charged lithium and sodium with ground-state helium and nitrogen atoms. For sake of simplicity, the considered collision systems are treated as three-body problems. The helium and nitrogen atomic targets are described within the single active electron approximation using a Garvey-type distance-dependent model potential where only the ground-state outermost electron is involved in the collision dynamics as an active electron while the other bound electrons are considered inactive [1,2]. The interactions between the projectile and target system are also described by the Garvey-type potential. The scattering problem is solved within the frame of the classical trajectory Monte Carlo (CTMC) [3].

We found that the classical treatment of the collision problem describes reasonable well both the total and differential cross sections. Our present CTMC results are in good agreement with available theoretical and experimental data.

### References

1. R. H. Garvey, C. H. Jackman, A. E. S Green, *Phys. Rev. A* 12(4), 1144 (1975).
2. A. E. S. Green, *Advances in Quantum Chemistry* 7, 221 (1973).
3. K. Tőkési et al., *Nucl. Instrum. Methods Phys. Res. B: Beam Interact. Mater. At.* 86, 201 (1994).

### Acknowledgements

This work has been carried out within the framework of the EUROfusion Consortium, funded by the European Union via the Euratom Research and Training Programme (Grant Agreement No 101052200 — EUROfusion).



## Improving opacity predictions through optimization of atomic data calculations

**Ricardo Ferreira da Silva<sup>1</sup>, Andreas Flörs<sup>2</sup>, Gerrit Leck<sup>2</sup>, Jorge M. Sampaio<sup>1</sup>, Pedro Amaro<sup>3</sup>, Luke Shingles<sup>2</sup>, Gabriel Martínez-Pinedo<sup>2</sup>, José Pires Marques<sup>1</sup>**

<sup>1</sup>*Laboratório de Instrumentação e Física Experimental de Partículas (LIP) and Faculdade de Ciências, Universidade de Lisboa, Portugal*

<sup>2</sup>*GSI Helmholtzzentrum für Schwerionenforschung, Darmstadt, Germany*

<sup>3</sup>*LIBPhys-UNL, Faculdade de Ciências e Tecnologia da Universidade Nova de Lisboa (FCT, Nova University of Lisbon), Portugal*

The 2017 observation of the electromagnetic counterpart to the gravitational wave signal GW170817 provided direct evidence that r-process elements are created in neutron-star mergers. The electromagnetic transient, also known as a kilonova, has revealed two distinct ejecta components: one containing heavy r-process material, including lanthanides and potentially actinides, and a second one characterized by low lanthanide abundance [1]. Spectroscopic data can often be used to identify features due to specific elements (e.g., Sr II [2]). However, having accurate atomic data is crucial for the interpretation of observed spectra, as even small relative errors (e.g., a few percent) in the transition wavelengths, or larger errors (tens of percent) in the transition strengths can make the task more difficult or even impossible to achieve [3]. The lack of atomic data has led to a number of computations of weakly ionised r-process opacities, primarily focussing on lanthanides, being published in recent years. Nevertheless, if the merging process results in the ejection of material with an electron fraction ( $Y_e$ ) of 0.15 or less, nucleosynthesis should progress to actinides, which are projected to possess photon opacities similar to, or perhaps higher than, lanthanides [4,5]. Moreover, large discrepancies can still be found in the opacities, which are related to the uncertainty of the atomic data produced using different methodologies. [5]

To address this issue, we have developed an optimization procedure to provide atomic data (energy levels and oscillator strengths) that is consistent with available experimental data. The Flexible Atomic Code software package [6] is used, as it allows for the calculation of both radiative and collisional processes. We investigate how this optimization technique affects our calculations as well its impact on line-by-line and grey opacity data. The goal is to provide a more reliable, while still complete, set of atomic data for relevant lanthanides and actinides in the expanding ejecta.

### References

1. D. Kasen, B. Metzger, J. Barnes, E. Quataert, and E. Ramirez-Ruiz, Origin of the Heavy Elements in Binary Neutron-Star Mergers from a Gravitational-Wave Event, *Nature* 551, 7678, 80–84, 2017.

- 
2. D. Watson et al., Identification of Strontium in the Merger of Two Neutron Stars, *Nature*, vol. 574, no. 7779, 497–500, 2019.
  3. N. Domoto, M. Tanaka, D. Kato, K. Kawaguchi, K. Hotokezaka, and S. Wanajo, Lanthanide Features in Near-infrared Spectra of Kilonovae, *The Astrophysical Journal* 939, 1, 8, 2022.
  4. R. F. Silva, J. M. Sampaio, P. Amaro, A. Flörs, G. Martínez-Pinedo, and J. P. Marques, Structure Calculations in Nd III and U III Relevant for Kilonovae Modelling, *Atoms* 10, 1, 18 2022.
  5. A. Flörs et al., Opacities of Singly and Doubly Ionised Neodymium and Uranium for Kilonova Emission Modeling. *arXiv*, 2023. doi: 10.48550/arXiv.2302.01780.
  6. M. F. Gu, The Flexible Atomic Code, *Canadian Journal of Physics* 86, 5, 675–689, 2008.

---

## A hybrid fine-structure and super transition array calculation using a consistent bound and continuum electron treatment

**Nathanael Gill**<sup>1</sup>

<sup>1</sup>*Los Alamos National Laboratory, USA*

Determining plasma opacities requires knowledge of the electronic structure of many atomic configurations. For dense plasmas, the number of configurations required to accurately represent the plasma is often intractably large when using methods that require explicit accounting of each configuration. The superconfiguration concept [1] allows one to use a representative atomic structure for groups of configurations, and the super transition array (STA) technique [1,2] then uses those superconfiguration structures to form an opacity that approximately retains the same statistical properties of opacities obtained using explicit accounting methods. The cost of this STA approach is that many spectral lines are merged into broader features, which reduces the number of so-called “windows” of low opacity in between spectral lines. Though this loss of spectral resolution is necessary to tractably account for the large number of configurations found in plasmas, quantities such as the Rosseland mean opacity are very sensitive to the absence of opacity windows. In this work, we build on prior STA development [3] and present the results from our hybrid fine-structure and STA approach, which uses superconfigurations to incorporate the influence of more exotic configurations and splits configurations that are closer to the ground state in energy into fine-structure levels. This hybrid approach gives an opacity that combines the strength of the STA formalism to capture all possible configurations with the increased spectral resolution obtained from fine-structure transitions.

### References

1. A. Bar-Shalom et al, Phys. Rev. A 40, 3183-93 (1989).
2. A. Bar-Shalom, J. Oreg, Phys. Rev. E 54, 1850-6 (1996).
3. N. M. Gill, C. J. Fontes, C. E. Starrett, J. Phys. B 56, 015001 (2023).

## A comparison of the relative sensitivities of Au and Zn ionization in buried layer targets

Edward Marley<sup>1</sup>

<sup>1</sup>*Lawrence Livermore National Laboratory, USA*

An experiment has been done at the National Ignition Facility (NIF) using a buried layer platform to study the radiative properties of non-local thermodynamic equilibrium (NLTE) gold plasma at an electron temperature of  $\sim 3$  keV and an electron density of  $\sim 10^{21} \text{cm}^{-3}$ . The targets used consisted of a 625  $\mu\text{m}$  diameter, 1900  $\text{\AA}$  thick dot with two different mixtures of Au and Zn: one at 1:2.25 atomic mix of Au and Zn and the other 1:4.5. The dot was placed in the center of a 2500  $\mu\text{m}$  diameter, 10  $\mu\text{m}$  thick beryllium tamper. Lasers heat the target from both sides for 4.0 ns. The size of the emitting volume vs time was measured side-on with time resolved x-ray imaging to infer the ion density versus time. The radiant x-ray power was measured with a low-resolution, absolutely calibrated x-ray spectrometer (DANTE). The Au L-shell and the Zn K-shell were measured simultaneously and time resolved with the same spectrometer and streak camera. The electron temperature was inferred from the measured zinc K-shell emission. A comparison is made of the relative sensitivities to the plasma conditions of the Au and Zn ionization which were inferred from the time resolved L- and K-shell emissions respectively.

### Acknowledgements

This work was performed under the auspices of the U.S. Department of Energy by Lawrence Livermore National Laboratory under Contract DE-AC52-07NA27344. LLNL-ABS-840296

## Measurement of the fine-structure splitting in Co-like Yb, Re, Os, and Ir to study QED and Breit interaction effects

Roshani Silwal<sup>1</sup>

<sup>1</sup>*Appalachian State University, USA*

With enhanced relativistic and quantum electrodynamics (QED) effects and reduced electron correlation at high  $Z$ , highly charged ions (HCI) offer a great test-bed to benchmark sophisticated atomic theory. Such ions can be reliably created in an electron beam ion trap (EBIT) by tuning the energy of the electron beam. Atomic spectroscopy of the EBIT plasmas can help explore the structure of unique electron configurations in multi-electron atomic systems, and to better understand the atomic processes in laboratory and astrophysical plasma.

Recently, highly accurate Breit and QED effects have been analyzed for the so-called “Layzer-quenched” systems [1–4]. With minimized electron correlations, these systems are proposed for testing QED predictions [5–6] in high- $Z$  HCI. Particularly interesting examples are the ground state configuration of  $2p^5$  (F-like),  $3d^9$  (Co-like), and  $4f^{13}$  (Pr-like) ions. To further test the accuracy of atomic calculations for the Co-like case, we have measured the magnetic-dipole  $3d^9 \ ^2D_{3/2} \rightarrow \ ^2D_{5/2}$  fine-structure transition in Co-like Yb, Re, Os, and Ir using the National Institute of Standards and Technology EBIT facility. It is worth noting that forbidden transitions in Co-like ions may be used for density plasma diagnostics under various conditions. Details of the measurements and their comparison with theoretical results will be presented.

### References

1. R. Si, X. L. Guo, T. Brage, C. Y. Chen, R. Hutton, and C. F. Fischer, *Physical Review A* 98,012504 (R) (2018).
2. M. C. Li, R. Si, T. Brage, R. Hutton, and Y. M. Zou, *Physical Review A* 98, 020502 (2018).
3. G. O’Neil et al, *Physical Review A* 102, 032803 (2020).
4. M.C. Li, G.L. Zhu, K. Wang, R. Si, C.Y. Chen, T. Brage, R. Hutton, *Journal of Quantitative Spectroscopy & Radiative Transfer* 287 108215 (2022).
5. T. A. Welton, *Physical Review* 74, 1157 (1948).
6. V. Shabaev, I. Tupitsyn, and V. Yerokhin, *Computational Physics Communications* 189, 175 (2015).

## Neutron spectra in hybrid fusion-fission nuclear reactors

J. Garcia Gallardo<sup>1</sup>, N. Gimenez<sup>1</sup>, J. L. Gervasoni<sup>1,2</sup>

<sup>1</sup>*Comisión Nacional de Energía Atómica (CNEA), Bariloche, Argentina*

<sup>2</sup>*Consejo Nacional de Investigaciones Científicas y Técnicas (CoNiCeT), Bariloche, Argentina*

The Hybrid Fusion-Fission Reactors (FFHR) are arrangements formed by a nuclear-fusion device and a subcritical-fission-set. The function of the fusion device is to provide neutrons to drive the subcritical assembly which then, uses those neutrons to generate energy. These parts are arranged concentrically forming a three-layer system to optimize the use of neutrons.

Nevertheless, achieving a reasonable neutron yield, in order to drive an FFHR, is difficult with current fusion devices, which is why the use of so-called multiplier cascades has been proposed [1]. These cascades consist of concentric shells where the fissile material is placed, separated by a very large empty space. The dimensions, shape, and fuel of the shells and the size of the empty space between them, determine the multiplying capacity of the system. A distinctive feature of the hybrid reactor is that, since it is actually made up of two reactors, it requires two different fuels: in addition to the fissile material, the use of Deuterium and Tritium is required. Deuterium is a reasonably readily available gas, but Tritium, given the complications involved in storage and transportation, is preferred to be generated on-site. For this reason, a hybrid reactor while using fusion technology, will need to be fitted with a Tritium Generating Shell (TGS). This shell is usually made of a Lithium compound, which generates Tritium by means of the  ${}^6\text{Li}(n, t){}^4\text{He}$  and  ${}^7\text{Li}(n, n't){}^4\text{He}$  channels. In this work we analyze a model of FFHR following these principles, where two shells of 8% enriched Uranium are placed as fuel, a Lithium silicate is used as TGS, and a Tungsten layer plays the role of reflector and shielding. This arrangement was simulated using MCNP5 to find the spectra of the whole system [2].

The spectra obtained show that the neutron spectra are quite similar to that expected in conventional fast reactors, and therefore, compatible with actinide burn.

---

## References

1. A. Clause, L. Soto, C. Friedli, L. Altamirano, *Annals Of Nuclear Energy* **78**, 10, (2015).
2. J. A. García Gallardo, M. A. N. Giménez, J. L. Gervasoni, *Annals of Nuclear Energy* **147**, 107739 (2020).

---

## Electron correlation energies, atomic masses and their applications in the search for physics beyond the standard model

Chunhai Lyu<sup>1</sup>, Christoph H. Keitel<sup>1</sup>, Zoltán Harman<sup>1</sup>

<sup>1</sup>*Max-Planck Institute for Nuclear Physics, Heidelberg, Germany*

Electron correlations play important roles in determining the structures and properties of atoms, molecules, and solid-state materials. However, due to complicated electron-electron interactions, it is challenging to accurately treat the correlation effects. In this contribution, we employ the *ab initio* fully relativistic multi-configuration Dirac-Hartree-Fock (MCDHF) and relativistic configuration interaction (RCI) methods to calculate the electron correlation energies and ionization potentials of complex atoms and ions. In collaboration with high-precision mass measurement of highly charged ions in Paul traps, our calculations would enable the determination of the absolute masses of neutral atoms with a relative accuracy of  $10^{-12}$ , and have applications in measuring the neutrino mass and in constraining the hypothetical fifth force.



## Dielectronic recombination study of $\text{Xe}^{3+}$

Suvam Singh<sup>1</sup>, Christoph H. Keitel<sup>1</sup>, Zoltán Harman<sup>1</sup>

<sup>1</sup>*Max Planck Institute for Nuclear Physics, Heidelberg, Germany*

Dielectronic recombination (DR) is a fundamental process in plasma physics, which involves the resonant capture of a free electron by an ion and the subsequent emission of photons or other particles. DR is important in the study of astronomical plasmas, such as those found in stars and the interstellar medium [1]. The study of DR can provide insight into the composition and physical conditions of these plasmas. The detection of singly charged strontium in a kilonova event has specifically pointed to the need for more detailed studies on the recombination of low-charged ions [2], as this process can significantly impact the ionization state of the plasma and ultimately the composition of the elements that are produced. In order to better understand how such ions behave in extreme astrophysical environments, recombination in heavy ions is an essential field of study.

The presence of  $\text{Xe}^{3+}$  ions in the universe has been detected in certain astronomical environments such as in the atmospheres of white dwarf stars [3], and in planetary nebulae, where it is thought to be produced through the ionization of neutral xenon by ultraviolet radiation from hot stars.

Theoretically and computationally demanding calculations are required for such multielectron systems. In this study, we have made theoretical calculations of cross sections and rate coefficients for various DR channels by using the flexible atomic code (FAC) [4]. The results of our calculations are compared with the cryogenic storage ring (CSR) experiment [5] of our institute and are in good agreement with the experimental data.  $\text{Xe}^{3+}$  ion is also very significant because it is one of the highest mass-to-charge ratio ions that is experimentally and theoretically studied simultaneously in this present work.

### References

1. S. Ali et al. *The Astrophysical Journal* 753.2 (2012): 132.
2. A. Müller, *Advances in Atomic, Molecular, and Optical Physics* 55 (2008): 293-417.
3. K. Werner et al., *The Astrophysical Journal Letters* 753.1 (2012): L7.
4. M. F. Gu, *AIP Conference Proceedings* 730, 1. American Institute of Physics, 2004.
5. R. von Hahn et al., *Review of Scientific Instruments* 87.6 (2016): 063115.

## Extreme-ultra-violet emission of W ions with open 4f-shell

Filipe Grilo<sup>1</sup>, Marc Botz<sup>2</sup>, José Paulo Santos<sup>3</sup>, José R. Crespo López-Urrutia<sup>2</sup>, Pedro Amaro<sup>3</sup>

<sup>1</sup>*Laboratory of Instrumentation, Biomedical Engineering and Radiation Physics, LIBPhys-UNL, Portugal*

<sup>2</sup>*Max-Planck-Institut für Kernphysik, Heidelberg, Germany*

<sup>3</sup>*LIBPhys-UNL, Nova de Lisboa (FCT, Nova University of Lisbon), Portugal*

The plasma divertor for the International Thermonuclear Experimental Reactor (ITER) will have target plates made out of tungsten (W) [1]. The inevitable W contamination will emit characteristic radiation that depends on the specific charge state balance, electron temperature and density conditions. Therefore, the respective emission spectra can be used as real-time diagnostics of the fusion reactor plasma physical conditions [1, 2]. Given the importance of the spectra of this elements, both its low and highly charged ions have already been extensively studied in the past in a wide range of the electromagnetic spectrum [2-5]. However, the emission of the open 4f-shell charges states, between 12+ and 28+, still remains largely understudied, has the emissions of this group of ions is usually observed mixed with each other. In our work, an Electron Beam Ion Trap (EBIT) was used to produce and individually observe the EUV spectrum (12 – 26 nm) of each of the charge states in the open 4f-shell complex. A slow electron beam energy scan between 300 and 1000 eV allowed us to observe the emissions for every individual charge state. The excellent resolution allows to retrieve each charge state contribution with the Non-Negative Matrix Factorization (NNMF) method. The decomposed data was matched with the respective theoretical wavelengths of the Unresolved Transition Arrays (UTA) calculated with Flexible Atomic Code (FAC) [6]. In this regime, we observed the O-O transitions derived from N-O collisional excitations. This data is of great importance, as it can be incorporated in diagnostic models relevant for fusion plasma monitoring.

### References

1. J. Clementson, P. Beiersdorfer, E. W. Magee, et al., *Journal of Physics B: Atomic, Molecular and Optical Physics*, 43, 14 (2010).
2. J. Clementson, T. Lennartsson, P. Beiersdorfer, *Atoms*, 3, 3 (2015).
3. T. Lennartsson, J. Clementson, P. Beiersdorfer, *Physical Review A*, 87, 6 (2013).
4. H. A. Sakaue, D.Kato, N. Yamamoto, et al., *Physical Review A*, 92, (2015). [5] T. Oishi, S. Morita, D. Kato, et al., *Atoms*, 9, 3 (2021).
5. <https://github.com/flexible-atomic-code/fac>

## **Theoretical study of ablation of cylindrical particulate in Plasma**

**Nopparit Somboonkittichai**<sup>1</sup>

<sup>1</sup>*Department of Physics, Faculty of Science, Kasetsart University, Thailand*

Pellet injection is the way to provide fuel replenishment in fusion devices. The technique has been also adopted, and actively studied to establish its variant as methodologies for instability suppression, e.g. ELMs using Li pellet, and protecting inner surface via mitigation by a shattered-pellet-induced radiation. Sometimes, such pellet is produced in a cylindrical shape, corresponding to its guiding tube. So, its ablation may deviate from a conventional ablation model assuming spherical shape.

In the study, upstream plasma electrons are assumed to satisfy Maxwellian distribution. Electron flux before reaching electrostatic sheath is modified by atomic processes. In an ablation cloud region, the electrons undergo inelastic collisions under the process of excitation and ionization. Maxwellian flux for electrons is modified by exploiting Saha equation for ionization and rate coefficient for excitation. Net ion flux is assumed to be equal to net electron flux to set up an equilibrium floating potential and net heating flux on a cylindrical particulate. Then, the ablation develops corresponding to the particulate shape and the plasma parameters. A magnetic field is not currently included in the study.

## Electron-driven reactivity of molecular cations in cold plasmas

**Zsolt J. Mezei<sup>1</sup>, Jeffrey Boffelli<sup>2</sup>, Riyad Hassaine<sup>2</sup>, Frédéric Gauchet<sup>2</sup>, Nicolina Pop<sup>3</sup>, Felix Iacob<sup>4</sup>, Sebastian Niyonzima<sup>5</sup>, Michel Douglas Epée Epée<sup>6</sup>, Kalyan Chakrabarti<sup>7</sup>, Ousmanou Motapon<sup>6</sup>, Jonathan Tennyson<sup>8</sup>, Ioan F. Schneider<sup>2</sup>**

<sup>1</sup>*Institute for Nuclear Research (ATOMKI), Hungary*

<sup>2</sup>*Université Le Havre Normandie, France*

<sup>3</sup>*Politehnica University Timisoara, Romania*

<sup>4</sup>*West University of Timisoara, Romania*

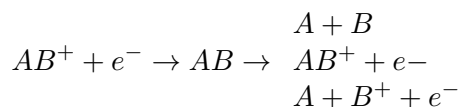
<sup>5</sup>*Université du Burundi, Bujumbura, Burundi*

<sup>6</sup>*University of Douala, Cameroon*

<sup>7</sup>*Scottish Church College, Kolkata, India*

<sup>8</sup>*University College London, UK*

Electron impact recombination, (ro-)vibrational, electronic and dissociative excitation of molecular cations:



are in the heart of the molecular reactivity in the cold ionized media [1], being major charged particles destruction reactions and producing often atomic species in metastable states, inaccessible through optical excitations. They involve super-excited molecular states undergoing predissociation and autoionization, having thus strong resonant character.

The methods based on the Multichannel Quantum Defect Theory (MQDT) [1,2] are the most suitable for modeling these processes, since they account the strong mixing between ionization and dissociative channels, open – direct mechanism – and closed – indirect mechanism, via capture into prominent Rydberg resonances correlating to the ground and excited ionic states - and the rotational effects. These features will be illustrated for several cations of high astrophysical, planetary atmosphere and fusion edge plasma relevance, such as  $H_2^+$  [3],  $BeH^+$  [4-6],  $SH^+$  [7],  $N_2^+$  [8],  $NeH^+$ ,  $NS^+$  [9],  $N_2H^+$  [10],  $C_2H^+$ , etc.

Comparisons with other existing theoretical and experimental results, as well as the isotopic effects, will be displayed.

---

## References

1. I. F. Schneider, O. Dulieu, J. Robert, eds., EPJ Web of Conferences 84 (2015).
2. J. Zs. Mezei et al, ACS Earth and Space Chem 3 2276 (2019).
3. M. D. Epée Epée et al, MNRAS 512 424 (2022).
4. S. Niyonzima et al, At. Data Nucl. Data Tables 115-116 287 (2017).
5. S. Niyonzima et al, Plasma Sources Sci. Technol. 27 025015 (2018).
6. N. Pop et al, ADNDT 139 101414 (2021).
7. J. Boffelli et al, submitted to MNRAS (2023).
8. A. Abdoulanziz et al, J. Appl. Phys. 129 052202 (2021).
9. F. Iacob et al, Journal of Physics B: At. Molec. Optical Phys. 55, 235202 (2022).
10. J. Zs. Mezei et al, submitted to EPJST (2023).

## Acknowledgements

Research supported by the Normandy region, LabEx PTOLEMEE, IEPE, CNRS-CEA CNES/PCMI and FR-FCM, ANR-MONA, NKFIH-OTKA and IAEA.

## Electron-impact excitation of Ar II for application in magnetically confined fusion plasmas

Connor Ballance<sup>1</sup>, Niall McElroy<sup>1</sup>, Catherine Ramsbottom<sup>1</sup>

<sup>1</sup>*Queen's University Belfast, UK*

Detailed, accurate, complete atomic datasets, including energy levels, radiative transition probabilities, excitation and ionisation cross sections and recombination rates, are vital for accurately modelling fusion plasmas. The R-Matrix approach is well known to be one of the most powerful and reliable methods for calculating these atomic parameters.

Recent and ongoing developments of the relativistic parallel DARC codes have enabled an order of magnitude advance in the accuracy of the atomic structure and subsequent collision calculations that are now feasible for lowly ionised high  $Z$  ions, such as W I, W II and W III; additionally, this method remains viable for low  $Z$  ions, opening those ionisation stages to possible relativistic and semi-relativistic treatments.

Characterising the impurity influx, erosion and deposition of W ions in tokamaks is important for their future development. However, on occasion, it may be necessary to inject specific impurity ions into the plasma deliberately. For example, redistribution of the power radiated from the core to the reactor wall may be required to reduce any damage that may be caused to the plasma-facing wall components due to a high heat load and prolong tokamak lifespan. Impurities such as argon, nitrogen or neon improve plasma control and limit plasma disruptions that impede magnetic confinement. Unfortunately, there is currently a paucity of fine structure resolved atomic data in the literature for the first three ionisation stages of Argon, a key priority for the fusion plasma community.

To address these issues, the QUB group are undertaking a series of calculations for the electron-impact excitation of Ar II, results from which will be presented at the conference.

The fully relativistic DARC codes have been used to compute excitation rates for two models incorporating 15 and 31 configurations in the expansion of the target wavefunctions. These data will be compared and contrasted to a full Breit-Pauli pseudo-state calculation comprising all levels up to  $n = 12$ . The data presented will significantly impact the modelling and characterisation of magnetically confined fusion tokamaks and numerous astrophysics applications.

## Microsecond electrical breakdown in water: advances using emission analysis and cavitation bubble theory

Xavier Duten<sup>1</sup>, Truong Son Nguyen<sup>2</sup>, Cathy Rond<sup>3</sup>

<sup>1</sup>*Université Paris 13 Nord*

<sup>2</sup>*Vietnam Academy of Sciences and Technology*

<sup>3</sup>*French National Centre for Scientific Research*

Electrical discharges in water are a subject of major interest because of both the wide range of potential applications and the complexity of the processes. This topic aimed to provide significant insights to better understand processes involved during a microsecond electrical discharge in water, especially during the propagation and the breakdown phases. Two different approaches were considered. The first analysis focused on the emission produced by the discharge during the propagation using fast imaging measurements and spatially resolved optical emission spectroscopy. The excited species H, O, and OH were monitored in the whole interelectrode gap. The second analysis concerned the thermodynamic conditions induced by the breakdown of the discharge. The time evolution of the bubble radius was simulated and estimation of the initial pressure of the cavitation bubble was performed using the Rayleigh–Plesset model. Values of about  $1.7 \times 10^7$  Pa and  $1.2 \times 10^8$  Pa were reported for the cathode and anode regimes, respectively. This multidisciplinary approach constitutes a new step to obtain an accurate physical and chemical description of pin-to-pin electrical discharges in water.

## On the transient spatial localization model

Carlos Iglesias<sup>1</sup>, Michael Kruse<sup>1</sup>

<sup>1</sup>*Lawrence Livermore National Laboratory, USA*

Significant discrepancies relevant to helioseismology between experimental and theoretical photon absorption by plasmas remain unresolved. Interestingly, a new process called transient spatial localization (TSL), where the plasma perturbs the final states in photon ionization processes, ostensibly enhances cross-sections resolving the extant discrepancies. The TSL model, however, is shown to involve *ad hoc* formulas not derived from fundamental principles and systematic approximations. In addition, a variant of the TSL model, which claimed to enhance electron collisional ionization, is inconsistent with the Schrodinger equation and fails to reproduce known results.



## Effect of the ionization potential depression on electron-impact ionization cross-sections in dense plasmas

Djamel Benredjem<sup>1</sup>, Annette Calisti<sup>2</sup>, Sandrine Ferri<sup>3</sup>, Jean-Christophe Pain<sup>4</sup>

<sup>1</sup>*Université Paris-Saclay*

<sup>2</sup>*CNRS*

<sup>3</sup>*Aix Marseille University, CNRS, PIIM*

<sup>4</sup>*CEA, DAM, DIF*

Collisional-radiative calculations can provide reliable emission and opacity spectra if the cross-sections of the various microscopic processes occurring in a dense plasma are accurate. In this work, we focus on electron impact ionization (EII). Since the EII cross-section depends strongly on the ionization energy and since the latter is very sensitive to the plasma environment (“density effects”), we need to take into account the ionization potential depression (IPD). The IPD can be calculated by using the Stewart-Pyatt [1] or Ecker-Kröll [2] formulas. A recent model, based on classical molecular dynamics [3], was developed at Aix-Marseille University. It simulates multi-component plasmas, and accounts for all the charge correlations, providing a distribution of ionization energies for each ion charge state. This distribution is a result of the fluctuations of the environment. In this work, we compare calculated IPDs to experimental results obtained at LCLS (Stanford) [4]. Following a recent work [5], we discuss the distribution of the ionization energy in an aluminum plasma, and propose an alternative formulation of the cross-section, suitable for the inclusion of the IPD.

### References

1. J. C. Stewart and K. D. Pyatt, *Astrophys. J.* 144, 1203 (1966).
2. G. Ecker and W. Kröll, *Phys. Fluids* 6, 62 (1963).
3. A. Calisti, S. Ferri, C. Mossé and B. Talin, *J. Phys.: Conf. Ser.* 810, 012009 (2017).
4. O. Ciricosta et al, *Nat. Commun.* 7, 11713 (2016).
5. D. Benredjem, J.-C. Pain, A. Calisti and S. Ferri, *J. Phys. B: At. Mol. Opt. Phys.* 55, 105001 (2022).

## Effect of cold atmospheric pressure plasma on the control and reduction of cell growth in breast cancer

Mahdiyeh Bakhtiyari-Ramezani<sup>1</sup>, Mojtaba Nohekhan<sup>1</sup>, Sharareh Mirshahvalad<sup>2</sup>

<sup>1</sup>*Plasma and Nuclear Fusion Research School, Nuclear Science and Technology Research Institute (NSTRI), Atomic Energy Organization of Iran (AEOI)*

<sup>2</sup>*Plasma Technology Development Company, Atomic Energy Organization of Iran (AEOI)*

*Introduction:* Breast cancer has become the most prevalent cancer in the world since 2021. The out-of-control growth of breast cells results in breast cancer. The type of breast cancer depends on which cell in the breast becomes cancerous. Due to the high incidence and limitations of surgery, chemotherapy, and radiotherapy including non-selective and incomplete tumor ablation, non-thermal plasma (NTP) technology has been reported as a novel therapeutic way in different fields of medical science such as oncology and dermatology. In vitro and in vivo studies have reported that NTP has anticancer effects and can selectively inhibit the growth of cancer cell lines. The combination of physical and chemical factors in the interaction between NTP and cells is the basis of the anti-cancer effect [1-3]. Plasma can affect target cells and tumors in two ways, direct and indirect. In direct treatment, plasma directly interacts with cells and tumors while in indirect treatment, first a solution or medium is activated by a plasma device then the activated solution or medium is added to the cell culture medium or injected to the tumor. In this study, atmospheric pressure argon and helium plasma jets was used to investigate and compare the effect of cold plasma on the control and reduction of cell growth in breast cancer in in-vitro and in-vivo studies.

*Material and method:* The configuration of argon and helium plasma jets is shown in Fig1.a. 4T1 mammary carcinoma cell lines were purchased from Iranian Biological Resource Center and were cultured in DMEM medium. The culture medium containing cells (expect control) was exposed to He or Ar plasma in direct treatment and, the plasma-activated medium (PAM) was added to the cells in indirect treatment. The cell cycle and apoptotic rate were inspected using flow cytometry. Twenty female BalbC mice were randomly divided into 5 groups: breast tumor without treatment (control), breast tumor + direct He plasma, breast tumor + indirect He plasma, breast tumor + direct Ar plasma, and breast tumor + indirect Ar plasma. The treatment time was adjusted to 3 minutes. The variation of weight and H&E staining was investigated.

*Conclusion:* The apoptosis rate increased compared to the control group, and the presence of cells in the S phase of the cell cycle decreased in all groups except the control group (Fig1.b). The pathology images of tumors indicated that cell proliferation and angiogenesis were controlled by direct and indirect plasma treatment (Fig1.c). The results of this research provide medical experts with a clear perspective on the treatment of breast cancer.

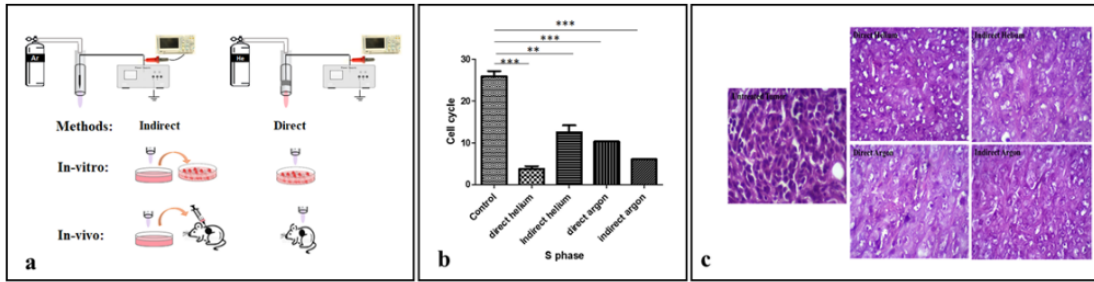


Fig. 1: a. Experimental setup, b. Cells in the S phase, c. Tumor pathology.

## References

1. S. Lee et al., "Epigenetic silencing of miR-19a-3p by cold atmospheric plasma contributes to proliferation inhibition of the MCF-7 breast cancer cell.", *Scientific reports* 6.1 (2016): 30005.
2. Y. Ma et al., "Non-thermal atmospheric pressure plasma preferentially induces apoptosis in p53-mutated cancer cells by activating ROS stress-response pathways.", *PloS one* 9.4 (2014): e91947.
3. Murphy, William, Caitlin Carroll, and Michael Keidar. "Simulation of the effect of plasma species on tumor growth and apoptosis." *Journal of Physics D: Applied Physics* 47.47 (2014): 472001.

## Investigation of the efficacy of dielectric barrier discharge jets (DBD-Jet) and plasma activated water (PAW) in wound treatment: an in-vivo study

Mahdiyeh Bakhtiyari-Ramezani<sup>1</sup>, Mojtaba Nohekhan<sup>1</sup>, Fatemeh Shakeri<sup>2</sup>, Sharareh Mirshahvalad<sup>2</sup>

<sup>1</sup>*Plasma and Nuclear Fusion Research School, Nuclear Science and Technology Research Institute (NSTRI), Atomic Energy Organization of Iran (AEOI)*

<sup>2</sup>*Plasma Technology Development Company, Atomic Energy Organization of Iran (AEOI)*

*Introduction:* The effects of cold plasma, such as antimicrobial, anti-inflammatory, tissue regeneration, cell proliferation, and angiogenesis have made this technology a therapeutic option for wound healing [1]. These effects not only are related to the treatment duration and type of tissue but also depend on the plasma configuration, working gas, and plasma source distance.

The dielectric barrier discharge jet (DBD-Jet) is a special type of plasma jet that guarantees the safety of the treatment. While using a ring electrode in this configuration weakens the discharge inside the dielectric tube [2], it led us to investigate the effectiveness of DBD-Jet on wound healing in direct and indirect methods.

*Material and method:* DBD-Jet was developed by the Plasma Technology Development Company (Tehran, Iran). In this study, the electrode is connected to an AC power supply ( $V_{pp}=12$  kV,  $f= 55$ kHz), the helium gas rate flow is kept at 5 l/min. The plasma-activated water is prepared by applying the plasma jet on the surface of 2ml distilled water for 2 to 4 minutes.

The rats were randomly divided into 4 groups ( $n = 6$ ): a wound without treatment (control), a wound treated with DBD-Jet plasma for 2 minutes (wound + DBD-Jet plasma), a wound treated with 2- minute plasma-activated water (wound + 2 min PAW), and a wound treated with 4-minute plasma-activated water (wound + 4 min PAW). The protocol is summarized in Fig. 1. A thermal camera (Testo 881) was used to measure the wound temperature during the plasmatherapy. The appearance of wounds was recorded using a Canon camera and pictures were analyzed with Image J (version 1.8.0). The variation of wound microbial load and histopathology was investigated.

*Conclusion:* We found that DBD-Jet plasma and rinsing of wounds by PAW can support wound healing and tissue regeneration. Interestingly, our results showed that the 2-minute PAW has proved to have more effectiveness in wound healing compared to the 4-minute one.

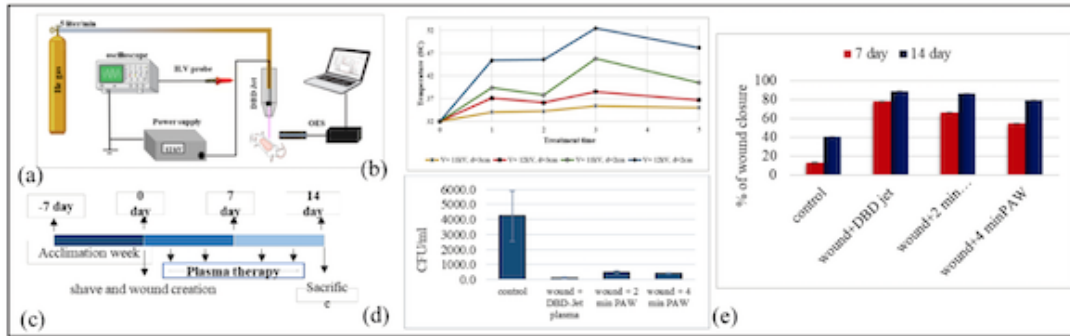


Fig. 1. (a) Plasma jet device, (b) plasma temperature vs treatment time, (c) Experimental Procedure (d) microbial load of the wound, (e) Rate of wound closure

Figure 2: (a) Plasma jet device, (b) Plasma temperature vs. treatment time, (c) Experimental Procedure (d) Microbial load of the wound, (e) Rate of wound closure.

## References

1. A. A. Fridman, G. G. Friedman, Plasma Medicine, Chichester, John Wiley & Sons, UK, 2013.
2. X. Lu, M. Laroussi, V. Puech. "On atmospheric-pressure non-equilibrium plasma jets and plasma bullets.", Plasma Sources Science and Technology 21.3 (2012): 034005.

## Electron scattering from neutral tin atoms and doubly-charged tin ions

Dmitry Fursa<sup>1</sup>, H. Umer, Igor Bray<sup>1</sup>

<sup>1</sup>*Curtin University, Australia*

A cross section dataset has been calculated for electron scattering from the ground and first four excited states of neutral tin using the Relativistic Convergent Close-Coupling method. Integrated cross sections have been produced over a projectile energy range of 0.1 eV to 1000 eV for all major processes. Maxwellian rate coefficients with analytical fits are available for electron temperatures ranging from 0.5 eV to 200 eV. Electron collisions with Sn<sup>+2</sup> have also been studied and cross sections have been produced for various excitations, total-inelastic scattering and total-single ionisation.

With recent developments in the fields of fusion research and nano-lithography, collision datasets for tin are becoming increasingly important. Plasma-facing components in tokamak fusion reactors such as ITER experience large amounts of erosion due to bombardment from the plasma [1]. This damage from erosion is especially an issue for the divertor region of such fusion reactors [2]. To combat this, liquid metal designs for the divertor are currently in development for the European DEMO reactor which promises major improvements over the current tungsten mono-block design adopted in ITER. The primary candidate material for this new design is tin. Extreme-ultraviolet (EUV) lithography is an advanced microchip manufacturing technique which uses a tin plasma to generate the 13.5 nm light [3]. However, the details on how this light is produced in the plasma are not well understood. Ongoing research in both fusion and EUV requires reliable electron collision datasets for tin and its ions.

The Relativistic Convergent Close-Coupling method (RCCC) [4] has been applied to calculate integrated cross sections for elastic scattering, various excitations, total scattering (TCS), total-inelastic scattering (inel-TCS), and single-ionisation of the ground and first four excited states of neutral tin. State-resolved cross sections have been produced for excitations to all states in the the  $5p^2$ ,  $5p6s$ ,  $5p5d$  and  $5p6p$  manifolds. Previous studies for tin have not been as extensive and used first-order approximations which are accurate only at high projectile energies. This is the first study in which accurate results have been produced for all transitions studied over the entire projectile energy range from 0.1 eV to 1000 eV. Rate coefficients with analytical fits to a simple formula have been included for use in modelling applications. The RCCC approach has been also used to calculate cross sections for many important excitations from the ground state of Sn<sup>+2</sup>, for which there is no previous data.

### References

1. Foster A *et al.* 2007 *Journal of Nuclear Materials* **363** 152

- 
2. Rindt P *et al.* 2021 *Fusion Engineering and Design* **173** 112812
  3. O'Sullivan G *et al.* 2015 *J Phys B: At. Mol. Opt. Phys.* **48** 144025
  4. Fursa D V and Bray I 2008 *Phys. Rev. Lett.* **100** 113201§

## Absolute measurement of dielectronic recombination rates at storage ring

X. Ma<sup>1,2,3</sup>, Z. K. Huang<sup>1,2</sup>, W. Q. Wen<sup>1,2</sup>, S. X. Wang<sup>4</sup>, H. B. Wang<sup>1,2</sup>, C. Chen<sup>5</sup>, C. Zhang<sup>5</sup>, W. L. Ma<sup>4</sup>, D. Y. Chen<sup>1,2</sup>, H. K. Huang<sup>1,2</sup>, L. Shao<sup>1,2</sup>, X. Liu<sup>1,2,5</sup>, L. F. Zhu<sup>4</sup>, L. J. Mao<sup>1,2</sup>, J. Li<sup>1,2</sup>, M. T. Tang<sup>1,2</sup>, J. C. Yang<sup>1,2</sup>, Y. Yuan<sup>1,2</sup>, and DR Collaboration

<sup>1</sup>*Institute of Modern Physics, Chinese Academy of Sciences, Lanzhou, China*

<sup>2</sup>*University of Chinese Academy of Sciences, Beijing, China*

<sup>3</sup>*College of Physics and Electronic Engineering, Northwest Normal University, Lanzhou, China*

<sup>4</sup>*Department of Modern Physics, University of Science and Technology of China, Hefei, China*

<sup>5</sup>*Shanghai EBIT Laboratory, Institute of Modern Physics, Fudan University, Shanghai, China*

Dielectronic recombination (DR) is one of the most important atomic processes in various plasmas, which is relevant to the charge balance, radiative diagnostics, and energy transportation in the plasma evolution. Accurate DR rates as well as the plasma rates are crucial parameters in plasma modeling. However, measured absolute rates are scarce due to the experimental difficulties. DR measurements has developed into a high precision spectroscopy and furthermore, absolute DR rates for highly charged ions can be obtained at storage rings [1–3]. We have performed a series of DR experimental at the cooler storage ring CSR in Lanzhou China, for ions including Ar<sup>12+,13+,14+,15+</sup>, Ca<sup>14+,16+,17+</sup>, Ni<sup>19+</sup> and Kr<sup>25+,30+</sup> [4–13]. The typical DR spectrum of the Ar<sup>14+</sup> ion and the plasma rate coefficients of different ions will be presented. A comparison between the plasma rates deduced from measured DR rates with the results of various theoretical models will be discussed. It is noticed that the electron–electron interactions in the multiple electron ion system should be considered appropriately in the models in order to explain the measured results.

### References

1. A. Müller, in *Advances in Atomic, Molecular, and Optical Physics*, Vol 55, E. Arimondo, P. R. Berman, and C. C. Lin (eds), Elsevier Academic Press Inc, San Diego, 2008, pp. 293.
2. C. Brandau and C. Kozhuharov, in *Atomic Processes in Basic and Applied Physics*, V. Shevelko and H. Tawara (eds), Springer Berlin Heidelberg, Berlin, Heidelberg, 2012, pp. 283.
3. S. Schippers, Nucl. Instrum. Methods B. 350, 61 (2015).
4. Z. K. Huang et al., Phys. Scr. T166, 014023 (2015).



- 
5. S. Mahmood et al., *J. Phys. B* 53, 085004 (2020).
  6. Z. K. Huang et al., *X-Ray Spectrometry* 49, 155 (2020).
  7. Z. K. Huang et al., *Astrophys. J. Suppl. Ser.* 235, 2 (2018).
  8. W. Q. Wen et al., *Astrophys. J.* 905, 36 (2020).
  9. S. Wang et al., *Astrophys. J.* 862, 134 (2018).
  10. N. Khan et al., *J. Phys. B: At., Mol. Opt. Phys.* 55, 035001 (2022).
  11. S. X. Wang et al., *A&A* 627, A171 (2019).
  12. Z. K. Huang et al., *Phys. Rev. A* 102, 062823 (2020).
  13. W.-L. Ma et al., *J. Phys. B: At., Mol. Opt. Phys.* 56, 095203 (2023).

## **Plasma pinch produced by a low energy plasma focus discharge**

**Seong Ling Yap**<sup>1</sup>

<sup>1</sup>*Plasma Technology Research Centre (PTRC), University of Malaya, Malaysia*

This paper presents the results of recent experiments performed within a low energy plasma focus of 3 kJ. The main goal of the investigation is to determine the correlation of the plasma discharge dynamics to the neutron emission characteristics. Two set of identical indium foil activation counters are employed to monitor the neutron yields from the end-on and the side-on direction. A simultaneous measurement of the discharge current and voltage are obtained with a high voltage probe across the electrodes and a Rogowski coil. A set of PIN diodes covered with different filters, are used to perform time-resolved measurements of the X-ray radiation. The array of PIN diodes detectors give the time profiles of the plasma emission, while by means of different filters also resolved the plasma temperature. They are compared and the neutron emission and other time-resolved signals. Results and discussion will be presented to show their correlations.

## CollisionDB: an online repository of plasma collisional data sets

**Christian Hill<sup>1</sup>, Dipti<sup>1</sup>, Martin Haničinec<sup>2</sup> Kalle Heinola<sup>1</sup>**

<sup>1</sup>*Atomic and Molecular Data Unit, Nuclear Data Section, International Atomic Energy Agency*

<sup>2</sup>*University College London, UK*

CollisionDB [1] is a repository for the longterm curation of collisional cross sections and rate coefficients. Any data set described in a peer-reviewed article which has been assigned a DOI and is published in a recognised scientific journal is, in principle, eligible for inclusion in the database. As of May 2023 the resource contains 122 352 data sets.

Each data set included in CollisionDB is associated with metadata providing an unambiguous description of its units, provenance, method of calculation or measurement and citation. Fit functions and the corresponding coefficients are provided, where available. An online interface allows data sets to be searched by reactant and product species (including by quantum state where this is resolved), publication DOI, author name and process type (identified as one of a set of documented process codes [2], e.g. EIN = electron-impact ionization).

The online interface also allows all data sets matching a query to be downloaded in a single, compressed archive and for individual data sets to be visualized in an interactive, browser-based plot.

CollisionDB exposes an Application Programming Interface (API), which can be used to request data from the database from users' own code using JSON-based queries. A Python package, `pycollisiondb`, [3] has been released to provide a high-level access to CollisionDB, with library functions for aggregating, visualizing and transforming data sets.

### References

1. <https://db-amdis.org/collisiondb/>
2. C. Hill et al., *Classification of Processes in Plasma Physics*, v2.4, March 2022, <https://amdis.iaea.org/databases/processes/>
3. <https://github.com/xnx/pycollisiondb>

## Application of multi-physical states injection technology in fusion plasma disruption mitigation

Yunbo Dong<sup>1</sup>, Chengyuan Chen<sup>1</sup>, Yipo Zhang<sup>1</sup>

<sup>1</sup>*Southwestern Institute of Physics, Chengdu, China*

Disruption mitigation is considered an essential part of the control system in tokamaks and fusion reactors. The goal of massive impurity injection is to dissipate the stored thermal and poloidal magnetic energy of the plasma radiatively over the entire surface of the first wall, avoiding the concentrated heat load near the strike point on the divertor that occurs when confinement is lost in an unmitigated disruption. At present, the massive gas injection (MGI) and shattered pellet injection (SPI) techniques are regarded as the primary injection methods for disruption and RE mitigation. Both of them have their own character and can be used in different applications. In order to combine the advantages of gas injection and pellet injection for avoidance and mitigation of disruptions, a new hybrid injection system, which including an MGI system and Li pellet injection system, had been developed successfully on HL-2A tokamak. It can realize the global simultaneous cooling of the plasma core and boundary. This impurity injection method is more conducive to enhance the mixing effect of impurities. The hybrid injection system is installed at the midplane port on HL-2A. The MGI injector with a short response time (0.25 millisecond), and adjustable throughput ( $10^{21} \sim 10^{23}$ ) allows to meet the requirement of disruption mitigation. The Li pellet injection system has automatic supplying system and turntable adjustment system to adjust the number of Li pellet. The Li pellet can be injected with a speed of 200 – 400 m/s. Several different injection scenarios were performed using different gases and Li pellet in various amounts on HL-2A. Gas (He, Ar) and pellet Li injected into steady (non-disrupting) discharges are shown to mix into the plasma core dominantly via magnetohydrodynamic activity during the plasma thermal quench (TQ). Mixing efficiencies of injected impurities into the plasma core are measured to be of order 0.05 – 0.4. At this large amount of injected impurities, the fuelling efficiency ( $F_{\text{eff}}$ ) remained at the level of 30 % for plasmas with a modest thermal energy ( $E_{\text{th}} < 0.4$  MJ). The preliminary experiments, presented in this contribution, show that the new hybrid injection system has a significantly higher  $F_{\text{eff}}$  than the MGI.

## Development of test-carbon-ion transport simulation code with atomic and collision process in HL-2M tokamak

W. J. Chen<sup>1</sup>, D. L. Yu<sup>1</sup>, L. W. Yan<sup>1</sup>, G. Z. Hao<sup>1</sup>, L. Liu<sup>1</sup>, C. F. Dong<sup>1</sup>, X. F. He<sup>1</sup>, X. X. He<sup>1</sup>, Y. L. Wei<sup>1</sup>, N. Zhang<sup>1</sup>, Y. P. Zhang<sup>1</sup>, L. Nie<sup>1</sup>, Z. B. Shi<sup>1</sup>, Y. Liu<sup>1</sup>, Q. W. Yang<sup>1</sup>

<sup>1</sup>*Southwestern Institute of Physics, Chengdu, China*

The HL-2M tokamak (Huan Liu Qi-2 Modification) is a new tokamak with an advanced divertor configuration. At the first stage, the carbon material will be applied to the first wall and divertor. Therefore, study of carbon impurity behavior in HL-2M is extremely important for realizing steady-state operation. In general, impurity ions give rise to degradation of the plasma performance through fuel dilution and radiation loss. Now, a space-resolved extreme ultraviolet (EUV) spectrometer system has been developed in the HL-2A/2M tokamak for impurity monitoring and transport studies [1]. And a tri-band high spectral resolution spectrometer is developed to measure the plasma parameters such as ion temperatures, rotation velocities as well as ion density profiles of He, C and D simultaneously [2]. These measurements can provide rich data for impurity transport research.

There have been developed two types of impurity transport models, one is a fluid model, such as EMC3-ERINCE [3] and SOLIP-ITER [4], and the other is a test particle model [5]. Although the test particle model takes longer computational time, it has several advantages compared with the fluid model: (1) the model directly follows the charged particle trajectories, and therefore, it can simulate the advanced divertor configuration for HL-2M, (2) various atomic and collisional effects on impurities (ionization, recombination, charge exchange and Coulomb collision with background particles) and (3) the interaction with wall materials can be simulated more directly.

Our initial goal is to develop a test-ion particle code to simulate the spatial distribution of carbon impurity in HL-2M configuration. The motion of charged particles are in the guiding-center phase space [6]. The neoclassical transport is caused primarily by the varying depth of particle trapping in the magnetic well along the magnetic field with collision. The Monte Carlo pitch angle scattering model of the Lorentz collision operator is implemented to update the particle pitch angle [7]. A new random velocity sampling is adopted, which plays a key role in plasma heating, instead of conserving total momentum and energy. In order to make the charge of carbon ions evolve self-consistently, some atomic processes are considered, including ionization, charge exchange and recombination [8].

### References

1. C.F. Dong et al, "Space-resolved extreme ultraviolet spectrometer for impurity diagnostics in HL-2A", *Fusion Engineering and Design*, 159 (2020)111785.

- 
2. L. Liu et al, “The Tri-Band High Spectral Resolution Spectrometer for the CXRS Diagnostic System on HL-2A Tokamak”, *Rev. Sci. Instrum.* (2023) in press.
  3. Y. Feng, et al “3D fluid modelling of the edge plasma by means of a Monte Carlo technique”, *J. Nucl. Mater.* 266-269(1999),812.
  4. Wiesen S. et al, “The new SOLPS-ITER code package”, *J. Nucl. Mater.* 463(2015) 480
  5. Yuki Homma, Akiyoshi Hatayama, ”Numerical modeling of thermal force in a plasma for test-ion transport simulation based on Monte Carlo Binary Collision Model”, *Journal of Computational Physics*, 231 (2012) 3211–3227.
  6. John R. Cary and Alain J. Brizard, ”Hamiltonian theory of guiding-center motion”, *Rev. Mod. Phys.* 81(2009), 693.
  7. Maciek Sasinowski, and Allen H. Boozer, ”A  $\delta f$  Monte Carlo method to calculate plasma parameters”, *Physics of Plasmas* 4(1997), 3509.
  8. Manfred von Hellermann et al, “Simulation of Spectra Code (SOS) for ITER Active Beam Spectroscopy”, *Atoms*, 7(2019), 30.

# **TUTORIAL LECTURES**





## **Atomic processes in plasmas**

**Yuri Ralchenko**<sup>1</sup>

<sup>1</sup>*National Institute of Standards and Technology (NIST), USA*

A short overview of atomic processes in plasmas will be presented. We will briefly outline the current state of art in atomic structure analyses, discuss basic types of radiation and their importance for plasma spectroscopy, and review plasma diagnostics with dielectronic satellites. The main ideas of plasma population kinetics such as local thermodynamic equilibrium, coronal equilibrium, and collisional-radiative modeling will be presented with examples. A brief summary of the basic mechanisms of spectral line broadening will be given as well.

### **Further Reading**

1. H.-J. Kunze, *Introduction to Plasma Spectroscopy*, Springer (2009)
2. V. P. Shevelko and L. A. Vainshtein, *Atomic Physics for Hot Plasmas*, IOP Publishing (1993)

## A non-perturbative R-matrix tutorial for single photon ionization of atoms and ions

**Connor Ballance**<sup>1</sup>, **Nigel Badnell**<sup>2</sup>, **Franck Delahaye**<sup>3</sup>

<sup>1</sup>*School of Maths and Physics, Queen's University of Belfast, UK*

<sup>2</sup>*Department of Physics, Strathclyde University, UK*

<sup>3</sup>*LERMA, Observatoire de Paris; PSL Research University; CNRS; Sorbonne University, France*

This joint lecture will present two generalized approaches for calculating the cross sections of fundamental atomic processes, with an emphasis on the single photon ionization of atoms and ions. The distorted-wave method is categorized as a perturbative approach and shall be presented by Dr Fontes, whereas the R-matrix method, which is a non-perturbative method will be presented by myself.

A summary overview of the R-matrix method and associated terminology given in greater detail in the R-matrix review book of P. G. Burke [1] shall be given. A discussion concerning the strengths and weaknesses of the method, sometimes in relation to the distorted-wave method will be provided highlighting the computational bottlenecks and how we address them. These include the description of Rydberg resonance structure in the two methods and how we optimize the structure for photo-ionization calculations.

A simple He-like Fe test case for those attendees that would like to pursue a calculation themselves and the step-by-step process from atomic structure to photo-ionization cross sections will be presented.

For the vast majority of highly charged ions there is wide applicability of both distorted-wave and R-matrix methods and excellent agreement found between them in terms of the fundamental photo-ionization cross sections. In terms of application, the R-matrix approach provides the bound-bound and bound-free component of opacity calculations [2] for many ion stages. Opacities shall be discussed in greater detail by Dr Fontes.

### Further Reading

1. P. G. Burke, "R-Matrix Theory of Atomic Collisions", Springer (2011); doi:10.1007/978-3-642-15931-2.
2. F. Delahaye, C. P. Ballance, R. Smyth and N. R. Badnell, "Quantitative comparison of opacities calculated using the R-matrix and Distorted-Wave methods: Fe XVII", *Monthly Notices of the Royal Astronomical Society* **508**, 421 (2021); doi:10.1093/mnras/stab2016.

---

## Atomic cross section calculations: the distorted-wave method

**Christopher J. Fontes<sup>1</sup>**

<sup>1</sup>*Computational Physics Division, Los Alamos National Laboratory, USA*

Over the past sixty years, steady and significant progress has been made in the ability to calculate the vast amount of atomic data that is required to model spectra produced by plasmas, under both local thermodynamic equilibrium (LTE) and non-LTE conditions. Ab initio methods for calculating the cross sections associated with fundamental atomic processes typically fall under two categories: close-coupling theory and distorted-wave theory. The former is sometimes referred to as a “non-perturbative” approach, in which the continuum and bound electrons are treated on an equal footing, and are coupled (or mixed) in a single wavefunction. The latter is considered to be a perturbative approach, in which the continuum-electron wavefunctions are calculated in the presence of a distortion potential that is produced by previously calculated bound-electron wavefunctions. In this case, the continuum and bound electrons are not formally mixed.

This presentation is the second half of a joint talk given by Dr. Ballance, who will discuss the non-perturbative R-matrix method, and myself. The goal of this talk is to provide a basic explanation of the distorted-wave method, particularly in the context of so-called “resonances” that can appear in the atomic cross sections. Resonances may occur when a continuum electron appears in a fundamental atomic process, either at the start or the end of the process, and at least two bound electrons are present in the target atom or ion. More specifically, resonances can appear in the cross sections associated with the processes of electron-impact excitation, electron-impact ionization and photoionization, as well as their inverse processes. In the distorted-wave approach, the resonance contribution can be calculated via a two-step process that begins with a specific bound state, followed by a short-lived autoionizing state that spontaneously decays (via the Auger-Meitner process) to a specific final bound state of interest. The calculation of resonances via this two-state approach was pioneered, for the process of dielectronic recombination, by Bates and Dalgarno [1] and subsequently applied in the analysis of solar spectral features by Gabriel, Jordan and Paget [2,3], while the process of electron-impact excitation was investigated by Seaton [4] and Cowan [5].

In this talk, I focus on the process of photoionization, which is important from both a fundamental-theory perspective and the practical need to provide the so-called “bound-free” contribution to the radiative opacity, which is important for an understanding of stellar structure. I use the Los Alamos Suite of Atomic Physics Codes [6] to calculate photoionization cross sections for some simple examples and demonstrate, for highly charged ions, that the resulting cross sections produce very similar results to those obtained with the R-matrix solution to the close-coupling equations.

---

## Further Reading

1. D.R. Bates and A. Dalgarno, in *Atomic and Molecular Processes*, Ed. D.R. Bates (New York: Academic) pp. 258–61 (1962).
2. A.H. Gabriel and C. Jordan, *Nature* **221**, 941 (1969).
3. A.H. Gabriel and T.M. Paget, *J. Phys. B: Atom. Molec. Phys.* **5**, 673 (1972).
4. M.J. Seaton, *J. Phys. B: Atom. Molec. Phys.* **2**, 5 (1969).
5. R.D. Cowan, *J. Phys. B: Atom. Molec. Phys.* **13**, 1471 (1980).
6. C.J. Fontes, H.L. Zhang, J. Abdallah, Jr., R.E.H. Clark, D.P. Kilcrease, J. Colgan, R.T. Cunningham, P. Hakel, N.H. Magee and M.E. Sherrill, *J. Phys. B* **48**, 144014 (2015).

## Acknowledgements

This work was performed under the auspices of the U.S. Department of Energy by Los Alamos National Laboratory under Contract No. 89233218CNA000001.

---

## FAC for intermediate users

M. F. Gu<sup>1,2</sup>

<sup>1</sup>*Prism Computational Sciences, WI, USA*

<sup>2</sup>*Space Science Laboratory, UC Berkeley, CA, USA*

In this tutorial, we will discuss practical usage of the Flexible Atomic Code (FAC) for intermediate users. Basic knowledge of atomic physics and plasma spectroscopy is assumed, but familiarity with FAC in particular is not required. The topics covered in the tutorial include:

- Download and installation.
- Atomic processes implemented in FAC.
- SFAC and PFAC interfaces.
- Handling FAC binary and ascii output files.
- Basic usage for simple atomic systems.
- Coupling atomic calculations and collisional radiative modeling.
- Advanced features: Many-body perturbation theory and R-Matrix.

We will follow the tutorial through several practical examples, both simple and more advanced. Simple examples will demonstrate the use of FAC in obtaining limited sets of atomic parameters, such as energy levels, radiative rates, and collisional cross sections. More complex examples will demonstrate the use of PFAC interface (via the Python scripting language) to generate large scale datasets, and use them as input to collisional radiative models for spectroscopic modeling applications.

## Density effects on plasma spectroscopy

**Stephanie Hansen**<sup>1</sup>

<sup>1</sup>*Sandia National Laboratories, USA*

1. Atomic kinetic effects:
  - (a) Ladder ionization
  - (b) Metastable states
  - (c) Local thermodynamic equilibrium
  - (d) Degenerate electron distributions
2. Atomic structure effects:
  - (a) Plasma screening
  - (b) Pressure ionization
  - (c) Ion correlations
  - (d) Line broadening

### Further Reading

1. Modern Methods in Collisional-Radiative Modeling, Y. Ralchenko (ed.), Springer (2016).

---

## Electron-molecule collisions

**Mourad Telmini**<sup>1</sup>

<sup>1</sup>*University of Tunis El Manar, Tunisia*

Electron-molecule collisions play an important role in plasma physics, particularly in cool plasma and discharges where they are the dominant process. In this tutorial lecture, the main processes occurring when an electron collides with a molecule, or a molecular ion, will be briefly introduced. Then, the case of  $(e+H_2^+)$  will be presented in detail, not only because of its simplicity as a prototype, but also in relation with its importance in plasma fusion physics.

A key point in modelling the collision, is the formation of an intermediate neutral super-excited compound ( $H_2^{**}$  in the prototype case), which governs the various outcome channels and gives rise to sharp complex variations in the cross sections at low-energy, especially in the important case of dissociative recombination.

The main theoretical approaches for studying this problem will be introduced, with an emphasis on the method that combines the eigenchannel  $R$ -matrix formalism with Generalized Quantum Defect Theory. We will show how this approach, so-called Halfium  $R$ -matrix, is able to take into account simultaneously the bound spectrum and the fragmentation channels, leading to the key quantities needed for the calculation of the electron-molecule collisions cross-sections and rates of the various processes.

### Further Reading

1. M. Aymar, C.H. Greene, E. Luc-Koenig, *Rev. Mod. Phys.* **68** 1015 (1996).
2. M. Telmini, Ch. Jungen, *Phys Rev. A* **68** 062704 (2003).
3. J. Tennyson, *Physics Reports* **491** 29-76 (2010).
4. O. Motapon, N. Pop, F. Argoubi, J. Zs Mezei, M. D. Epee Epee, A. Faure, M. Telmini, J. Tennyson, I. F. Schneider, *Phys Rev. A* **90** 012706 (2014).

## X-ray lasers

**Nina Rohringer**<sup>1,2</sup>

<sup>1</sup>*Center for Free-Electron Laser Science (CFEL), Deutsches Elektronen-Synchrotron DESY, Hamburg, Germany*

<sup>2</sup>*The Hamburg Centre for Ultrafast Imaging, Universität Hamburg, Hamburg, Germany*

The advent of x-ray free-electron lasers providing femtosecond x-ray pulses of unprecedented high intensities opened the field of nonlinear x-ray science and the study of collective x-ray matter interaction. In this tutorial I will give an overview over the development of inner-shell x-ray lasers based on superfluorescence of K- $\alpha$  emission. The concept of single-pass x-ray laser amplifiers based on stimulated emission on transitions involving inner-shell electronic levels has been developed by Duguay and Rentzepis [1] soon after the invention of the optical laser. The idea is relatively simple: tuning x-rays with frequencies tuned above K-shell ionization edges predominantly promotes electrons from this shell to the continuum. The resulting inner-shell hole decays on a femtosecond timescale predominantly via Auger decay (for atoms with  $Z < 21$ ) or K- $\alpha$  fluorescence decay (for atoms with  $Z > 20$ ). For intensities achievable at XFELs, the K-shell ionization rates are comparable to these decay rates, resulting in a sizable, transient population inversion, that can be exploited for stimulated K- $\alpha$  emission. The first proof-of-principle experiment on inner-shell x-ray amplification has been performed in 2010 on the K- $\alpha$  transition in neon gas [2], in a cylindrical gain medium of large aspect ratio, in which a short XFEL pulse creates a channel of population inverted ions propagating through the sample in swept gain geometry. Spontaneously emitted photons propagating in the forward direction of the propagating XFEL pulse meet ions in an inverted state, eventually resulting in an avalanche of stimulated emission processes (superfluorescence, or amplified spontaneous emission). Exponential gain of stimulated x-ray emission has been demonstrated over four orders of magnitude, with small signal gains of  $\approx 20$ . This concept of inner-shell x-ray amplification has been also established in the hard x-ray spectral range on K- $\alpha$  transitions in solid Cu [3], and Mn, and on Mn atoms in solution [4]. Interestingly, it has been demonstrated that the spectroscopic information on the oxidation state of the metals – the chemical shift of K- $\alpha$  emission – is preserved in the stimulated x-ray emission [4], thereby opening the pathway towards stimulated emission spectroscopy [5]. Theoretical modeling [6,7] predicts that the emitted x-ray superfluorescence can result in almost transform limited femtosecond x-ray pulses, despite the process starting from spontaneous emission. Being pumped with a stochastic XFEL source, also phase-stable pairs of fs pulses can be generated, as recently demonstrated [8]. Currently, concepts of x-ray laser oscillators based on the inner-shell x-ray lasing are investigated [9], potentially providing fully coherent x-ray pulses of unprecedented spectral brightness with properties comparable to x-ray free-electron laser oscillators



---

## Further Reading

1. M.A. Duguay and G. P. Rentzepis, *Appl. Phys. Lett.* **10**, 350 (1967).
2. N. Rohringer et al., *Nature* **481**, 488 (2012).
3. H. Yoneda et al., *Nature* **524**, 446 (2015).
4. T. Kroll et al., *Phys. Rev. Lett.* **120**, 133203 (2018).
5. T. Kroll et al., *Phys. Rev. Lett.* **125**, 037404 (2020).
6. C. Weninger and N. Rohringer, *Phys. Rev. A* **90**, 063828 (2014)
7. A. Benediktovitch et al. arXiv:2303.00853 (2023).
8. Y. Zhang et al., *PNAS* **119**, e2119616119 (2022).
9. A. Halavanau et al., *PNAS* **117** (27), 15511 (2020).



---

# THINGS TO DO IN VIENNA

ChatGPT

Vienna is a city with a lot to offer, whether you are interested in history, art, music, or simply want to enjoy the local cuisine and experience the Viennese way of life. Here are some recommendations for things to see and do in Vienna:

- Visit Schönbrunn Palace: This is one of Vienna's most famous landmarks and an absolute must-see. It's a beautiful Baroque palace that was once the summer residence of the Habsburgs. You can take a tour of the palace and its gardens, or simply enjoy a stroll around the grounds.
- Attend a performance at the Vienna State Opera: This world-renowned opera house hosts some of the best performances in the world. Even if you're not an opera fan, the grandeur of the building and the quality of the performances are worth experiencing.
- St. Stephen's Cathedral: This Gothic masterpiece is located in the heart of Vienna's old town and is an iconic symbol of the city. You can take a guided tour of the cathedral or climb to the top of the tower for panoramic views of the city.
- Visit the Kunsthistorisches Museum: This art museum is home to an impressive collection of paintings, sculptures, and decorative arts from around the world. It's also home to one of the largest coin collections in the world.
- Explore the Naschmarkt: This open-air market is a foodie's paradise. You can find everything from fresh produce to spices, cheeses, meats, and more. It's a great place to sample some local cuisine or pick up some souvenirs.
- Take a stroll through the Hofburg Palace: This is another impressive palace that was once the residence of the Habsburgs. It's now home to several museums, including the Imperial Apartments and the Sisi Museum, which is dedicated to the life of Empress Elisabeth.
- Walk around the Prater: This large park is home to the famous Wiener Riesenrad, a giant Ferris wheel that offers stunning views of the city. You can also find a variety of other rides and attractions, as well as restaurants and cafes.
- Try some Viennese coffee and cake: Vienna is famous for its coffee culture, and there are many traditional coffeehouses throughout the city where you can enjoy a cup of coffee and a slice of cake. Some of the most famous cafes include Café Central, Demel, and Café Sacher.
- Visit the Belvedere Palace: This beautiful palace is home to an impressive collection of Austrian art, including works by Gustav Klimt. You can also enjoy a stroll through the palace's gardens and take in the stunning views of the city.
- Explore the MuseumsQuartier: This cultural complex is home to several museums, including the Leopold Museum, the Museum of Modern Art, and the Kunsthalles Wien. It's also a great place to relax and enjoy some food and drinks in one of the many outdoor cafes.

---

If you're looking for something a little different to do in Vienna, here are some alternative recommendations:

- Take a street art tour: Vienna is home to a vibrant street art scene, and there are several tour companies that offer guided walks through the city's neighborhoods to see the murals and graffiti.
- Visit the Hundertwasserhaus: This colorful apartment building was designed by artist Friedensreich Hundertwasser and is a great example of his unique style. You can take a guided tour of the building and learn about its history and architecture.
- Attend a wine tavern (Heuriger): Vienna is surrounded by vineyards, and there are several traditional wine taverns where you can taste local wines and enjoy traditional Austrian food. Some of the most popular areas for Heurigers include Grinzing and Neustift am Walde.
- Explore the Danube Island: This long, narrow island in the middle of the Danube River is a popular spot for outdoor activities. You can go for a bike ride or a run, swim in the river, or simply relax in one of the many parks.
- Take a day trip to Bratislava: Vienna is only about an hour away from the Slovakian capital of Bratislava, and it's easy to take a day trip to explore this charming city. You can take a boat tour along the Danube or simply wander through the old town.
- Visit the Prunksaal at the National Library: This stunning Baroque library is a hidden gem in the heart of Vienna. You can take a guided tour of the library and see its impressive collection of rare books and manuscripts.
- Take a cooking class: Vienna is famous for its cuisine, and there are several cooking schools that offer classes where you can learn how to make traditional dishes like Wiener Schnitzel and Sachertorte.
- See a movie at the Gartenbaukino: This classic movie theater has been showing films since 1960 and is a great place to catch a classic or independent film.
- Take a bike tour: Vienna has a great network of bike paths, and there are several tour companies that offer guided bike tours through the city's neighborhoods and parks.

## PARTICIPANTS

Pedro AMARO	Faculdade de Ciências e Tecnologia da Universidade Nova de Lisboa (FCT, Nova University of Lisbon), Portugal
Luc ASSINK	University of Groningen, Netherlands
Nigel BADNELL	University of Strathclyde, UK
Mahdiyeh BAKHTIYARI RAMEZANI	Nuclear Science and Technology Research Institute (NSTRI), Atomic Energy Organization of Iran (AEOI), Iran
Connor BALLANCE	Queen's University Belfast (QUB), UK
Sofia BALUGANI	European Synchrotron Radiation Facility (ESRF), France
Raúl BARRACHINA	Bariloche Atomic Centre (Centro Atómico Bariloche, CAB), Argentina
Matthew BARTON	United Kingdom Atomic Energy Authority (UKAEA), UK
Manuel BAUTISTA	Western Michigan University, USA
Sirine BEN NASR	Université de Mons, Belgium
Djamel BENREDJEM	Laboratoire Aimé Cotton, Université Paris-Saclay, France
Klaas BIJLSMA	University of Groningen, Netherlands
David BISHEL	University of Rochester, USA
Xavier BONNIN	ITER
Dmitriy BORODIN	Forschungszentrum Jülich (FZJ), Germany
Bastiaan BRAAMS	Centrum Wiskunde and Informatica (CWI), Netherlands
Annette CALISTI	Physique des Interactions Ioniques et Moléculaires (PIIM), Aix-Marseille Université (AMU), France
Helena CARVAJAL GALLEGO	Université de Mons, Belgium
Kalyan Kumar CHAKRABARTI	Scottish Church College, India
Wenjin CHEN	Southwestern Institute of Physics, China

Byoung-Ick CHO	Gwangju Institute of Science and Technology (GIST), South Korea
Ricardo Ferreira DA SILVA	Faculdade de Ciências e Tecnologia da Universidade Nova de Lisboa (FCT, Nova University of Lisbon), Portugal
Jérôme DEPRINCE	Université de Mons, Belgium
Corinne DESGRANGES	Centre d'Etudes Nucleaires de Cadarache, Association EURATOM-CEA, France
Xiaobin DING	Northwest Normal University (NWNNU), China
Yunbo DONG	Southwestern Institute of Physics, China
DIPTI	IAEA
Maylis DOZIÈRES	General Atomics, USA
Youssef EZZO	Advanced Research Center for Nanolithography (ARCNL), Netherlands
Erik FLOM	University of Wisconsin-Madison, USA
Christopher J. FONTES	Los Alamos National Laboratory (LANL), USA
Keisuke FUJII	Oak Ridge National Laboratory (ORNL), USA
Dmitry FURSA	Faculty of Science and Engineering, Curtin University, Australia
Marta GALBIATI	Polytechnic University of Milan, Italy
Xiang GAO	Institute of Applied Physics and Computational Mathematics (IAPCM), China
Simone GARGIULO	École Polytechnique Fédérale de Lausanne (EPFL), Switzerland
Juana GERVASONI	National Atomic Energy Commission (Comisión Nacional de Energía Atómica, CNEA), Argentina
Mohammad GHARAIBEH	Qatar University, Qatar
Nathanael GILL	Los Alamos National Laboratory (LANL), USA
Gabriel GRELL	NASA Goddard Space Flight Center (GSFC), USA
Filipe GRILO	Faculdade de Ciências e Tecnologia da Universidade Nova de Lisboa (FCT, Nova University of Lisbon), Portugal
Ming Feng GU	Prism Computational Sciences, USA

Rémy GUIRLET	Centre d'Etudes Nucleaires de Cadarache, Association EURATOM-CEA, France
Devki Nandan GUPTA	University of Delhi, India
Ibtissem HANNACHI	University of Batna 1, Algeria
Stephanie HANSEN	Sandia National Laboratories, USA
Kalle HEINOLA	IAEA
Christian HILL	IAEA
David HOARTY	Atomic Weapons Establishment, UK
Ronnie HOEKSTRA	University of Groningen, Netherlands
Suxing HU	University of Rochester, USA
Haikel JELASSI	National Center of Nuclear Sciences and Technologies (CNSTN), Tunisia
Curtis JOHNSON	Oak Ridge National Laboratory (ORNL), USA
Valdas JONAUSKAS	Vilnius University (Vilniaus universitetas), Lithuania
Alisher KADYROV	Faculty of Science and Engineering, Curtin University, Australia
Timothy KALLMAN	NASA Goddard Space Flight Center (GSFC), USA
Alina KONONOV	Sandia National Laboratories, USA
Michael KRUSE	Lawrence Livermore National Laboratory (LLNL), USA
Duck-Hee KWON	Korea Atomic Energy Research Institute (KAERI), South Korea
Vincenzo LAPORTA	Consiglio Nazionale delle Ricerche – Area della Ricerca di Bari (CNR Bari), Italy
Hai LE	Lawrence Livermore National Laboratory (LLNL), USA
Hae Ja LEE	Stanford Linear Accelerator Laboratory (SLAC), USA
Chunhai LYU	Max Planck Institute for Nuclear Physics (Max-Planck-Institut für Kernphysik, MPIK), Germany
Xinwen MA	Institute of Modern Physics (IMP), Chinese Academy of Sciences (CAS), China
Mike MACDONALD	Lawrence Livermore National Laboratory (LLNL), USA
P. Bharathi MAGESH	Institute for Plasma Research, Ahmedabad, India

Oleksandr MARCHUK	Forschungszentrum Jülich (FZJ), Germany
Edward MARLEY	Lawrence Livermore National Laboratory (LLNL), USA
Brian Edward MARRÉ	Helmholtz-Zentrum Dresden-Rossendorf (HZDR), Germany
Alessandro MAFFINI	Polytechnic University of Milan, Italy
Niall MCELROY	Queen's University Belfast (QUB), UK
János Zsolt MEZEI	Institute for Nuclear Research (ATOMKI), Hungary
Mohd Faiz Bin MOHD ZIN	Malaysian Nuclear Agency, Malaysia
Charisse MONFERO	IAEA
Caroline MOSSÉ	Physique des Interactions Ioniques et Moléculaires (PIIM), Aix-Marseille Université (AMU), France
Izumi MURAKAMI	National Institute for Fusion Science (NIFS), Japan
Taisuke NAGAYAMA	Sandia National Laboratories, USA
Bob NAGLER	Stanford Linear Accelerator Laboratory (SLAC), USA
Nobuyuki NAKAMURA	Institute for Laser Science (ILS), University of Electro-Communications (UEC), Japan
Truong Son NGUYEN	Vietnam Academy of Sciences and Technology, Vietnam
Anna NIGGAS	Technische Universität Wien (TU Wien), Austria
Joseph NILSEN	Lawrence Livermore National Laboratory (LLNL), USA
Martin O'MULLANE	Department of Physics, University of Strathclyde, UK
Sebastián OTRANTO	Instituto de Física del Sur (IFISUR), Universidad Nacional del Sur (UNS), Argentina
Marquidia PACHECO	Instituto Nacional de Investigaciones Nucleares (ININ), Mexico
Jean-Christophe PAIN	CEA / DAM / DIF, France
Marek PAJEK	Jan Kochanowski University in Kielce, Poland
Conor PERKS	Plasma Science and Fusion Center (PSFC), Massachusetts Institute of Technology (MIT), USA
Olivier PEYRUSSE	Laboratoire Lasers, Plasmas et Procédés Photoniques (LP3), Aix-Marseille Université (AMU), France
Yves PEYSSON	CEA/IRFM, France



Daniel PINHEIRO	Faculdade de Ciências e Tecnologia da Universidade Nova de Lisboa (FCT, Nova University of Lisbon), Portugal
Robin PIRON	CEA / DAM / DIF, France
Nicolina POP	West University of Timișoara, Romania
Banafsheh POURSHAHAB	Nuclear Science and Technology Research Institute (NSTRI), Atomic Energy Organization of Iran (AEOI), Iran
PRITI	National Institute for Fusion Science (NIFS), Japan
Pascal QUINET	Université de Mons, Belgium
Yuri RALCHENKO	National Institute of Standards and Technology (NIST), USA
Catherine RAMSBOTTOM	Queen's University Belfast (QUB), UK
Nina ROHRINGER	Deutsches Elektronen-Synchrotron (DESY), Germany
Marc SACKERS	Forschungszentrum Jülich (FZJ), Germany
Ioan F. SCHNEIDER	Université du Havre, France
Vladimir SCHOLTZ	University of Chemistry and Technology, Prague, Czechia
Howard SCOTT	Lawrence Livermore National Laboratory (LLNL), USA
Chintan SHAH	Max Planck Institute for Nuclear Physics (Max-Planck-Institut für Kernphysik, MPIK), Germany
Kajal SHAH	Pandit Deendayal Energy University, India
Fatemeh SHAKERI	University of Kashan, Iran
Lalita SHARMA	Indian Institute of Technology (IIT), Roorkee, India
Neelam SHUKLA	University of Nebraska at Kearney, USA
Roshani SILWAL	Appalachian State University, USA
Joseph John SIMONS	The Graduate University for Advanced Studies, SOKENDAI, Japan
Suvam SINGH	Max Planck Institute for Nuclear Physics (Max-Planck-Institut für Kernphysik, MPIK), Germany
Nicolas SISOURAT	Laboratoire de Chimie Physique – Matière et Rayonnement (LCPMR), Sorbonne Université, France
Michal ŠMÍD	Helmholtz-Zentrum Dresden-Rossendorf (HZDR), Germany

Jang Hyeob SOHN	Gwangju Institute of Science and Technology (GIST), South Korea
Nopparit SOMBOONKITTICHAJ	Kasetsart University, Thailand
Evgeny STAMBULCHIK	Weizmann Institute of Science, Israel
Roland STAMM	Physique des Interactions Ioniques et Moléculaires (PIIM), Aix-Marseille Université (AMU), France
Christine STOLLBERG	École Polytechnique Fédérale de Lausanne (EPFL), Switzerland
Chihiro SUZUKI	The Graduate University for Advanced Studies, SOKENDAI, Japan
Endre TAKACS	Clemson University, USA
Mourad TELMINI	University of Tunis El Manar (UTM), Tunisia
Károly TÓKÉSI	Institute for Nuclear Research (ATOMKI), Hungary
Pedro VELARDE	Universidad Politécnica de Madrid (Technical University of Madrid), Spain
Sam VINKO	Oxford University, UK
Richard WILHELM	Technische Universität Wien (TU Wien), Austria
Zhongshi YANG	Institute of Plasma Physics, Chinese Academy of Sciences (ASIPP), China
Yang YANG	Fudan University, China
Seong Ling YAP	Plasma Technology Research Centre (PTRC), University of Malaya, Malaysia
Jianmin YUAN	Atomic and Molecular Physics Group (AMPG), National University of Defense Technology (NUDT), China
Chunyu ZHANG	Department of Physics, University of Strathclyde, UK
Ling ZHANG	Institute of Plasma Physics, Chinese Academy of Sciences (ASIPP), China
Beata ZIAJA-MOTYKA	Centre for Free-Electron Laser Science - Deutsches Elektronen-Synchrotron (CFEL-DESY), Germany
Yaming ZOU	Fudan University, China

---

## AUTHOR INDEX

- Acebal, E. .... P77  
 Aich, S. .... #69  
 Al-Mustafah, E. .... P47  
**Amaro, P.** .... #106, P108, P43, P81  
**Assink, L.** .... #63  
 Atrey, P. .... #69  
 de Avillez, M. .... P43  
 Azuma, T. .... #34  
 Baczewski, A. .... #92  
 Badnell, N. .... P65, T2a  
 Bai, X. .... #70  
**Bakhtiyari-Ramezani, M.** P124, P125  
**Ballance, C.** .... #111, P114, T2a  
**Balugani, S.** .... #25  
 Banaś, D. .... #116  
 Bandhopadhay, M. .... #62  
 Baptista, G. .... P43  
 Baquero-Ruiz, M. .... #68  
 Barbui, T. .... #66  
 Barrientos, R. V. .... #50  
 Baruah, U. .... #62  
 Bastrakov, S. .... #40  
 Beach, M. .... #82  
**Ben Nasr, S.** .... #8  
 Benredjem, D. .... P123, #4  
 Berengut, J. .... #58  
 Bhuyan, M. .... #62  
 Bielecki, J. .... #71  
**Bijlsma, K.** .... P45, #63  
**Bishel, D.** .... #90  
 Bitter, M. .... #95  
 Blenski, T. .... #89  
 Boerner, P. .... #118  
 Boffelli, J. .... P113  
**Borodin, D.** .... #118  
 Botz, M. .... P108  
 Boumendjel, Y. .... #76  
 Brasseur, M. .... P10  
 Bray, I. .... #129, P130  
 Brezinsek, S. .... #118  
 Brown, G. .... #117  
 Burke, T. .... #100  
 Bussmann, M. .... #40  
**Calisti, A.** .... P123, #4  
**Chakrabarti, K.** .... P113, #26  
 Chakraborty, A. .... #62  
 Chen, Chongyang .... P138, P65  
 Chen, Chengyuan .... P141  
 Chen, D. Y. .... P138  
 Chen, H. .... #95  
**Chen, W.** .... P142  
 Cheng, Y. .... #107  
 Chin, D. .... #90  
**Cho, B.-I.** .... P74, #78  
 Choksi, B. .... #62  
 Chowdhuri, M. .... #69  
 Chung, H.-K. .... #127, P74  
 Cianfrani, F. .... #118  
 Cliche, D. .... #117  
 Collins, G. .... #90  
 Coteló, M. .... #137  
 Cowan, T. .... #40  
 Cuenca, A. .... P77  
 Dasgupta, A. .... #95  
 Deka, A. .... #62  
 Delahaye, F. .... T2a  
**Deprince, J.** .... P11, #8  
 Desgranges, C. .... #76  
 Dey, R. .... #69  
**Ding, X.** .... #107, P56  
 Dipti .... #100, P12, P140  
 Dolui, S. .... #69  
 Dong, C. .... P56  
 Dong, C. F. .... P142  
**Dong, Y.** .... P141  
 Doron, R. .... #95  
 Doyle, H. .... #25  
**Dozières, M.** .... #82  
 Duten, X. .... P119  
 Dworak, D. .... #71  
 Eakins, D. .... #25  
 Eftthimion, P. .... #95

Ennis, D. ....	#111	Hahn, S. J. ....	P74
Epstein, R. ....	#90	Haničinec, M. ....	P140
Epée Epée, M. D. ....	P113	<b>Hannachi, I.</b> ....	#6
Ertmer, S. ....	P12	<b>Hansen, S.</b> ....	#92, T4
Fedorczak, N. ....	#76	Hao, G. Z. ....	P142
Fernandes, A. ....	P43	Harman, Z. ....	P96, P97
Ferri, S. ....	P123, #4	Harris, A. ....	#66
Fiser, L. ....	#103	Hartwell, G. ....	#111
<b>Flom, E.</b> ....	#66	Hassaine, R. ....	P113
Flörs, A. ....	P81	He, X. F. ....	P142
<b>Fontes, C. J.</b> ....	T2b	He, X. X. ....	P142
Foord, M. ....	#117	Heeter, B. ....	#117
Formenti, A. ....	#104	Heeter, R. ....	#23
Fu, Y. ....	P56	Heinola, K. ....	P140
<b>Fujii, K.</b> ....	#58	Hentschel, T. ....	#92
Furno, I. ....	#68	Hernandez, J.-A. ....	#25
<b>Fursa, D.</b> ....	#129, P130	<b>Hill, C.</b> ....	P140
<b>Galbiati, M.</b> ....	#104	Hill, K. ....	#95
<b>Gallego, H. C.</b> ....	#8, P9	<b>Hoarty, D.</b> ....	#117, #23
<b>Gambari, M.</b> ....	P60	Hodziova, A. ....	#103
Gamrath, S. ....	P10	Hoekstra, R. ....	#63
Gao, L. ....	#95	Hosier, A. ....	#100
Garcia Gallardo, J. ....	P94	Hrudka, J. ....	#103
<b>Gargiulo, S.</b> ....	P67	Hu, A. ....	#107
Gauchet, F. ....	P113	<b>Hu, S.</b> ....	#128, #90
<b>Gervasoni, J. L.</b> ....	P94	Huang, H. K. ....	P138
<b>Gharaibeh, M.</b> ....	P47	Huang, Z. K. ....	P138
Ghosh, J. ....	#69	Huckins, J. ....	#82
Ghosh, R. ....	#26	Huebl, A. ....	#40
<b>Gill, N.</b> ....	P83	Iacob, F. ....	P113
Gimenez, N. ....	P94	Iglesias, C. ....	P122, #95, #99
Godinho, C. ....	P43	Indelicato, P. ....	P43
Golovkin, I. ....	#90	Jabłoński, L. ....	#116
Goto, M. ....	#42, #57	Jacquier, R. ....	#68
<b>Grell, G.</b> ....	P79	Jadeja, K. S. ....	#69
<b>Grilo, F.</b> ....	P108, P43	Jankovsky, M. ....	#103
Groth, M. ....	#118	Jardin, A. ....	#71
<b>Gu, M. F.</b> ....	T3	<b>Jelassi, H.</b> ....	P28
Guerra, M. ....	P43	Jiresova, J. ....	#103
<b>Guirlet, R.</b> ....	#76	<b>Johnson, C.</b> ....	#111
Guittienne, P. ....	#68	<b>Jonauskas, V.</b> ....	P30, #75
<b>Gupta, D. N.</b> ....	P49	Julak, J. ....	#103
Gupta, M. K. ....	#69	Kadi, L. ....	#68

Kadyrov, A. ....	#21	Lokajova, E. ....	#103
<b>Kallman, T.</b> ....	#32	London, R. ....	#117, #52
Karimov, R. ....	#68	<b>Lyu, C.</b> ....	P96
Kato, D. ....	P56, #57	López-Urrutia, J. R. C. ....	P108
Kauffman, B. ....	#95	Ma, W. L. ....	P138
Kawamoto, Y. ....	#57	<b>Ma, X.</b> ....	P138
Kawate, T. ....	#57	<b>MacDonald, M.</b> ....	#117, #95
Keitel, C. H. ....	P96, P97	MacPhee, A. ....	#95
Khun, J. ....	#103	Machado, J. ....	P43
Kimura, N. ....	#34	Machkova, A. ....	#103
Klenivskiy, M. ....	#103	Macwan, T. ....	#69
Kluge, T. ....	#40	Maffini, A. ....	#104
Koenig, R. ....	#66	<b>Magesh, P. B.</b> ....	#62
Koike, F. ....	P56	Manas, P. ....	#76
Kolake, B. K. M. ....	#69	Manchanda, R. ....	#69
Kono, Y. ....	#34	Mandelbaum, P. ....	#76
<b>Kononov, A.</b> ....	#92	Mao, L. J. ....	P138
Krauland, C. ....	#82	Marandet, Y. ....	#118, #6
Kraus, F. ....	#95	<b>Marchuk, O.</b> ....	P12, P39
Kreter, A. ....	P12	Marler, J. P. ....	#100
<b>Kruse, M.</b> ....	P122, #99	<b>Marley, E.</b> ....	P87
Kuma, S. ....	#34	Maron, Y. ....	#95
Kumar, A. ....	#69	Marques, J. P. ....	P43, P81
Kumar, R. ....	#69	<b>Marré, B. E.</b> ....	#40
Kučas, S. ....	#75	Martin, M. ....	#117, #52
Kwak, S. ....	#66	Martínez, S. H. ....	P77
Kynienė, A. ....	#75	Martínez-Pinedo, G. ....	P81
Küppers, B. ....	#118	Masys, Š. ....	#75
Lahmann, B. ....	#95	Mathon, O. ....	#25
<b>Le, H.</b> ....	#61, P72	Maurer, D. ....	#111
Leck, G. ....	P81	Mazon, D. ....	#71
Lei, L. ....	P56	<b>McElroy, N.</b> ....	P114
Leitão, R. G. ....	P43	McLean, K. ....	#23
Leutenegger, M. ....	P79	MesaDame, A. ....	#52
Li, J. ....	P138	<b>Mezei, Z. J.</b> ....	P113, #26
Li, W. ....	#70	Mirani, F. ....	#104
Liedahl, D. A. ....	#117, #95	Mirshahvalad, S. ....	P124, P125
Liu, H. ....	#107	Mori, N. A. ....	#129
Liu, L. ....	P142	Morita, S. ....	#107
Liu, X. ....	P138	Morton, J. ....	#23
Liu, Yi ....	P142	Motapon, O. ....	P113
Liu, Yile ....	P56	Mukherjee, N. ....	#26
Loch, S. ....	#111, #66	<b>Murakami, I.</b> ....	P56, #57

Méndez, L. ....	#63	<b>Quinet, P.</b> .....	P10, #8
<b>Nagayama, T.</b> .....	#29	Rabadán, I. ....	#63
<b>Nagler, B.</b> .....	#126	Racova, Z. ....	#103
Nagora, U. ....	#69	Rai, S. ....	#63
Nakamura, N. ....	#34, P56	<b>Ralchenko, Y.</b> .....	#100, P12, T1
<b>Nguyen, T. S.</b> .....	P119	Ramaiya, N. ....	#69
Nie, L. ....	P142	Ramsbottom, C. ....	P114
<b>Niggas, A.</b> .....	P38	Rathi, S. ....	P55
<b>Nilsen, J.</b> .....	#117, #52	Ravasio, A. ....	#25
Nilson, P. ....	#90	Rehill, U. S. ....	#129
Niyonzima, S. ....	P113	Reinke, M. ....	#112
Nohekhan, M. ....	P124, P125	Remington, B. ....	#23
Numadate, N. ....	#34	Ren, S. ....	#127
O’Neil, G. C. ....	#100	Rice, J. ....	#112
Oishi, T. ....	#57	Richardson, S. ....	#23
Oliva, E. ....	#137	Rilloraza, F. ....	#52
Opachich, Y. ....	#23	<b>Rohringer, N.</b> .....	T6
<b>Otranto, S.</b> .....	P77	Romazanov, J. ....	#118
Pablant, N. ....	#95	Rond, C. ....	P119
<b>Pacheco, M. J. P.</b> .....	#50	Rosato, J. ....	#6
<b>Pain, J.-C.</b> .....	P123, #4	Rose, S. ....	#23
<b>Pajek, M.</b> .....	#116	Rougier, J. ....	#23
Palmeri, P. ....	#8	Rubery, M. ....	#23
Pandya, K. ....	#62	Ruby, J. ....	#90
Parente, F. ....	P43	Rygg, R. ....	#90
Passoni, M. ....	#104	<b>Sackers, M.</b> .....	P12
Patel, K. ....	#69	Sahoo, A. K. ....	P55
Patel, M. ....	#117	Sakaue, H. A. ....	P56, #57
Patel, S. ....	#69	Sampaio, J. M. ....	P43, P81
Pathak, S. ....	#69	Santos, J. P. ....	P108, P43
Pativate, P. ....	#34	Sasaki, A. ....	#57
<b>Perks, C.</b> .....	#112	Scarlett, L. ....	#129
Perry, T. ....	#23	Schmitz, O. ....	#66
<b>Peyrusse, O.</b> .....	P37, P60, #76	Schneider, I. F. ....	P113, #26
<b>Peysson, Y.</b> .....	#71	Schneider, M. B. ....	#82, #95
<b>Pinheiro, D.</b> .....	P43	<b>Scholtz, V.</b> .....	#103
<b>Piron, R.</b> .....	#89	Scholz, M. ....	#71
Poirier, L. ....	#63	Schramm, U. ....	#40
Pop, N. ....	P113	Schwob, J.-L. ....	#76
<b>Pourshahab, B.</b> .....	P27	<b>Scott, H.</b> .....	#117, #61, P72, #95
Prahlad, V. ....	#62	Seely, J. ....	#82
<b>Priti</b> .....	#34	Sevelin-Radiguet, N. ....	#25
Purohit, S. ....	#69	<b>Shah, C.</b> .....	P33, P79

<b>Shah, K.</b> .....	#69	Vankova, E. ....	#103
Shakeri, F. ....	P125	de la Varga, A. G. ....	#137
Shao, L. ....	P138	<b>Velarde, P.</b> .....	#137
<b>Sharma, L.</b> .....	P55	Versolato, O. ....	#63
Sharma, S. ....	#62	Vezenet, D. ....	#112
Sheil, J. ....	#63	<b>Vinko, S.</b> .....	#127
Shepherd, R. ....	#117	Vázquez, E. ....	#137
Shi, Y. ....	#127	Walkowiak, J. ....	#71
Shi, Z. B. ....	P142	Wang, H. B. ....	P138
Shingles, L. ....	P81	Wang, S. X. ....	P138
Shukla, G. ....	#69	Wark, J. ....	#127
<b>Shukla, N.</b> .....	P53	Wei, Y. L. ....	P142
<b>da Silva, R. F.</b> .....	P81	Wen, W. Q. ....	P138
<b>Silwal, R.</b> .....	P93	Werl, M. ....	P38
<b>Simons, J. J.</b> .....	#42	Whitley, H. ....	#117
Singh, K. ....	#69	Widera, R. ....	#40
Singh, M. ....	#62	Widmann, K. ....	#117
<b>Singh, S.</b> .....	P97	Wilhelm, R. ....	P38
Smith, E. ....	#90	de Wit, E. ....	#63
<b>Šmíd, M.</b> .....	#109	Wu, C. ....	P56
<b>Sohn, J. H.</b> .....	P74	Xu, G. ....	#70
<b>Somboonkittichai, N.</b> .....	P110	Yadava, N. ....	#69
Sotelo, J. P. ....	#50	Yan, C. ....	#70
Soutome, K. ....	#34	Yan, L. W. ....	P142
<b>Stambulchik, E.</b> .....	#95	Yang, J. C. ....	P138
<b>Stamm, R.</b> .....	#6, P64	Yang, P. ....	P56
<b>Stollberg, C.</b> .....	#68	Yang, Q. W. ....	P142
Stoupin, S. ....	#82, #95	<b>Yang, Y.</b> .....	#107, P56, #70
Sustelo, L. ....	P43	Yao, K. ....	#107, P56
<b>Suzuki, C.</b> .....	P41	<b>Yap, S. L.</b> .....	P139
Svensson, J. ....	#66	Yu, D. L. ....	P142
Swatton, D. ....	#23	<b>Yuan, J.</b> .....	#35, P138
Tabimina, J. ....	#82	Zammit, M. S. ....	#129
<b>Takacs, E.</b> .....	#100	Zeng, J. ....	#35
Tang, M. T. ....	P138	<b>Zhang, C.</b> .....	P138, P65
Tanna, R. ....	#69	Zhang, F. ....	#107, P56
<b>Telmini, M.</b> .....	T5	<b>Zhang, L.</b> .....	#107, P56
Tennyson, J. ....	P113, #26	Zhang, N. ....	P142
Thompson, N. ....	#82	Zhang, W. ....	#107
Thorn, D. B. ....	#95	Zhang, Y. ....	P141
Tian, H. ....	#70	Zhu, L. F. ....	P138
Torchio, R. ....	#25	Zhang, Y. P. ....	P142
<b>Tókési, K.</b> .....	P80	<b>Ziaja-Motyka, B.</b> .....	#22
Umer, H. ....	P130		